Remote sensing of night lights: a review and an outlook for the future

Special issue '50 Years of Environmental Remote Sensing Research: 1969 – 2019'

Noam Levin[1,2], Christopher C. M. Kyba[3,4], Qingling Zhang[5], Alejandro Sánchez de Miguel[6,7], Miguel O Román[8], Xi Li[9], Boris A. Portnov[10], Andrew L. Molthan[11], Andreas Jechow[3,4], Steve Miller[12], Zhuosen Wang[13,15], Ranjay M Shrestha[14,15], Christopher D. Elvidge[16]

[1] Department of Geography, The Hebrew University of Jerusalem, Israel

[2] Remote Sensing Research Center, School of Earth and Environmental Sciences, University of Queensland, Australia

[3] GFZ German Research Centre for Geosciences, Germany

[4] Leibniz-Institute of Freshwater Ecology and Inland Fisheries, Germany

[5] School of Aeronautics and Astronautics, Sun Yat-Sen University, China

[6] Environment and Sustainability Institute, University of Exeter, Penryn Campus, Penryn, Cornwall, TR10 9FE, United Kingdom

[7] Dept. Física de la Tierra y Astrofísica, Universidad Complutense de Madrid, 28040 Madrid, Spain

[8] Earth from Space Institute, Universities Space Research Association, Columbia, MD, USA

[9] State Key Laboratory of Information Engineering in Surveying, Mapping and Remote Sensing, Wuhan University, Wuhan, China

[10] Department of Natural Resources and Environmental Management, Faculty of Management, University of Haifa, Mt. Carmel, Haifa 3498838, Israel

[11] Earth Science Branch, NASA Marshall Space Flight Center, Huntsville, AL, United States

[12] Cooperative Institute for Research in the Atmosphere, Colorado State University; Foothills Campus, 1375 Campus Delivery, Ft. Collins, CO 80523-1375, USA

[13] Earth System Science Interdisciplinary Center, University of Maryland, College Park, MD, United States

[14] Science Systems and Applications, Inc., Lanham, MD, United States

15 Terrestrial Information Systems Laboratory, NASA Goddard Space Flight Center, Greenbelt, MD, United States

[16] Earth Observation Group, NOAA National Centers for Environmental Information, United States

Abstract

Remote sensing of night light emissions in the visible band offers a unique opportunity to directly observe human activity from space. This has allowed a host of applications including mapping urban areas, estimating population and GDP, monitoring disasters and conflicts. More recently, remotely sensed night lights data have found use in understanding the environmental impacts of light emissions (light pollution), including their impacts on human health. In this review, we outline the historical development of night-time optical sensors up to the current state of the art sensors, highlight various applications of night light data, discuss the special challenges associated with remote sensing of night lights with a focus on the limitations of current sensors, and provide an outlook for the future of remote sensing of night lights. While the paper mainly focuses on space borne remote sensing, ground based sensing of night-time brightness for studies on astronomical and ecological light pollution, as well as for calibration and validation of space borne data, are also discussed. Although the development of night light sensors lags behind day-time sensors, we demonstrate that the field is in a stage of rapid development. The worldwide transition to LED lights poses a particular challenge for remote sensing of night lights, and strongly highlights the need for a new generation of space borne night lights instruments. This work shows that future sensors are needed to monitor temporal changes during the night (for example from a geostationary platform or constellation of satellites), and to better understand the angular patterns of light emission (roughly analogous to the BRDF in daylight sensing). Perhaps most importantly, we make the case that higher spatial resolution and multispectral sensors covering the range from blue to NIR are needed to more effectively identify lighting technologies, map urban functions, and monitor energy use.

1. Introduction

Human society has modified the Earth to such an extent, that the present geological era has been termed as the Anthropocene (Crutzen, 2002). Monitoring human activity from space has largely been directed at mapping land cover and land use changes, such as deforestation (Hansen et al., 2013). Remote sensing of artificial lights, on the other hand, provides a direct signature of human activity. Global images of the Earth at night are now iconic, thanks to NASA media releases such as the “Bright Lights, Big City” (published in Oct 23rd, 2000, https://earthobservatory.nasa.gov/Features/Lights) or the “Earth at Night” (published in April 12th, 2017, https://earthobservatory.nasa.gov/Features/NightLights) and other communication channels (Pritchard, 2017).

The availability of artificial lights is often associated with wealth and a modern society (Hölker et al., 2010a, Green et al. 2015). Brighter lights are strongly associated with increased security in the public consciousness, despite little evidence of a causal link. As a result, total installed lighting increased rapidly during the past centuries (Fouquet & Pearson 2006), and has continued to increase in most countries during recent years (Kyba et al. 2017). An example of recent lighting changes is shown in Figure 1. Nightscapes change when objects or areas are illuminated for the first time, as in new roads or neighbourhoods, or when lighting technologies change (Figure 1). As a result, economic development goes in tandem with lighting.

Artificial lights at night can also provide insights on negative impacts, such as disasters (Molthan et al., 2012), and armed conflict (Román and Stokes, 2015). The importance of monitoring the Earth at night is also demonstrated by the growing recognition of artificial light as a pollutant (Navara and Nelson, 2007; Hölker et al., 2010b), the development of new lighting sources (such as LEDs, which can increase ecological light pollution; Pawson and Bader, 2014), and the continuing growth in extent and radiance of artificially lit areas (Kyba et al., 2017). Light pollution can be defined as “the alteration of natural light levels in the night environment produced by the introduction of artificial light” (Falchi et al., 2011). Artificial light can alter species abundance or behavior due to changes in their circadian rhythms or due to their attraction to or repulsion from light (ecological light pollution; Longcore & Rich, 2004, Rich & Longcore, 2006), can decrease our ability to observe stars at night (astronomical light pollution), and also leads to negative health impacts to humans through the suppression of melatonin production and insomnia (Hölker et al., 2010b; Falchi et al., 2011, Lunn et al. 2017).

Figure 1: Lighting changes in Calgary, Alberta (Canada) between 24/12/2010 (top) and 28/11/2015 (bottom). The neighborhood at left has converted from high pressure sodium to white LED lights, while the highway at right is newly illuminated with sodium lamps. The area has a roughly 7.5x3 km extent. Images based on astronaut photographs ISS026-E-12438 and ISS045-E-155029.

With the development of new space borne, airborne and ground sensors for quantifying light at night, new research opportunities are emerging (Kyba et al., 2015a; Hänel et al., 2018). The first comprehensive review on remote sensing of night lights was published by Doll (2008). Since that time, a variety of new sensors have become available (Figure 2; Table 1). More recent reviews on remote sensing of night lights have either focused solely on applications of the DMSP/OLS sensor (Elvidge et al., 2009c; Huang et al., 2014; Li and Zhou, 2017), on multi-temporal applications using DMSP/OLS and VIIRS/DNB (Bennett and Smith, 2017), on the various applications of night-time imagery (Li et al., 2016) and on the community of researchers active in this field (Hu et al., 2017). Since the recent review of Zhang et al. (2015b), new sensors, algorithms, and applications have emerged (Zhao et al., 2019). In this paper we therefore aim to provide a comprehensive review on the field of remote sensing of night lights, focusing on the visible spectral range, which is mostly related to artificial lights used by people to light the night so as to extend human activity hours. In our review we cover space borne, airborne, and ground based observations (recently reviewed in Hänel et al., 2018). We cover the historical development of this research area, the available sensors, the current state of the art algorithms for routine data processing, key applications, the differences to daytime remote sensing, upcoming space-based night lights missions, and future research challenges.

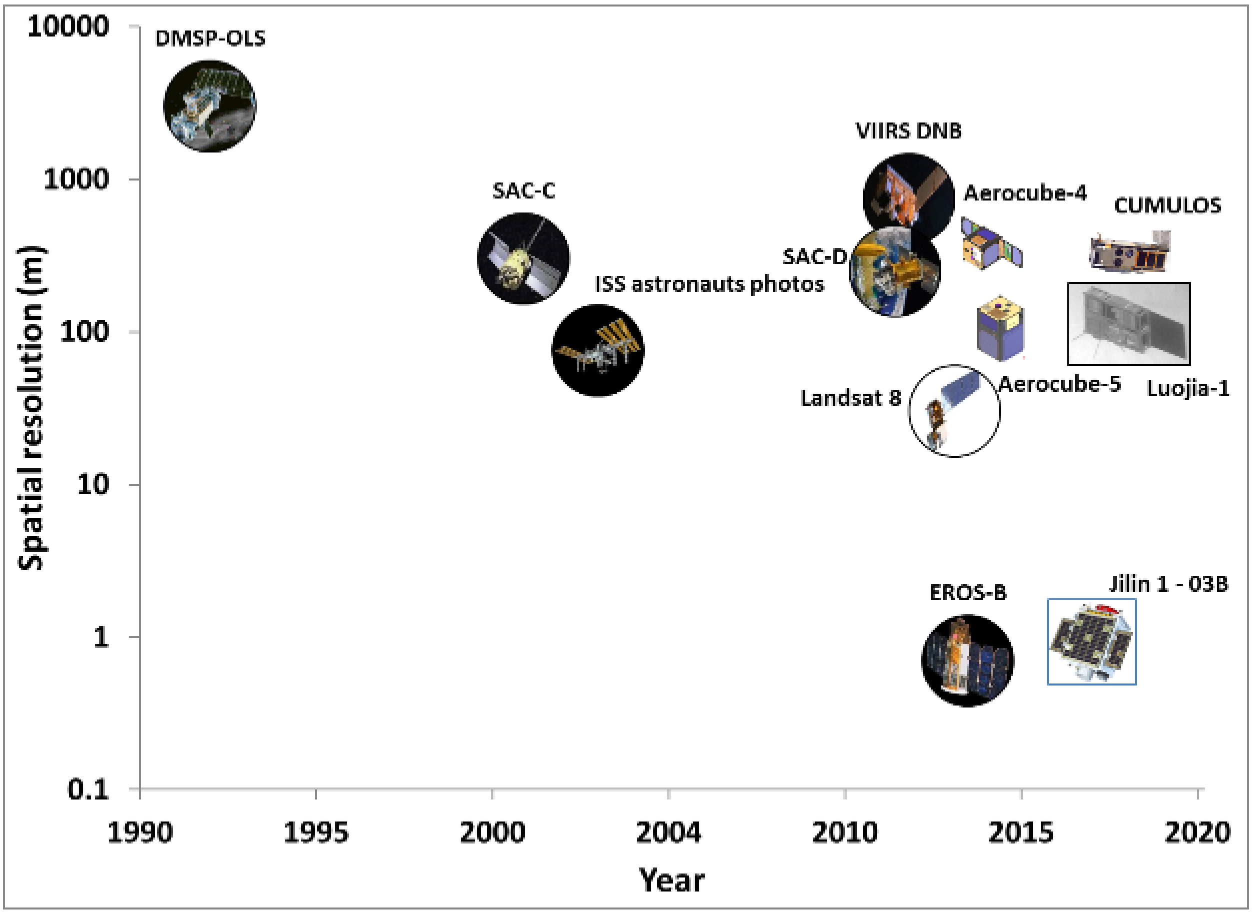

Figure 2: Space borne sensors with night-time lights capabilities, as a function of the year from which digital night-time images are available, and the spatial resolution of the sensor.

2. Historical overview

2.1 Earliest observations of night lights

Historically, technological developments in the energy industry (such as the transition from candles to gas, and later on to kerosene and then to electricity) have led over the past centuries to a gradual decrease in the price of lighting services, and were associated with increases in lighting efficiency and in the consumption of light per capita (Nordhaus, 1996; Fouquet and Pearson, 2006). The foundation of the Edison Electric Light Company can mark the modern era of lighting, and since the year 1800, the total consumption of light in the United Kingdom alone has grown by 25,600 times (Fouquet and Pearson, 2006). Walker (1973) reports that already in the 1930s sky illumination has started to preclude astronomical viewing from certain observatories (and see Rosebrugh, 1935), and as Bertrand Russell famously wrote in 1935, "*In the streets of a modern city the night sky is invisible; in rural districts, we move in cars with bright headlights. We have blotted out the heavens, and only a few scientists remain aware of stars and planets, meteorites and comets.*" (Russell, 1975).

The Artificial Light at Night (ALAN) Research Literature Database (http://alandb.darksky.org/, accessed September 16th, 2019) which covers 2,545 publications on the topic of light pollution (Figure 3; note however, that the ALAN database does not include all publications on light pollution or on remote sensing of night lights), has as one of its first papers that of Edison (1880). However, publications on light pollution were scarce until the mid-20th century (Figure 3; compare with Davies and Smyth, 2018). The first paper mentioning light pollution in its title (within this database) was only published in 1972, and it already suspected possible negative health impacts from exposure to artificial light at night (Burne, 1972). Other papers published in the early 1970s on light pollution were more concerned with the negative impacts that artificial lighting has on the ability of astronomers on view the night sky (e.g., Riegel, 1973), and the front cover of Vol. 179 No 4080 of Science shows the dramatic increase of city lights in Los Angeles between 1911 and 1965, as observed from Mount Wilson.

One of the first famous observations of cities' lights from space is attributed to US astronaut John Glenn, who in his orbit of the Earth in February 20th, 1962, saw Perth as the "City of Lights", thanks to local citizens and businesses who have turned on as many lights as they could as a sign of support for his mission (Biggs et al., 2012). In many ways, the subsequent development of remote sensing of night lights, can be compared to the general development of Earth observation using daytime images for environmental monitoring. However, as will be described below, remote sensing of night lights suffers from a lack of sensors, and consequently there is a temporal lag in the development of algorithms and customer-ready products.

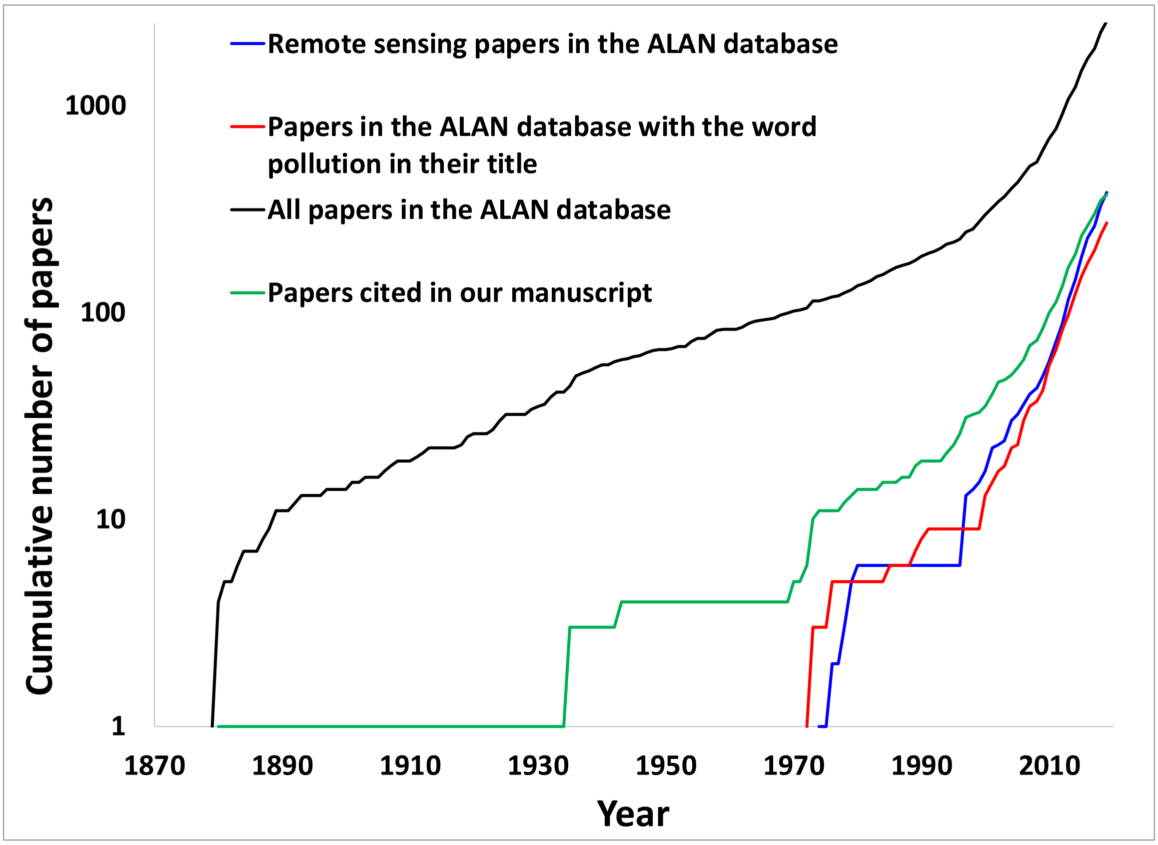

Figure 3: Cumulative number of papers on artificial lights in the Artificial Light at Night (ALAN) Research Literature Database (n = 2545) (http://alandb.darksky.org/, accessed September 16th, 2019). Also shown are papers where the title of the paper included the word pollution (n = 271), and papers published in remote sensing journals or where either one of the words "remote", "sensing", "satellite", "DMSP", "VIIRS", "Luojia", "SQM" appeared in the title of the paper or that Chris Elvidge was one of the co-authors (n = 380). The green line shows the yearly numbers of papers cited in our manuscript (n = 372).

2.2 Space borne sensors for measuring night lights

During nighttime, most passive remote sensing applications have focused on the thermal or microwave spectral regions, measuring radiation related to heat emission (Weng, 2009). In the following sections we detail the various sensors and platforms from which remote sensing of night lights has been performed.

2.2.1 DMSP/OLS

The first American satellites for Earth observation, launched in the 1960s, were either aimed for weather monitoring (TIROS-1, launched on April 1, 1960; Rao et al., 1990) or for military reconnaissance – the Corona program (McDonald, 1995). The Defense Meteorological Satellite Program (DMSP), started in the mid-1960s as the meteorological program of the US Department of Defense, aiming to collect global cloud cover data day and night. The era of global satellite observation of electric lighting started in 1971 with the launch of the SAP (Sensor Aerospace vehicle electronics Package) instrument flown by the Defense Meteorological Satellite Program. The SAP collected global imaging data in a panchromatic band spanning from 500 nm to 900 nm and a long-wave infrared channel. The signal from the visible band was intensified using a photomultiplier tube. Dickinson et al. (1974) presented a November 1971 SAP image showing nighttime lights of Northern Europe and gas flares in the North Sea. The purpose of the low light imaging was to enable the detection of clouds in the visible using moonlight as the illumination source (see e.g. Figure 4). The requirement for this came from Air Force meteorologists. A second generation low light imager, known as the Operational Linescan System (OLS) was carried on DMSP Block 5D satellites, with a first launch in 1976. A series of nineteen OLS instruments have been flown and data collection continues to the present (2018). However, the overpass times vary, with some satellites in dawn-dusk orbits and others in day-night orbits (Figure 5). Only the day-night satellites provide nighttime data in sufficient quantities to produce global nighttime lights products. While the existence of DMSP system was acknowledged in 1972, the use of night-time images of the Earth within the remote sensing community was very limited until the 1990s (Figure 3). This is mostly because until 1992 DMSP/OLS images were written to film and were not available in digital form. The University of Colorado, National Snow and Ice Data Center operated a film archive. Nonetheless, early scientific papers using DMSP/OLS observations of artificial lights from space were already published in the 1970s, with regards to astronomical light pollution (Hoag et al., 1973; Walker, 1973) and concerning the ability to monitor various human activities such as cities' lights, waste gas burning, agricultural fires and fishing fleets who use lights (Croft, 1973, 1978, 1979; Welch, 1980) (Figure 6). Sullivan (1989) produced the first global map of DMSP nighttime lights by mosaicking hand selected DMSP film segments (Figure 7). In comparison, the Corona satellite program and its associated photos were declassified much later than the DMSP program, in 1995, and have since allowed the development of various applications (Dashora et al., 2007).

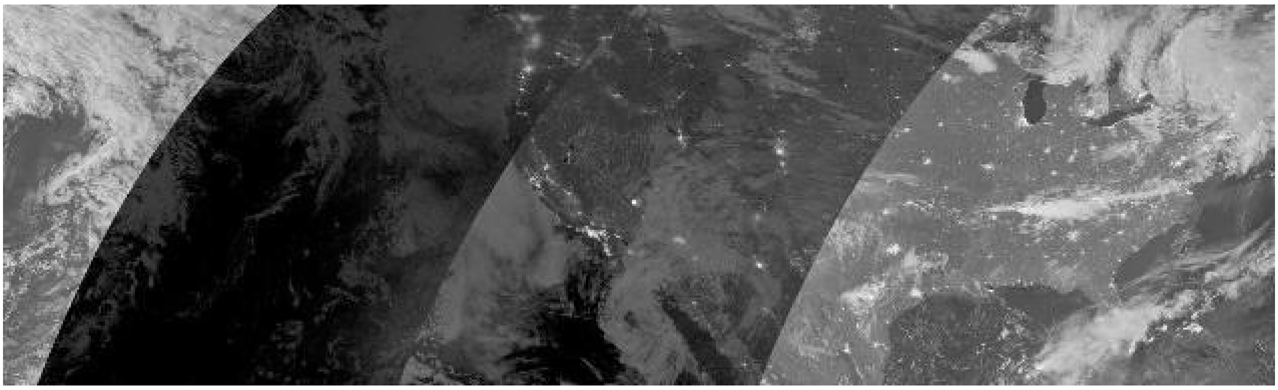

Figure 4: Lunar eclipse over North America on 2014/10/08, viewed by VIIRS DNB. At far right, the eclipse had not yet begun, and the instrument observed clouds illuminated by full moonlight. The next strip was taken with the moon partially eclipsed, and the dark strip when the moon was near to fully eclipsed. The final strip (at left) was taken one day earlier. Image prepared by Christopher Kyba based on image and data processing by NOAA's National Geophysical Data Center. Image available under a CC BY license at https://tinyurl.com/us-eclipse-20141008.

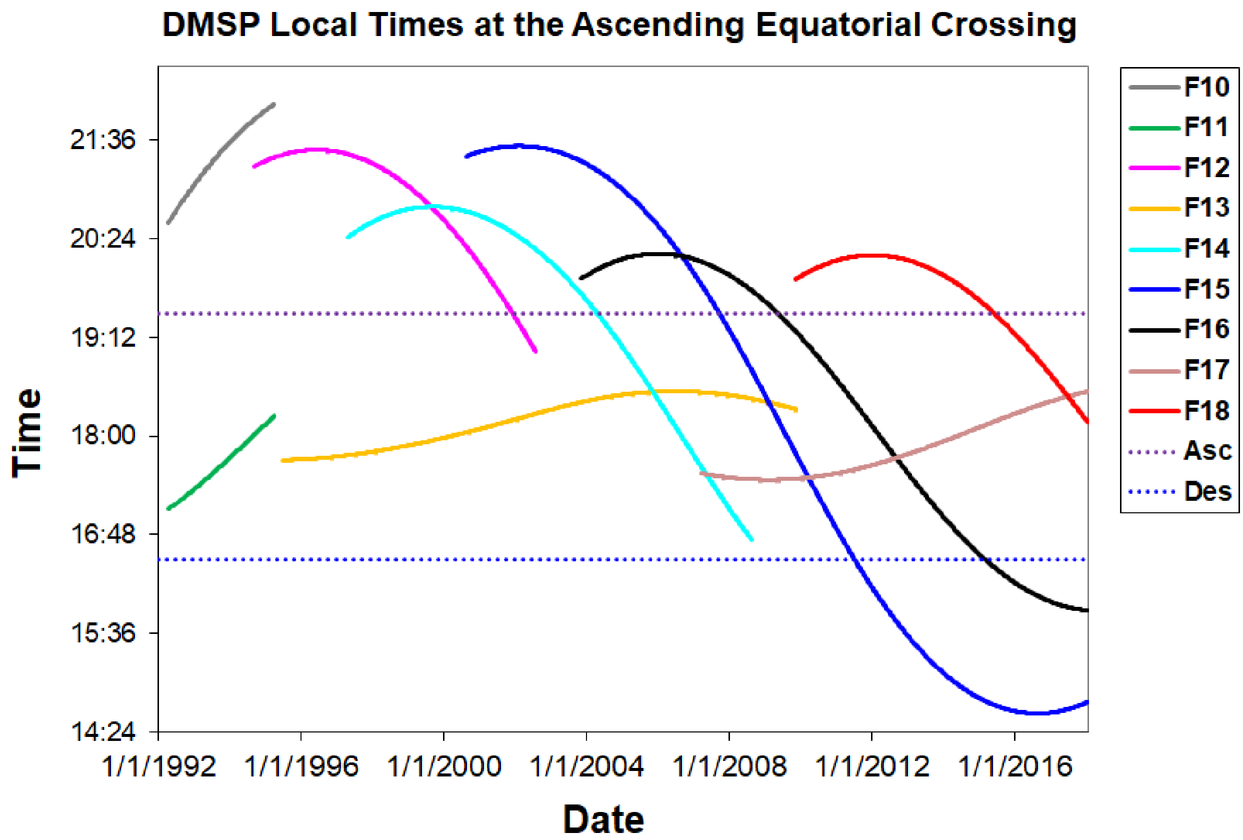

Figure 5: DMSP local times at the ascending equatorial crossing

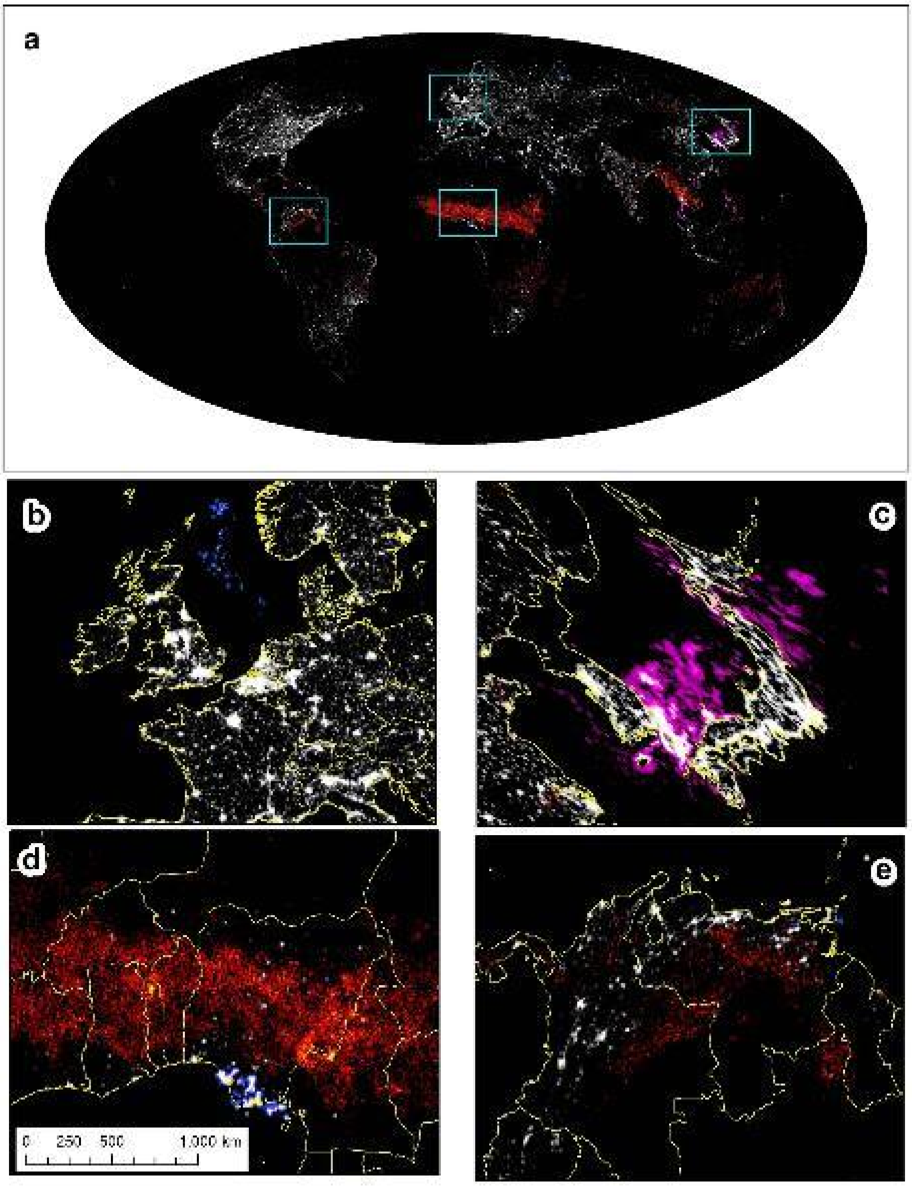

Figure 6: DMSP colorized night lights. The white represents lights generated from electricity, the red shading shows fires, the pink shading indicates light from squid fishing boats, and the blue spots are gas flares from oil rigs. Each is one year's worth of data. The differentiation of fires, boats, electric lights and gas flares was all done by temporal analysis (do the lights stay constant and do they move). The instrument itself is not able to distinguish between them. Zoomed in areas are shown for northern Europe (b), Japan and Korea (c), western Africa (d), and northern South America (e). Source of dataset: https://sos.noaa.gov/datasets/nighttime-lights-colorized/

Figure 7: Section of the first global map of DMSP nighttime lights, produced by mosaicking film segments by Woody Sullivan, University of Washington.

The launch of NOAA Advanced Very-High-Resolution Radiometer (AVHRR) weather satellites in the late 1970s (on TIROS-N in 1978 and on NOAA-6 in 1979; Rao et al., 1990), enabled the development of global 1km products for monitoring vegetation, surface temperature and land cover changes, with datasets going back to the early 1980s (Ehrlich et al., 1994). Similarly, a digital archive for DMSP data was established at the NOAA National Geophysical Data Center in 1992. In 1994, Chris Elvidge and Kimberly Baugh embarked on a program to produce global DMSP nighttime lights and fire products from digital DMSP data at NOAA's National Geophysical Data Center (NGDC) in Boulder, Colorado. This team pioneered the development of global satellite observed maps of nighttime lights. Algorithms were developed to geolocate OLS images and screen out sunlit and moonlit data. The first NGDC test product was of the USA and had 29 orbits as input. This product was clearly missing large numbers of lights from known cities and towns (Figure 8). To address the shortcoming regarding the large numbers of missing lights, the team realized they had no assurance that each area had cloud-free observations. This led to formal tracking of the numbers of observations and cloud-free coverages to ensure a comprehensive and standardized compilation of lighting features. A cloud detection algorithm was developed using the long wave infrared OLS data. The second NGDC product, made with 236 orbits with cloud screening is shown in Figure 9. For the global products, full years of data are used to ensure that there are multiple observations remaining after filtering out sunlit, moonlit and cloud data. Because fires are so readily detected by both DMSP and VIIRS, NGDC developed an outlier removal process tuned to filter out fires and retain areas with electric lighting (Baugh et al. 2010; Elvidge et al., 2017). One of the major shortcomings of the operational DMSP data collections is signal saturation in bright urban cores. In part, this is due to the fact that the visible band gain is gradually turned up as lunar illuminance declines. To produce a global nighttime lights product free of saturation, NOAA worked with the Air Force to schedule reduced gain OLS data (Elvidge et al., 1999). Global nighttime lights products were generated for seven years between 1996 and 2010 based on the preflight OLS calibration (Hsu et al., 2015). A sample of this data is shown in Figure 10. An additional shortcoming of the DMSP data is that its images are blurred, a phenomena termed as "blurring", "blooming" or "overglow". This is caused by scattering in the atmosphere (Sánchez de Miguel et al. 2019a), and discussed further in section 2.4.2. Abrahams et al. (2018) demonstrated that this blurring follows a Gaussian point-spread function, and developed an approach to deblur DMSP data. Other approaches for reducing and correcting the "blooming" effect on DMSP data were suggested by Townsend and Bruce (2010), Hao et al. (2015) and Cao et al. (2019).

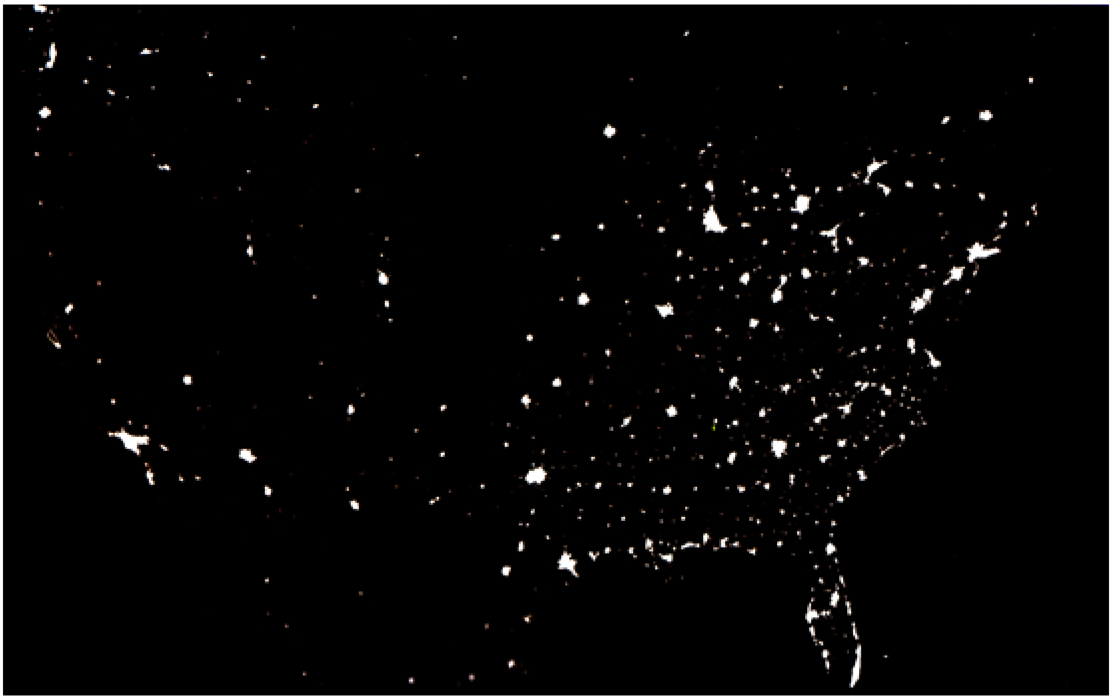

Figure 8: NGDC's first map of DMSP nighttime lights, produced from 29 orbits and no cloud screening.

Figure 9: NGDC's second generation DMSP nighttime lights product produced with cloud-screening from 236 orbits acquired in a six month period in 1995.

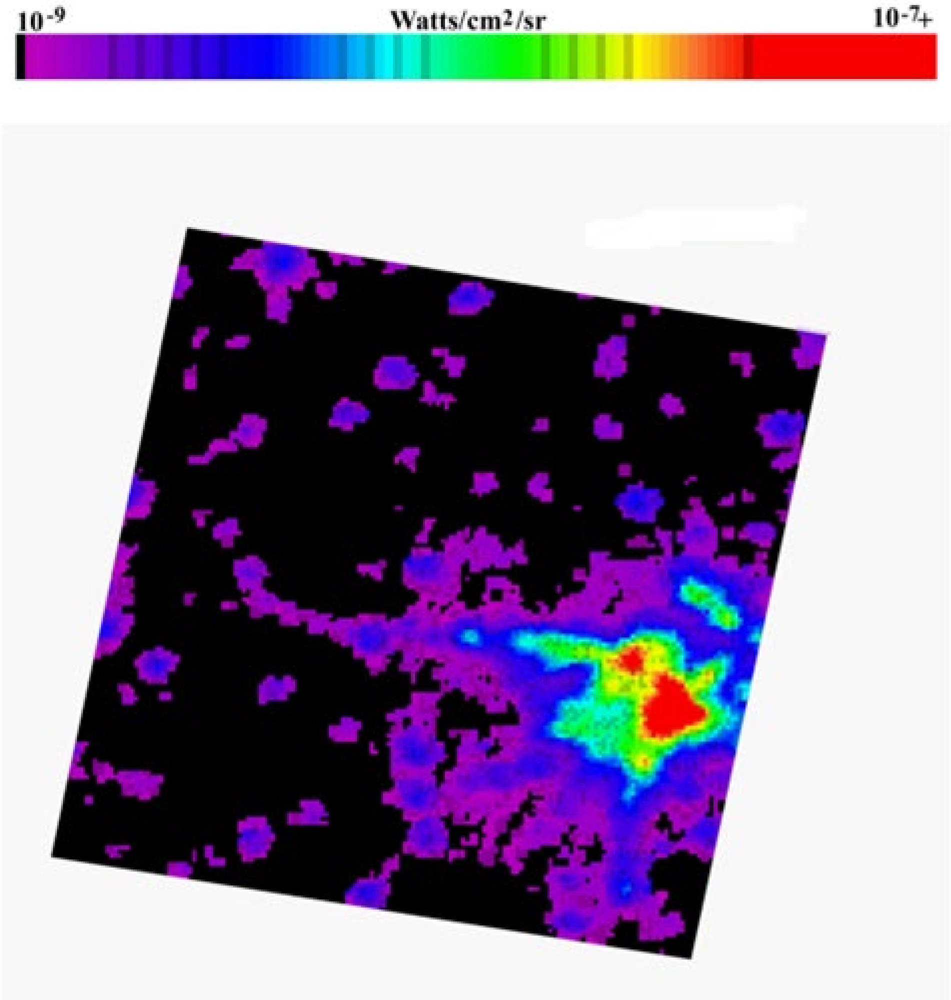

Figure 10: DMSP radiance nighttime lights for St. Louis, Missouri.

Christopher Elvidge and his team NOAA-NGDC have led the development of the various annual products of DMSP/OLS (covering the years between 1992 and 2013), which have been widely used, and are freely accessible online at https://ngdc.noaa.gov/eog/dmsp/downloadV4composites.html . The two major 1km global products of DMSP/OLS include average visible stable lights, and average lights × percentage, and are further described below (Baugh et al., 2010), however a host of other products have also been developed with time from DMSP/OLS data, including Global Radiance Calibrated Nighttime Lights, global impervious surface area (Elvidge et al., 2007a), global gas flare time series (Elvidge et al., 2009a), and more. By providing global time series of night lights, numerous papers have been published utilizing this unique source to study urbanization, socio-economic changes and threats to biodiversity (Bennett and Smith, 2017). False color composites of DMSP stable lights from different years have proven to be an effective way to visualize changes in artificial lighting and to follow patterns of urbanization, expansion of road networks, economic expansion or decline and damages to infrastructure as the result of armed conflicts (Figure 11).

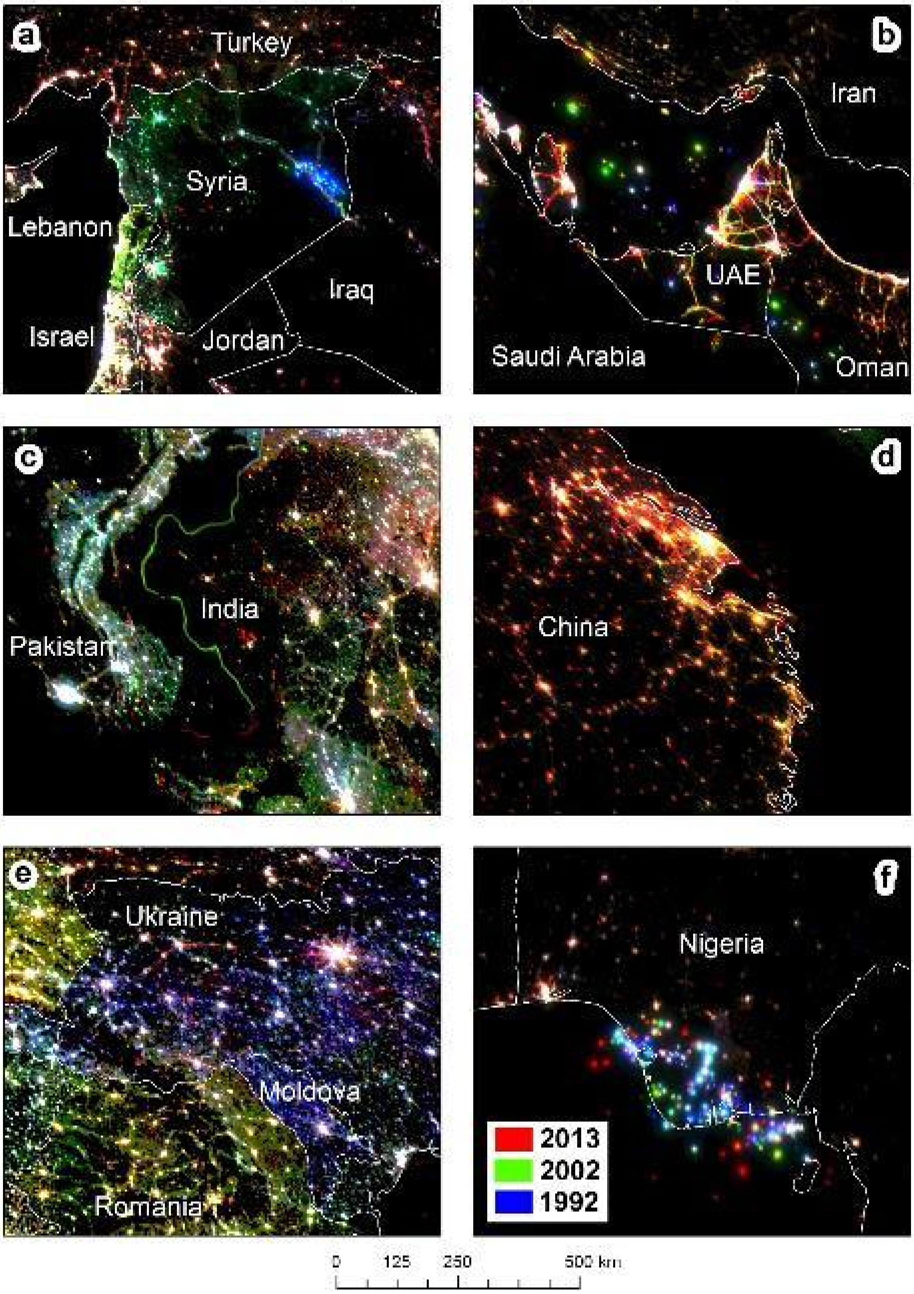

Figure 11: False color composites of DMSP stable lights version 4, showing: (a) decrease in lights following the war in Syria; (b) expansion of roads in the United Arab Emirates (UAE); (c) the lit border between India and Pakistan; (d) urbanization in China; (e) economic decline in Ukraine and Moldova following the collapse of the Soviet Union; (f) temporal changes of oil wells in Nigeria.

2.2.2 Landsat and Nightsat

Environmental monitoring of the Earth has been dramatically boosted by the launch of the first Landsat satellite in 1972, and the ongoing continuation of Landsat missions (whose entire archives became free to the public in 2009), and other civilian governmental satellites, offering medium spatial resolutions between 5 and 100 m at various spectral and temporal resolutions (Lauer et al., 1997; Roy et al., 2014). While Landsat satellites do acquire night-time images, these are mostly useful for their thermal information, as the optical sensors onboard the TM and ETM+ sensors were not designed for low light levels prevalent at night-time. However, the OLI sensor onboard Landsat 8, with its improved radiometric sensitivity, has been shown to be able to detect night-time lights from very bright areas such as gas flares and city centers (Levin and Phinn, 2016). Unfortunately, no sensor has been launched yet which offers operational multispectral monitoring of the Earth's night lights at medium spatial resolution. Nonetheless, the requirements of radiometric, spectral, spatial and temporal resolutions for such a sensor (termed NightSat) have been defined in a series of papers (Elvidge et al., 2007b,c, 2010), and are discussed in section 4.8 of this review paper. While two panchromatic sensors designed for observing night lights and offering a spatial resolution of about 300m have been launched in joint missions of CONAE and NASA (the SAC-C HSTC in 2000, and the SAC-D HSC in 2011; Colomb et al., 2003; Sen et al., 2006), images from them are hardly available and few papers have utilized them (but see Levin and Duke, 2012).

2.2.3 Remote sensing of night lights from the International Space Station

Night-time astronauts photographs

Astronaut photography from various NASA missions, including the Space Shuttle missions and the International Space Station (ISS), have long been used for observing a variety of environmental phenomena from low Earth orbits (Stefanov et al., 2017). The database of these photos is extensive, includes both daytime and nighttime photos, and is freely accessible via the Gateway of Astronaut Photography of the Earth (https://eol.jsc.nasa.gov/). The very first human acquired images from the Earth at night that we know of were the images taken by the astronauts of the Space Shuttle during Hercules/MSI mission (Simi et. al. 1995). For example a picture of Charlotte, US taken in 1993 was used to find the major sources of light at night, with the result of identifying vertical signs near the roads toward the airport that were lit on both sides with lights directed upwards to illuminate the signs[1]. This pioneer and other works were lost during the pre-internet era.

[1] Private communication. William Howard, 12 Aug 2015.

From 2001 until the present, the crew of the ISS has been taking images of Earth, space, and activities upon the station using digital single lens reflex (DSLR) cameras. Their nighttime images are the oldest multispectral images of the visible wavelengths emitted by Earth at night. Most images of Earth and space were taken either for outreach purposes or for the astronaut's pleasure, offering a unique perspective on our planet (Figure 12). Nevertheless, they comprise a unique and valuable dataset. Although there are technical challenges associated with radiometric calibration of such images (e.g. accounting for window extinction), work done at the Complutense University of Madrid over the last decade proves that calibration of ISS night light images is possible (Zamorano et. al. 2011, Sánchez de Miguel et. al. 2013a, 2018b; Sánchez de Miguel, 2015). One of the main problems of the astronaut photography is the motion blur produced by the orbital movement of the ISS. To solve this problem, astronaut Donald Pettit created a handmade device to compensate the movement of the ISS on the mission 006 (Pettit, 2009). Later, ESA created a special tripod called Nightpod (Sabbatini, 2014) used from the ISS030 to the ISS040 at least (precise date of decommissioning is unknown) (Figure 13). While DSLR cameras can be modified and have their IR-filter removed, so as to measure incoming light also in the infrared band (which is useful both for astrophotography purposes and for monitoring artificial lights sources which emit light in the near infra-red; Andreić and Andreić, 2010), the vast majority of astronaut night-time photography of the Earth, was limited to the visible range alone.

Figure 12: Night lights of the Levant, Astronaut photograph ISS053-E-50422, taken on 28/9/2017, 00:10:11 GMT. At the bottom of the image the densely populated Delta of the Nile can be seen, while the center of the image covers Israel, the West Bank, Jordan and Lebanon. The consequences of the conflict in Syria are hinted in this photo, where Syria is mostly dark, in contrast with lit towns and cities in Turkey to the north.

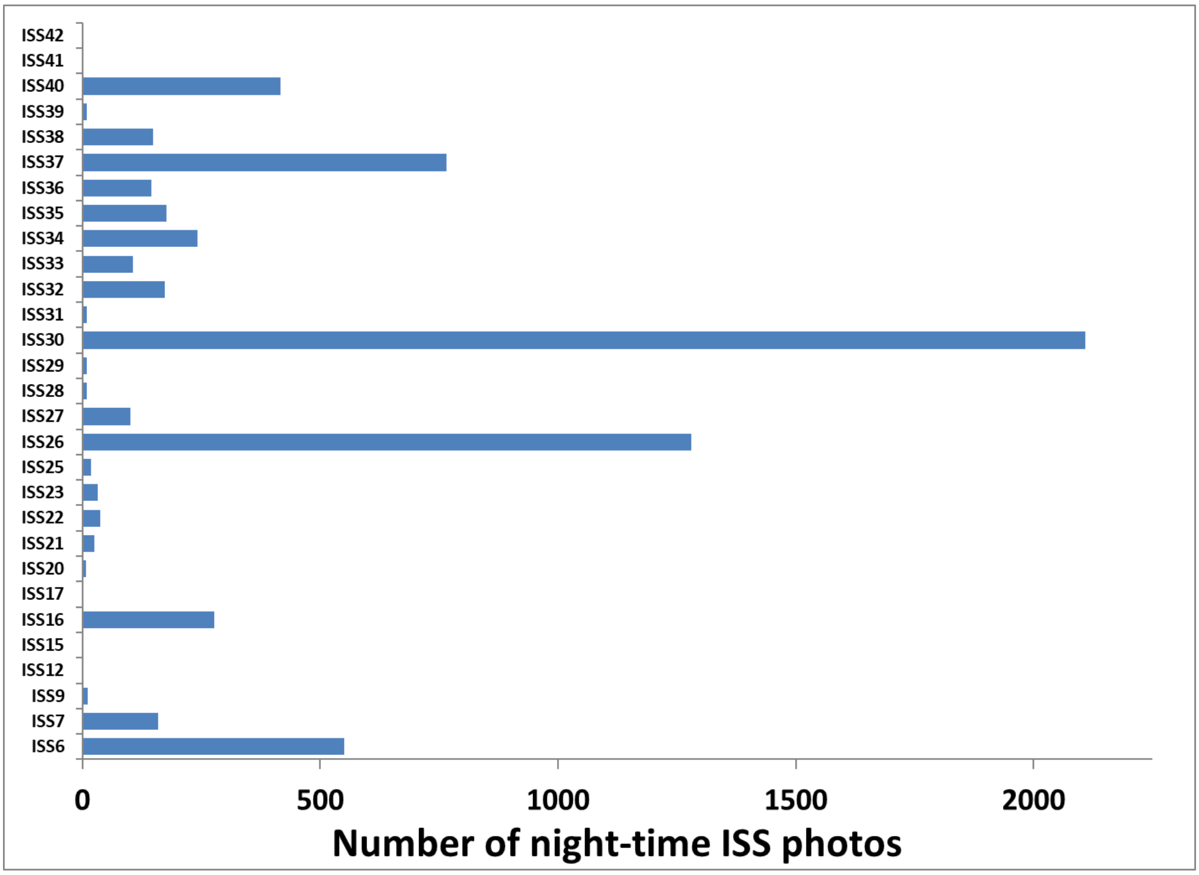

Figure 13: The number of night-time ISS photos identified by the Cities at Night crowdsourcing project (http://citiesatnight.org/index.php/maps/). Note that in several ISS missions many night-time photos were taken, while in other mission hardly any night-time photos were taken. The data shown does not include the recent three years.

The greatest advantages of night-time astronaut photos over other sources, are in their moderate spatial resolution (often between 5 – 200 m), and in being the first to provide color space borne night-time images (Kyba et al., 2015a; Figure 14), of hundreds of cities globally, albeit without any ordered acquisition program (Figure 13). Various studies have shown the value of those photos for studying socio-economic properties of cities at finer spatial resolutions than available by the DMSP/OLS (e.g., Levin and Duke, 2012; Kotarba and Aleksandrowicz, 2016; Kuffer et al., 2018). Calibrated DSLR images from the ISS have been used for epidemiological studies (Garcia-Saenz et. al. 2018), energy use and lighting technology studies (Kyba et al., 2015), environmental impact studies (Pauwels, et. al. 2019) and ecological studies (Mazor et al., 2013). In some cases, researchers have used ISS images without using, or at least without explaining, a radiometric calibration. Two companies currently provide calibration on demand of ISS images: www.noktosat.com and Eurosens. The "Cities at Night" project team has occasionally produced radiance calibrated images for scientific collaborations, and a project based at the University of Exeter is currently working on a data processing pipeline to produce a public database of calibrated images. The first mosaic of high resolution ISS images was made by Schmidt (2015), covering the administrative boundaries of the country of the Netherlands, and low resolution mosaics were made using time lapses by Sánchez de Miguel and Zamorano (2012), covering large parts of the US, Europe and middle-east.

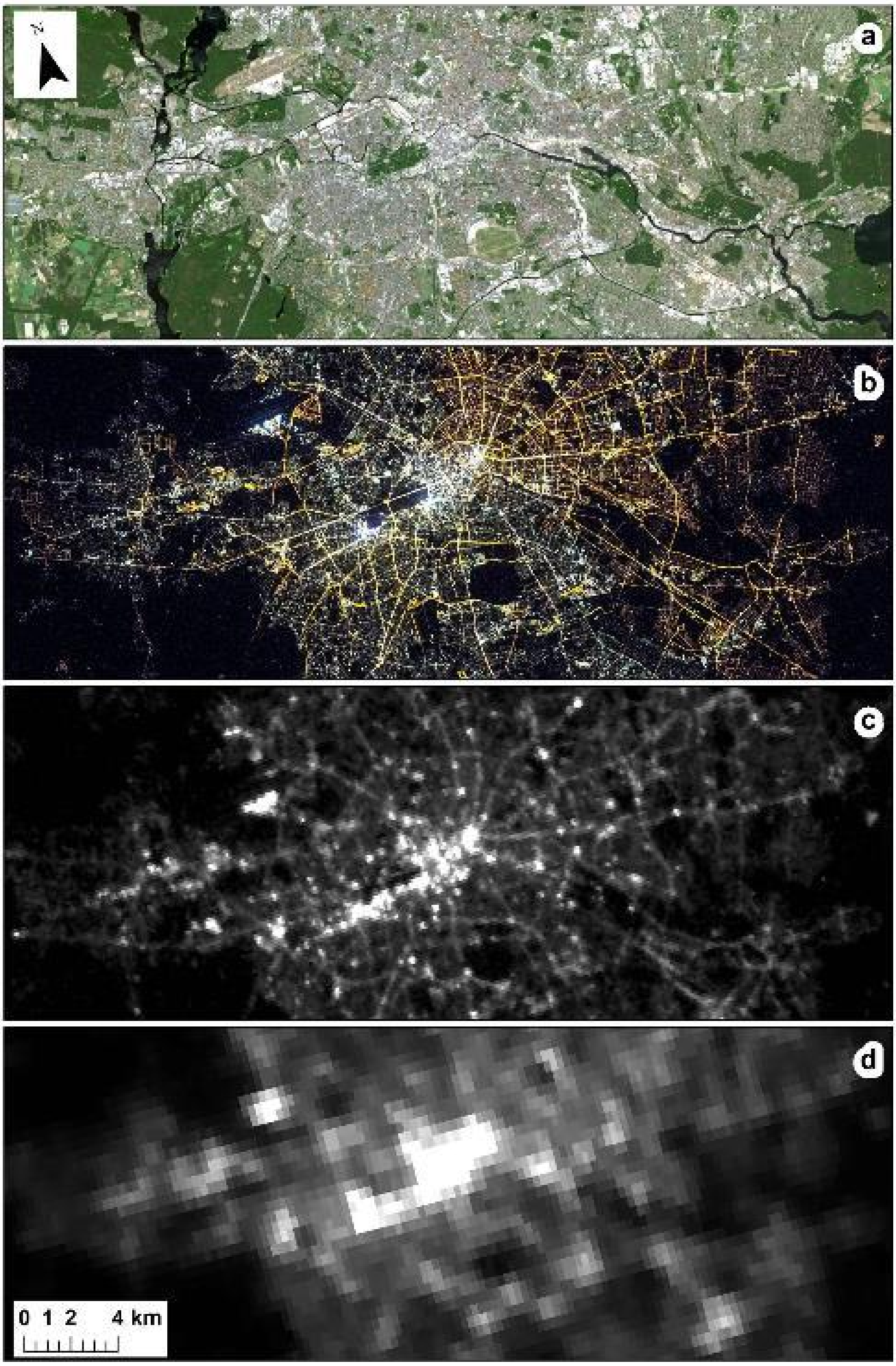

Figure 14: Berlin at day and night: (a) Landsat 8 OLI, April 2017, true color composite; (b) Astronaut photography from the International Space Station, ISS047-E-29989, March 2016; (c) Luojia01 night-time image, August 25th, 2018; (d) VIIRS/DNB October 2016.

Citizen science: Cities at Night

Currently, the astronaut photographs from the ISS are the largest online multispectral archive of night-time images of the Earth (https://eol.jsc.nasa.gov), with a unique potential for light pollution studies and to track changes in lighting technologies. However, these images lack precise location and georeferencing, and in addition, all the images of the Earth at night are mixed with images of astronomical and meteorological images, making it difficult to identify night-time images from the ISS, as they are often not tagged adequately. A citizen science program called "Cities at Night" was therefore launched with its major aim to provide an improved catalogue of night-time images from the ISS (Sánchez de Miguel et al., 2014). The project has three steps, classification/tagging to find the cities images called "Dark skies", location of the cities called "Lost at Night" and georeferencing called "Night cities". Thanks to the collaboration of more than 20,000 volunteers, the project has been able to tag more than 190,000 nocturnal images of mid and high spatial resolution (resolution from 5 - 200 m). The project was also able to locate more than 3000 images of cities with at least one control point and 700 images of cities with enough control points to be georeferenced (Sánchez de Miguel 2015). A fourth app had been created as a gamified version of "Dark Skies" called "Night Knights" with all the unprocessed answers of the project available from the beginning, but also some products (a large processed tagged catalogue of images with low precise location and smaller sample precise located images) have been released and are available of the web page of the project (Sánchez de Miguel et. al. 2018a). The images located by the volunteers and the researchers have already been used on several papers concerning light pollution monitoring (Sánchez de Miguel. 2015), epidemiological studies (Garcia-Saenz et. al. 2018) and ecological studies (Pauwels et. al. 2018). Several groups have used the "Cities at Night" as training sample for computer vision proposes, including Minh Hieu (2016), Calegari et al. (2018) and Sadler (2018). Based on this catalogue it can be seen that ISS night-time photos are not representing all parts of the world, and are more common in the urban areas of North America, Europe, the Middle East, eastern China and Japan (Figure 15a).

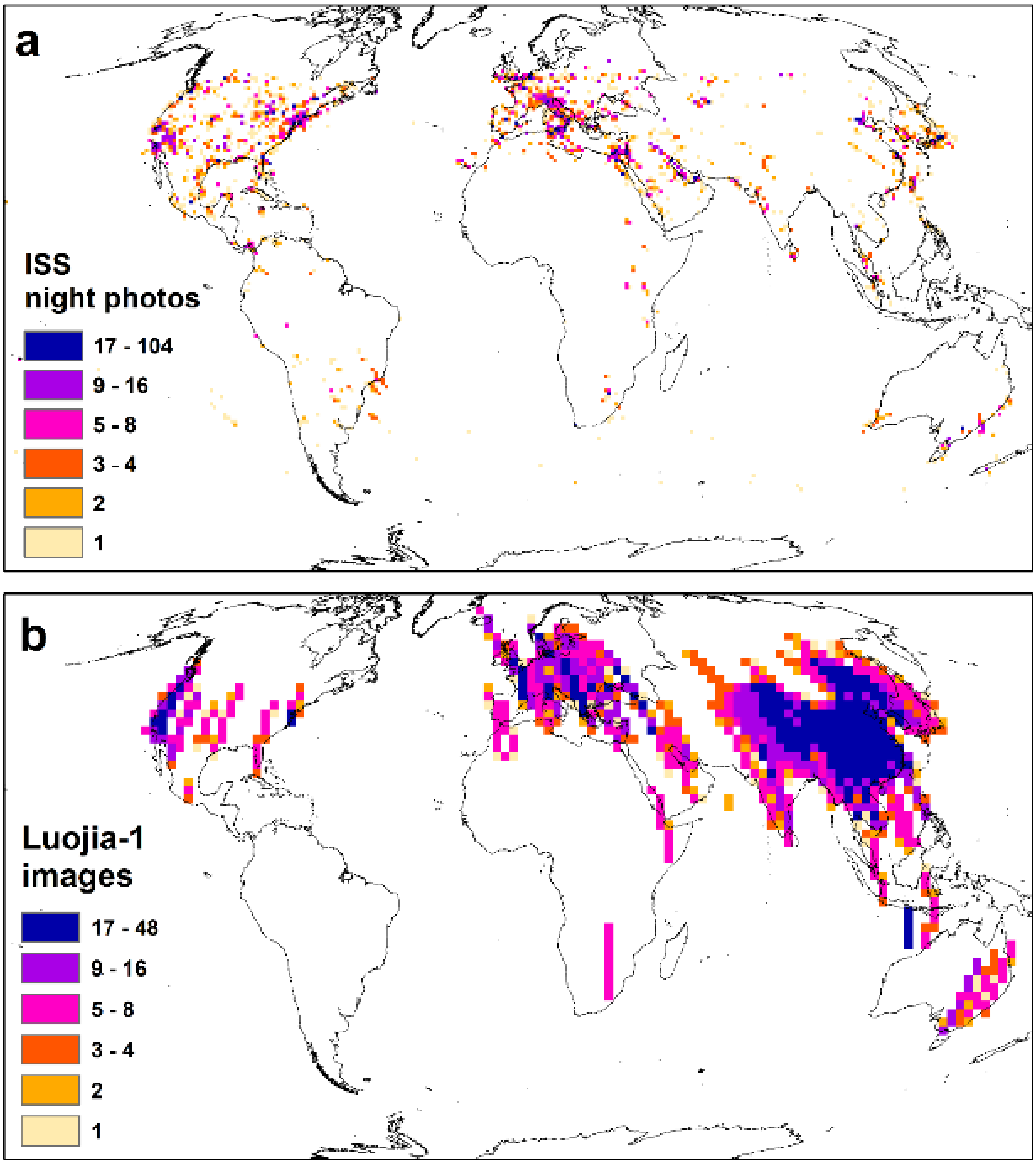

Figure 15: (a) The number of night-time ISS photos identified by the Cities at Night crowdsourcing project (http://citiesatnight.org/index.php/maps/), within 100x100 km grid cells;. (b) The number of all night-time Luojia-1 images acquired so far (n = 8675, May 2019), as received from Wuhan University, with 250x250 km grid cells.

Additional night-time sensors on the ISS

Another source of images of the Earth at night from the ISS is dedicated instrumentation on the ISS. For example, the experiment LRO (Lightning and Sprites Observation) (Farges et. al. 2016) was able to produce around at least 100 night-time images of urban areas (see Figure S1 in Farges et al., 2016); such imagery constituted the largest sample of medium spatial resolution (at about 400 m) images of Earth at night taken before the ISS026 mission. However, these images include sensitivity in the infrared regime, so they are difficult to compare to other images. Other instruments of similar science cases as ASIN recently arrived to the ISS might also be able to acquire some light pollution measurements. Since 2011, the Japanese Space Agency (JAXA) has been using a series of highly sensitive cameras on the ISS for the study of transient luminous event (TLEs) such as lightning of sprites, or other projects (Yair et. al. 2013). In the first videos, the main goal was the detection of TLEs, but light emissions from the Earth were also obvious. The second generation of these cameras was installed in 2016, and there is currently an ongoing collaboration between the University of Exeter and JAXA to provide radiometric calibration of this data.

2.2.4 VIIRS/DNB

The two MODIS sensors, onboard the Terra and Aqua satellites (launched in 1999 and 2002, respectively), with their 36 spectral bands, have led to the development of dozens of global products at various spatial and temporal resolutions, for monitoring vegetation, snow, fires, surface temperature etc. (Justice et al., 2002). Providing continuity to MODIS, the Visible Infrared Imaging Radiometer Suite (VIIRS) sensor onboard the Suomi NPP (Murphy et al., 2001) was launched in October 2011, and has been fitted with a specific panchromatic sensor designed for measuring night time lights – the Day and Night Band (DNB) (Miller et al., 2012, 2013). The VIIRS/DNB presents a significant improvement over the DMSP/OLS sensor, in data availability (with daily images provided for free), in its higher spatial resolution (750 m, instead of about 3 km for the DMSP), in providing radiometrically calibrated data which is sensitive to lower light levels and does not saturate in urban areas, and in the reduced overglow (Elvidge et al., 2013a, 2017; Figure 12). Therefore, global nighttime lights product generation has switched over from DMSP to VIIRS data in 2012, with the last annual products of DMSP produced for the year 2013 (Elvidge et al., 2017). The first products made available based on VIIRS/DNB data provided global monthly composites of night lights, starting in April 2012 (available at https://eogdata.mines.edu/download_dnb_composites.html), which have already allowed to advance our understanding on various topics, such as seasonal changes in night-time brightness (Levin, 2017), and detecting the negative impacts of military conflicts (Li et al., 2017). A novel product released in 2019, is NASA's Black Marble nighttime lights product suite (VNP46A1), at a spatial resolution of 500 m (Román et al., 2018). This product provides cloud-free, atmospheric-, terrain-, vegetation-, snow-, lunar-, and stray light-corrected radiances for estimating daily nighttime lights (NTL) (Román et al., 2018), thus enabling fine tracking of conflict affected displaced populations, damages to the electricity grid following disasters, and identification of events when and where people congregate (Román and Stokes, 2015).

2.2.5 Commercial satellites and cubesats

A new phase in space ushered in 1999 with the launch of Ikonos – the world's first high spatial resolution commercial satellite, and the first to offer a 1 m panchromatic band from space (Belward and Skøien, 2015). Since then additional companies have joined in, and at present the state of the art Earth observation commercial satellites are Digital Globe's WorldView 3 and 4 (launched in 2014 and 2016, respectively), offering a panchromatic band of 31 cm, and 28 additional spectral bands at various spatial resolutions of 1.24 m, 3.7 m and 30 m. The first commercial satellite with high spatial resolution night-time capabilities (at 0.7 m), was the Israeli EROS-B satellite, which was launched in 2006, but only started offering night-time acquisition publicly in 2013 (Levin et al., 2014). The first commercial satellite to offer multispectral (red, green and blue) night-time lights images (at 0.92 m) was launched in 2017: the Chinese JL1-3B (Jilin-1) satellite (Zheng et al., 2018). Such high spatial resolution satellites enable to study urban land use in finer details (as in Katz and Levin, 2016) and possibly to start and classify lighting sources.

The current revolution in space borne remote sensing is that of using small satellite missions (Sandau, 2010). The first company offering global daily multispectral high spatial resolution (3 m) coverage of the entire Earth is Planet Labs, with its constellation of about 150 nano satellites (Strauss, 2017). In coming years, researchers may benefit from similar cubesats offering night-time capabilities (such as NITEsat, presented in Walczak et al., 2017). Various cubesats have been launched in recent years, such as the CUbesat MULtispectral Observing System (CUMULOS), and the multispectral AeroCube, demonstrating the capabilities these new sensors provide for night time imaging (Pack and Hardy, 2016; Pack et al., 2017, 2018, 2019). An example of a recently launched cubesat which publicly offers global images of many regions on Earth at night is LJ1-01 (Luojia-1). This satellite, Luojia-1, was built by Wuhan University and was launched in June 2018, providing night-time images at 130 m (Figure 14; Jiang et al., 2018; Li et al., 2018b, 2019; images can be downloaded freely from http://59.175.109.173:8888/app/login_en.html), with each image covering about 250×250 km. So far, the acquired Luojia-1 images (n = 8675, as of May 2019) provide a complete and frequent coverage of China, as well as some additional areas such as south-east Asia and Europe. Recent studies have shown that Luojia-1 images are capable to accurately map urban extent and to monitor the construction of infrastructure at a moderate spatial resolution (Li et al., 2018b, 2019). Additional night-time sensors will also become available in coming years, such as TEMPO, a geostationary satellite which will offer two images per night over North America (Zoogman et al., 2017).

2.3 Airborne remote sensing of night lights

Topographic mapping using daytime aerial photos started back in World War I (Collier, 1994). The first aerial night-time photos we are aware of were taken during World War II, showing anti-aircraft searchlights, bombs exploding and incendiary fires (Figure 16). In addition to space based observations, remote observation of night lights can be accomplished from aircraft, drone, and balloon-based platforms. However, proper imaging of city lights from aerial platforms began much later. Such platforms allow higher spatial resolutions, and do not require the intensive testing for use in space. While there were some efforts to map urban night-time lights at fine spatial resolutions using airborne sensors such as the hyperspectral AVIRIS (over Las Vegas; Kruse and Elvidge, 2011), a panchromatic camera (over Berlin, at 1 m; Kuechly et al., 2012), or using a multispectral camera (at 10 cm over Birmingham or 1 m over Ottawa; Hale et al., 2013, Xu et al. 2018), dedicated aerial campaigns cannot provide continuous global monitoring of urban areas. Another flight over Berlin with a multispectral camera was performed in 2014, but the radiometric calibration of the data is not yet complete (Kyba et. al. 2015a, Sánchez de Miguel 2015). Nighttime imagery from aircraft has been frequently taken, but less frequently published. For example, flights over London (Royé 2018), Amsterdam, Friesland, and Deventer (http://nachtscan.nl/) have produced night imagery without leading to research publications. Aerial data from the state of Upper Austria is available online (https://doris.ooe.gv.at/themen/umwelt/lichtverschmutzung.aspx), but a report about the flight is available only in German (Ruhtz et al. 2015). In some cases, night light images have been acquired chiefly for artistic purposes (Laforet and Pettit 2015), in still others, there is not sufficient information to allow radiometric calibration.

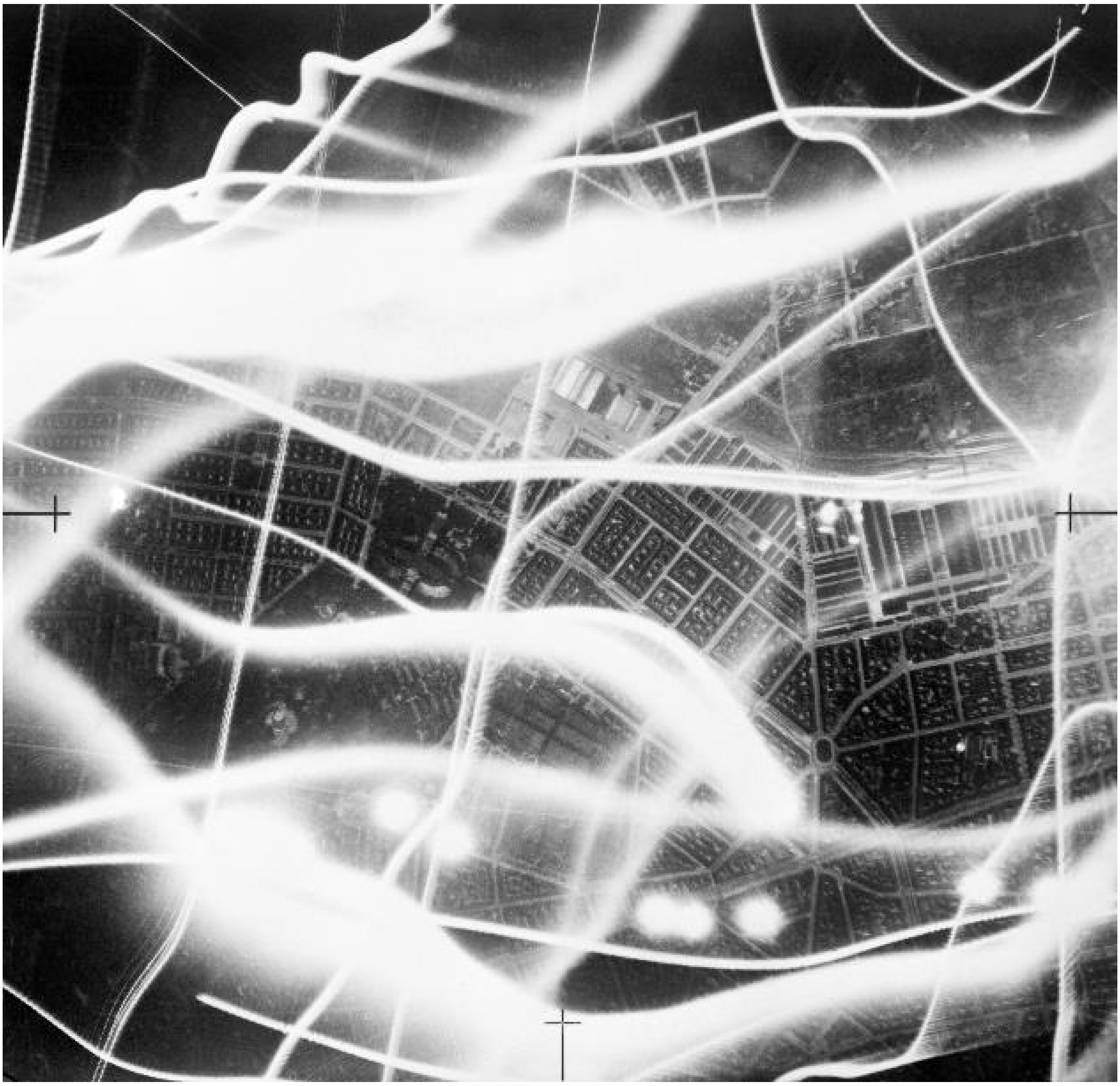

Figure 16: A vertical aerial photograph taken during a raid on Berlin on the night of 2-3 September 1941. The broad wavy lines are the tracks of German searchlights and anti-aircraft fire. Also illuminated by the flash-bomb in the lower half of the photograph are the Friedrichshain gardens and sports stadium, St Georgs Kirchhof and Balten Platz.

Few hyperspectral flights have been taken at night-time, perhaps because the instrumentation is much more complex. However, there have been a few cases, for example over Los Angeles (Stark et. al. 2011) and Las Vegas (Metcalf 2012), the ESA-Desirex and CM flights over Madrid performed by the Instituto Nacional de Técnica Aerospacial in 2008 (Moreno Burgos et al. 2010, Sorbino et. al. 2009, Sánchez de Miguel 2015), and the flights over Tarragona-Reus-La Bisbal de Falset (Cataluña, Spain) in 2009 (Tardá 2011). The main limitation of these datasets is the low signal to noise that hyperspectral instruments produce in some areas of the city. Although the spatial resolution is limited compared to photography, it can reach up to 5 meters. The most promising aspect of hyperspectral flights is the potential to unambiguously identify the light source technology. This has been demonstrated, for example, by Metcalf (2012).

Some experimental projects have made observations using drones (Sánchez de Miguel 2015, Fiorentin et. al. 2018, Regean 2018), and new studies are starting to explore the potential of acquiring data on night time lights from drones, given the flexibility in deploying them at different times during the night, the ability to acquire multi-angular images (Kong et al., 2019), and their potential for providing some near-sensing validation to space borne measurements. To some extent, the limited use of drones for remote sensing of night lights may be due to regulations restricting the use of drones at night over urban areas. However, the potential of drones is clearly seen by their use in the film industry, for example in TV productions like "España a ras de cielo" (RTVE 2013; http://www.rtve.es/alacarta/videos/espana-a-ras-de-cielo/espana-ras-cielo-espana-noche/4692661/) and "Bron/Broen" (SVT 2011). Balloons offer a more flexible platform for night imagery, as the regulations are not as strict as for drones. Pioneering experiments were performed by the Daedalus team (Ocaña et. al. 2016), where they combined detection of meteors with observation of night light emissions. These tests were mainly performed as technological demonstrations. The Far Horizons Project of the Adler planetarium of Chicago has also made several balloon flights. The purpose of these was to test the camera of a cubesat that will be launched in the future to monitor the conversion of street lamps in Chicago from sodium vapor lamps to white LEDs (Walczak et. al. 2017).

2.4 Ground based measurements of night sky brightness

A major gap in the remote sensing of night lights, stretching back to the time that DMSP/OLS data first became available, has been the lack of field data to "ground truth" the observations. Most optical remote sensing is mainly obtained done during the day with very different illumination conditions, as the only light source is the Sun, and atmospheric corrections are performed to derive the surface reflectance of objects, which can be ground truthed using field or lab measurements using a spectrometer (Vermote et al., 1997). At night-time, we are not interested in surface reflectance but in the emission of artificial lights; however, there are many relevant light sources in the visible band that can be equally important under some conditions such as city lights, gas flares, volcanos, lightning, moonlight, starlights or airglow. In addition, the dynamic range of the phenomena observed goes from 0.01 nW/cm^2/sr to more than 1000 nW/cm^2/sr (for sensors with higher spatial resolutions sensors than VIIRS/DNB, the radiance from upward directed sources will be far larger). The factors that make observing night lights challenging (see Section 4) also complicate acquiring ground reference data. For example, changing lights and changing atmospheric factors such as aerosols and water vapor mean that even aerial data acquired several hours before or after a satellite overpass cannot be directly compared. One indirect solution to the problem has been to compare ground based night sky brightness measurements to either the light observed from space directly, or else to models of diffuse sky brightness based on night lights data.

The brightening of the night sky by artificial light emissions is referred to as "skyglow", and is one of the most familiar forms of light pollution (Rosebrugh 1935, Riegel 1973, Kyba & Hölker 2013, Aubé 2015). Generally speaking, the artificially illuminated clear sky is brightest in the direction of nearby light sources, and darkest either at zenith or slightly displaced from zenith in the direction of undeveloped areas (Figure 17). The main source of skyglow is light emitted towards the horizon, because the path length to space is longest in this direction, greatly raising the scattering probability (Falchi et al. 2011). It is important to note that remote sensing of night lights is usually done towards nadir, so these emissions are not generally imaged during night light observations (however see Kyba et al. 2013b). Observations of night sky brightness therefore complement remote sensing of night lights in two ways: first, they can be used as a ground truth, and second, they provide indirect information about light emissions at angles that are not directly imaged from space.

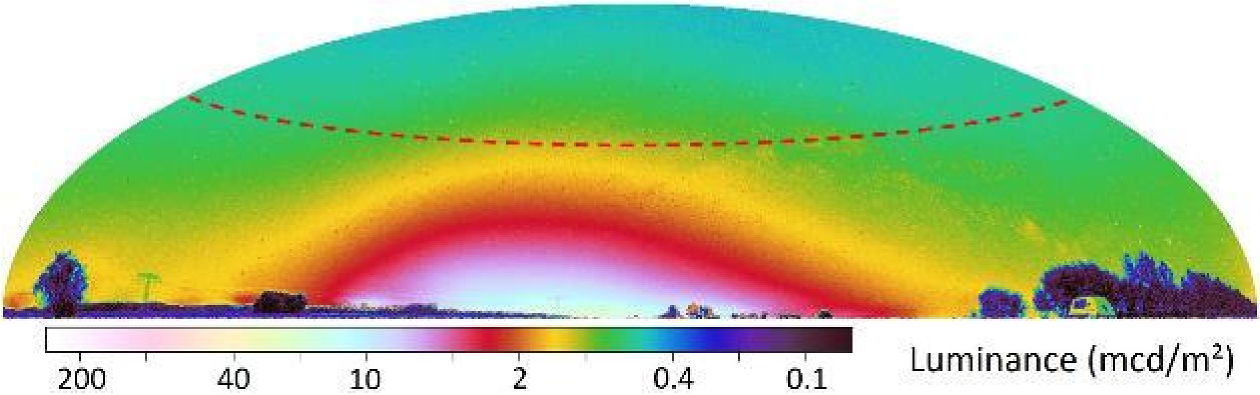

Figure 17: All-sky luminance map based on a photograph taken 15 kilometers outside of Berlin's city limits (30 km from the city center). Photograph and image processing by Andreas Jechow. The dashed line shows 40º from zenith (equivalently 50º elevation). A natural starlit sky has a luminance near 0.2-0.3 mcd/m^2 (Hanel et al 2018).

The influence of cloud cover on the surface light environment is important for understanding the ecological impacts of skyglow (Rich & Longcore 2006, Kyba et al. 2011, Kyba & Hölker 2013). In areas with little or no artificial lighting, clouds darken the night sky, while in areas with artificial lighting they make it considerably brighter. Some locations can experience both at once, in different viewing directions (Figure 18, Jechow et al. 2018a). Atmospheric scattering is biased towards blue light on clear nights (Kocifaj et al., 2019), but clouds scatter at all wavelengths. For this reason, the artificially illuminated clear night sky is far bluer than the overcast night sky, or in other words the "amplification" of light caused by clouds is far stronger in the red (Kyba et al. 2012, Aubé et al. 2016). At the moment, understanding of the light environment on overcast and partly cloudy nights remains poor (Jechow et al. 2018a). While local models exist (e.g. Solano Lamphar & Kocifaj 2016), global models of skyglow on overcast nights are not available, relatively few observations of cloudy sky radiance have been published, and local models of skyglow on overcast nights have not been validated with experimental data.

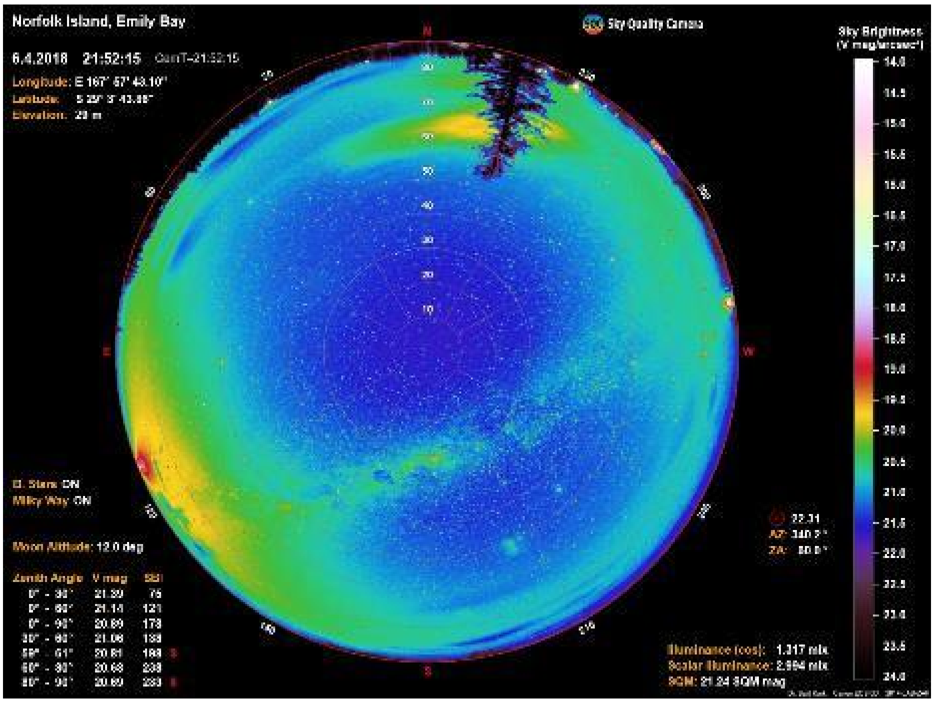

Figure 18: Night-time hemispheric photo at Emily Bay, Norfolk Island, Australia (April 6th, 2018, 21:52 local time). The upper image shows the raw image, while the bottom image presents sky brightness as calculated by the Sky Quality Camera software. The bright light at the east (azimuth 112, left side of the image) is the moon rising over the horizon. Notice the difference between bright clouds above artificial light sources, and the dark clouds above dark areas. Photo taken by Noam Levin.

2.4.1 Current status of ground based observations of the artificially illuminated night sky

Hänel et al. (2018) recently reviewed the commonly used techniques for observing the night sky brightness and skyglow, so only a brief summary is provided here. There are three basic techniques: point observations with broadband radiometers (most common), multispectral all-sky photographic observations, and point observations with spectrometers (most rare). Of the three techniques, Hänel et al. (2018) concluded that all sky imaging techniques “provide the best relation between ease-of-use and wealth of obtainable information on the night sky” (see e.g. Jechow et al. 2017a,b, 2019). However, Hänel et al. noted that a combination of the different techniques is ideal, as point observations can be used for long-term tracking, while being occasionally supplemented with all-sky photography. Note that both point observations taken in multiple directions (Zamorano et. al 2013) and image mosaicking (Duriscoe et al. 2007) can also be used to acquire information about the full sky dome.

In the past, night sky brightness observations were mainly performed by professional observatories and institutionally affiliated scientists (e.g. Walker 1970, Zhang et al. 2015a). The recently introduction of low-cost night light radiometers, starting with the Sky Quality Meter (SQM), has greatly expanded the number of surveyed sites, and enabled the active participation of citizen scientists. The SQM instrument enables monitoring night-time brightness in a rapid fashion, either along transects while walking, biking (Katz and Levin, 2016) or attached to a car (Xu et al., 2018), or temporally, allowing to monitor temporal changes in night sky brightness (Pun et al., 2014; den Outer et al., 2015). In addition to instrumental observations, citizen scientists are able to make visual observations of night sky brightness by examining stellar visibility. The most widespread of these projects is “Globe at Night” (Walker et al. 2008), which has been running since 2006. While visual observations have lower precision than instrumental observations (Kyba et al. 2013a), they have the advantage of correctly accounting for spectral changes in night sky brightness due to changing lighting technology (Sánchez de Miguel et al. 2017, Kyba et al. 2018a). Other instruments and methodologies such as the TESS-W photometers (which is growing to provide a global monitoring network, with freely available data via http://tess.stars4all.eu/; Zamorano at al., 2019), the Sky Quality Camera software, and the Loss of the Night app are further discussed by Hänel et al. (2018) and by Jechow et al. (2019b). The Sky Quality Camera software allows one to use a DSLR camera (which has been properly calibrated) with a fish-eye lens, to measure hemispherical night-time brightness (Jechow et al. 2018b, 2019), to estimate cloud cover, and to create night sky brightness images with or without bright stars and the Milky Way (Figure 18).

2.4.2 Direct comparison of night sky brightness observations to light observed from space

In many space-based night light images, it is possible to see a fuzzy haze that surrounds cities, extending into areas which are unlikely to contain lights (such as forests or offshore regions). This diffuse light in DMSP/OLS and VIIRS/DNB images has often been referred to as "blooming" (e.g. Amaral et al. 2005, Ou et al. 2015), likely due to its visual similarity to the phenomena of CCD blooming in digital photography. However, a recent study suggests that rather than being an instrumental error, it is likely that the instruments are actually correctly observing light scattered by the atmosphere, or in some cases light scattered by the atmosphere and then reflected from the ground.

When Kyba et al. (2013a) found that citizen science observations of skyglow were highly correlated with DMSP observations, they hypothesized that this correlation arises because the point spread function of the DMSP acts as a de facto approximate atmospheric radiative transfer model. A similar correlation between DMSP-OLS and night sky brightness was verified on a smaller spatial scale by Zamorano et. al. (2016). However, using an intensive night sky brightness survey around the city of Madrid, Sánchez de Miguel (2015) demonstrated a strong correlation between diffuse light in space-based images from instruments with different intrinsic spatial resolutions. By comparing SQM ground based measurements using SQMs, with VIIRS/DNB imagery and ISS astronaut photos, Sánchez de Miguel et al. (2019a) have recently demonstrated that the diffuse light observed around cities is not an instrumental error, but is actually a direct observation of the component of urban skyglow that scatters upward, i.e., artificial sky brightness. Sánchez de Miguel et al. (2019a) also mention additional components of diffuse light in night-time imagery which remain to be quantified, such as albedo, natural airglow, sea fog, and real blooming.

2.4.3 Comparison of night sky brightness observations to radiative transfer models

Observations of night sky brightness can in principle be used to extract information about light emissions that are not available through direct observations. For example, there is considerable debate about what fraction of light from cities is emitted towards the horizon (Luginbuhl et al. 2009), which is difficult or impossible to directly observe from space (Kyba et al. 2013b), but may be inferred from night sky brightness data (Kocifaj 2017). Falchi et al. (2016) produced models of night sky brightness under three different assumptions of the upward angular distribution function: Lambertian, emissions peaking at 30º, and strong emissions towards the horizon. Because light is additive, it is possible to fit for the linear combination of models that most closely matches the data. In the case of Falchi et al. (2016), the data were SQM observations at zenith from a number of academically affiliated and citizen scientists, notably including Ribas (2016), Zamorano et al. (2016), and Globe at Night. A similar procedure could in principle be used with all-sky camera data.

The conditions under which skyglow models are accurate remains an open question. The global model of Falchi et al. (2016) does not consider shadowing by mountains, for example, so it is likely that errors are larger in mountainous regions. Ges et al. (2018) compared the predictions of Falchi et al. (2016) to SQM observations made along a transect from Barcelona out to sea. They found extremely good agreement with the model under atmospheric conditions similar to those upon which the model is based, but disagreement of up to 50% on a night with better optical conditions. In particular, they found that on a night with low aerosol load, the sky was darker than predicted near Barcelona, while far out to sea the sky was brighter than predicted.

There is a need for further comparison of models to observations, and direct comparisons of models to each other (e.g. Aubé & Kocifaj 2012). As skyglow models are used to make lighting policy recommendations (e.g. Aubé et al. 2018), it is important to verify that their predictions are correct. Bará (2017) recently examined how dense observations should be in order to provide reliable data on zenith night sky brightness. He concluded that observations on a 1 km grid provide sufficient resolution for interpolation between the points to accurately represent night sky brightness. A major challenge for comparing models to observations occurs in areas where natural light sources such as airglow and stars are brighter than the artificial component of night sky brightness (Bará et al. 2015). Finally, the shifting spectrum of skyglow due to the change to LED technology poses a challenge for both observations and modeling, and is discussed in detail in section 4.5.

3. Applications of remote sensing of night lights

In this section, we aim to provide a brief overview of some of the most common applications of night lights data made using the existing and historical sensors. The aim is to demonstrate the breadth of existing study, and to refer the reader to historical, key, and review papers about each topic. Readers should understand that for each topic, a considerably larger base of scholarship exists, and that not all applications of night lights are reviewed here. For example, we do not review studies on whether lighting benefits public safety (and/or the perception of safety), and on whether there is correspondence between higher night-time brightness, and decreased crime rates and car accidents (Painter, 1996; Marchant, 2004, 2017; Peña-García et al., 2015; Steinbach et al. 2015). Where relevant, we highlight some of the main challenges in the applications, and how these may be addressed with future sensors. These challenges and opportunities are then addressed in more detail in the following section.

3.1 Mapping urbanization processes

Our world has been rapidly urbanizing in recent decades. As of 2014, more than 54% of the global population live in urban areas, and by 2100, 70%–90% of the world's population, which is projected to increase by another three billion, will live in urban regions (United Nations, 2014). Due to broad impacts of the concentrated human activities and associated built environment, cities are now a major factor shaping the Earth system and are considered agents of global change (Mills, 2010). Cities worldwide now occupy only about 2% of the global land surface (Akbari, 2009), but produce more than 90% of the world gross domestic production (GDP) (Gutman, 2007), consuming more than 70% of the available energy (Nakićenović, 2012), and generating more than 71% of anthropogenic greenhouse gas emissions (Hoornweg et al., 2011). There is therefore an urgent need for timely and reliable information on the extent of urban areas to support sustainable urban development and management (Ban et al., 2015).

Due to the fact that cities are brightly lit during the night, urban areas can be easily identified in nighttime light remote sensing data. Indeed, one of the first uses of NTL data from DMSP/OLS was to delineate urban extents, and DMSP/OLS data is one of the earliest datasets available for mapping our urbanizing planet (Zhu et al., 2019). The panchromatic nature of DMSP/OLS NTL data first encouraged researchers to find an optimal threshold to separate urban areas from their backgrounds (e.g. Imhoff et al. 1997; Small et al. 2005). However, it turned out that it is not straightforward to find a single optimal threshold that can accurately delineate both large cities and small cities simultaneously (Zhou et al., 2015). While a larger threshold might be good for delineating large cities but tends to overlook small towns, a smaller threshold can bring back small towns but often leads to overestimating the extents of large cities. Such a situation becomes even more complicated due to the overglow effect in DMSP/OLS, and due to the use of different types of lighting together with different street lighting standards in different countries (Small 2005). Optimal thresholds vary across space and a scheme of dynamic thresholds is required for large-scale and temporal dynamic urban extent mapping (Zhou et al. 2014; Elvidge et al. 1997b; Imhoff et al. 1997; Small, Pozzi, and Elvidge 2005; Elvidge et al. 2009b; Cao et al. 2009).

Due to the saturation of DMSP/OLS within urban areas, these images lack textural information, making it very hard to map urban patterns within cities. However, with the improved radiometric performance of VIIRS/DNB, new methods are being developed, demonstrating for example the ability to map local urban centers (Chen et al., 2017). The newer VIIRS/DNB nighttime light data is also better than DMSP/OLS data in mapping urban extents (Shi, et al., 2014), and attention has been given to determine dynamic thresholds for mapping using ancillary information (He et al. 2006; Cao et al. 2009; Zhou et al. 2014; Liu et al. 2015). Recently, researchers have started to look into the potential of integrating DMSP/OLS with the Moderate Resolution Imaging Spectroradiometer (MODIS) (Guo et al., 2015; Lu and Weng, 2002; Zhang et al., 2013, Ouyang et al., 2019) or Landsat at a finer spatial resolution (Zhang et al., 2015b; Goldblatt et al., 2018), to improve the accuracy and performance of regional and global urban extent mapping, developing spectral indices such as the vegetation adjusted NTL urban index (VANUI) (Zhang et al., 2013).

The long historical archive of DMSP/OLS NTL data not only allows static urban extent mapping but also has high potential in characterizing urban extent dynamics at regional and global scales (Small and Elvidge, 2013). For example, Yi et al. (2014) utilized multitemporal DMSP/OLS NTL annual composites to study urbanization dynamics in Northeast China, Liu et al. (2012) and Ma et al. (2012, 2015) explored urbanization in all of China, Álvarez-Berríos et al. (2013) examined South America, Pandey et al. (2013) examined India, Zhang et al. (2014) examined the conterminous United States, and Castrence et al. (2014) in Hanoi, Vietnam, and Zhang and Seto (2011) did this for the entire globe. In a recent paper, Zhou et al. (2018) developed a new method to generate temporally and spatially consistent global urban mapping, finding that global urban area has increased from 0.23% in 1992 to 0.53% in 2013.

3.2 Estimating GDP and mapping poverty

The connection between artificial lighting and urban areas described above has motivated many researchers to examine the possibility of using night lights data as an indicator of economic activity. Night-time light has been found to be positively correlated with Gross Domestic Product (GDP) or Gross Regional Product (GRP) at different spatial scales (Elvidge et al. 1997; Forbes 2013; Li et al. 2013a). However, there are also considerable differences in per capita light emissions observed for countries with similar GDP (e.g. Henderson et al. 2012, Kyba et al. 2017; Levin and Zhang, 2017; Figure 19). The strength of incorporating night lights data into economic analyses is therefore in: (1) estimating GDP at finer levels of spatial resolution than are available through official statistics, (2) estimating GDP change (as opposed to levels) at high temporal frequency (e.g., in Bennie et al., 2014; Figure 20), and (3) estimating GDP in areas with poor or no reporting (Henderson et al. 2012).

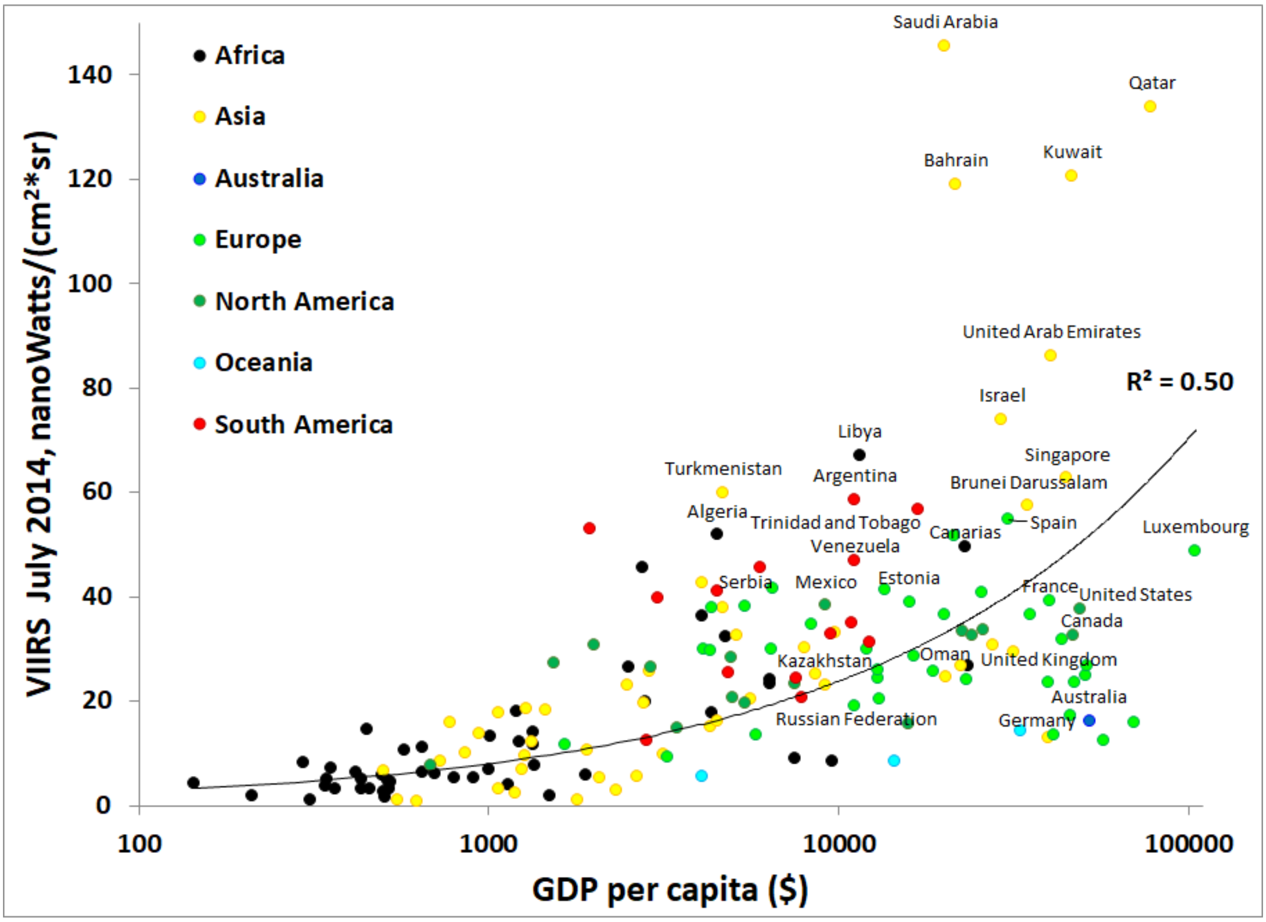

Figure 19: Mean VIIRS radiance values in July 2014 at the country level (averaging all cities within a country), as a function of national GDP per capita. Based on data from Levin and Zhang (2017). Note that GDP on its own is not enough to explain night-time brightness differences of urban areas between countries. Additional variables include albedo, whether countries have natural gas and oil resources, and lighting standards, among other factors.

An example of the first point above is disaggregating National GDP data to spatial grids. This was first carried out to produce 5 km resolution GDP map for 11 European Union countries and the United States (Doll et al. 2006), and it was further used, supported by ancillary data including a population density map (Landscan), to produce a global GDP map at 1 km resolution, showing that Singapore has the highest GDP density (Ghosh et al. 2010). Similarly, night-time lights can be used as a proxy of GDP for estimating wealth, allowing regional economic phenomenon such as inequality (Elvidge et al. 2012; Xu et al. 2015) and poverty to be mapped (Elvidge et al. 2009b; Wang et al. 2012; Yu et al. 2015; Jean et al., 2016). Henderson et al. (2016) showed that physical geography (such as climate, biomes, topography, etc.) has a strong influence on the spatial distribution of economic activity, however, that there are differences between developed and developing countries in the relative importance of agriculture and trade variables, to explain spatial variability in night-time lights.

An example of an application of the third point above is in correcting the statistical GDP or GDP growth rate data for developing countries. This is based on econometric models which regard the real GDP (or GDP growth rate) as a linear combination of statistical GDP (or GDP growth rate) and estimated GDP (or GDP growth rate) derived from night-time light images (Chen and Nordhaus 2011; Henderson et al. 2012; Henderson et al. 2011). Based on this framework, economists have concluded for example that China's real GDP growth rate is higher that the values from official statistics (Clark et al. 2017).

3.3 Monitoring disasters

Disasters can affect night light emissions through damage to and interruption of electric utility services. For example, tropical storms and hurricanes, heavy rains that cause flash or longer-term basin-wide flooding, damaging straight-line winds or tornadoes, widespread ice storms, fires, and earthquakes, frequently interrupt utility services for varying lengths of time. Outages can also occur from poorly maintained or damaged infrastructure, industrial accidents, or regional conflicts (see section 3.4). Disruptions can be on the order of hours for small, isolated events, to days, weeks, or even months, for particularly strong or long-lasting impacts such as those from major hurricanes (Román et al. 2018, 2019; Figure 20) or earthquakes (Kohiyama et al. 2004). For meteorological events, lingering cloud cover can impact the ability to reliably detect changes following natural disasters (Zhao et al., 2018). Therefore, monitoring of nighttime lights is particularly well-suited to assessment of impacts from major events over longer-time scales, or for non-meteorological events (e.g. failed infrastructure, earthquakes) where cloud cover may be less prevalent.

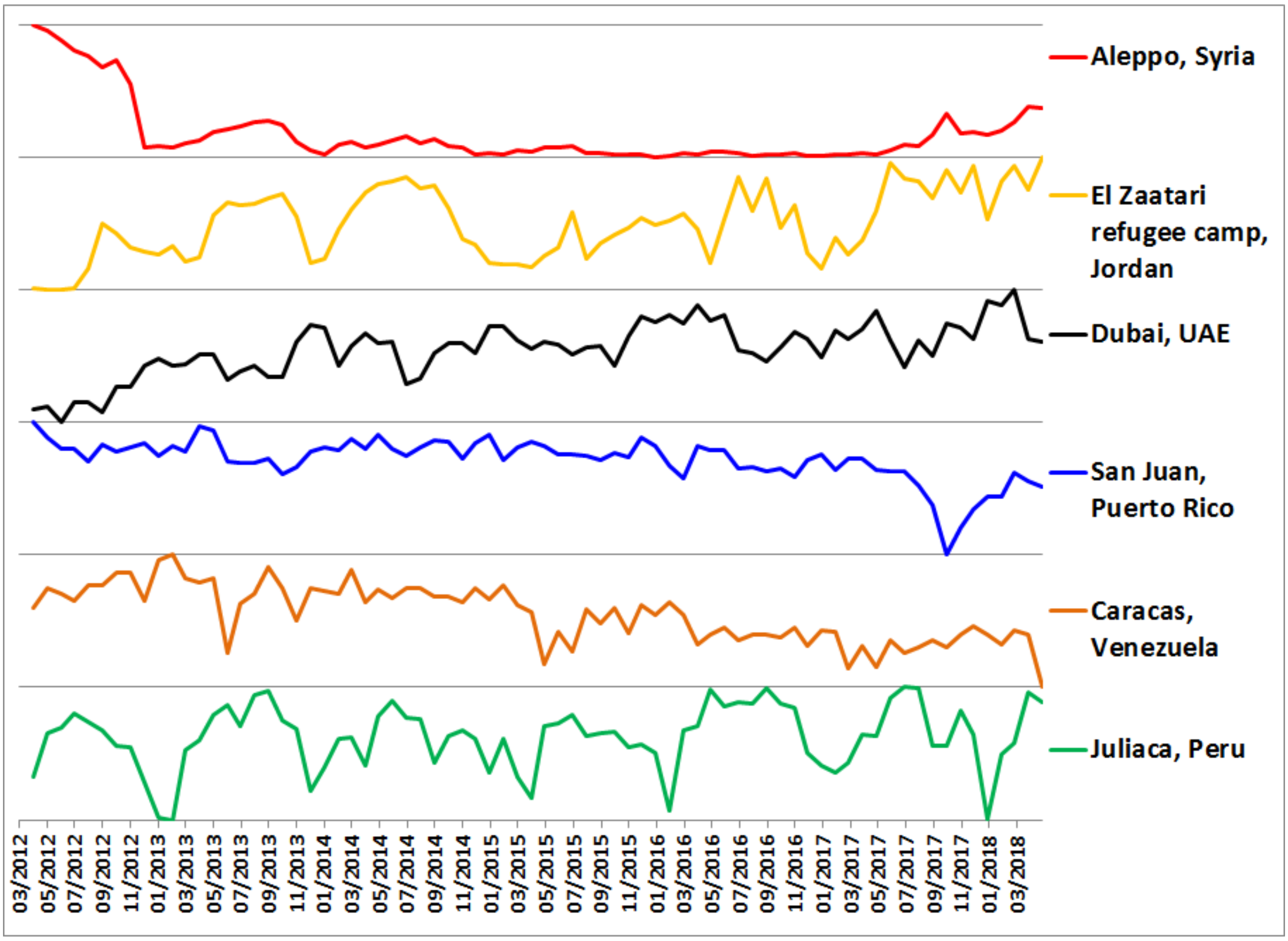

Figure 20: Temporal changes in monthly VIIRS night-time brightness, demonstrating various patterns (each of the sites was normalized between its own minimum and maximum values).

Aleppo, Syria: dramatic decrease in night-time lights due to the war in Syria.
El Zaatari refugee camp, Jordan: influx of refugees from Syria makes this refugee camp one of the largest cities in Jordan.
Dubai, UAE: A global city and a business hub in the Middle East, with a growing economy.
San Juan, Puerto Rico: Hurricane Maria (September 20th, 2017) led to power outages throughout Puerto Rico.
Caracas, Venezuela: In 2014 Venezuela entered an economic recession, with a decrease in its GDP, evident in a decrease of night lights in its capital city.
Juliaca, Peru: A seasonal pattern is evident in night-time lights, commonly attributed to seasonal changes in albedo related to vegetation and snow cover.

Gillespie et al. (2014) demonstrated the use of DMSP/OLS annual to monitor the damage and recovery of areas affected by the December 2004 earthquake and the tsunami which followed it, in Sumatra, Indonesia. Such applications have expanded with the advantages of VIIRS/DNB night-time imagery. VIIRS/DNB has been used to capture power outage and recovery from severe storms, for example. False color composites of pre- and post-event lights were used by Department of Defense and other partners in their response to Hurricane Sandy (Molthan et al. 2012). Cao et al. (2015) used comparisons of pre- and post-event emissions to identify loss and recovery of nighttime lights in Washington D.C. area from a derecho event (a wide-spread straight-line wind event), as well as following Hurricane Sandy, when Department of Energy utility reports were used as validation. Cole et al. (2017) combined nighttime light information, population data, and utility information to model likely future outages and affected populations, and documented outages and recovery following Hurricane Sandy in the northeastern states. Miller et al. (2018) used a long-term pre-event nighttime light composite and cloud-free scenes following Hurricane Matthew as a false color composite, in order to estimate outages. This work compared favorably to reported utility outages, and nighttime lights imagery also captured unique physical phenomena associated with the cyclone.

Zhao et al. (2018) investigated outages and recovery from earthquakes, major tropical cyclones, and floods with validation of outages against SAR-derived damage proxy estimates and flood mapping. They adopted the methodology of Cole et al. (2017) to derive a “percent of normal” condition as the ratio of a post-event scene to pre-event normal. For long-term outages in Puerto Rico following 2017’s Hurricane Maria, Zhao et al. found a strong correlation between percent of normal light (low values) and reported outages (R^2=0.94), though obtaining cloud-free pre-event and post-event scenes were difficult. Finer-scale observations of nighttime lights and change have been developed from the NASA Black Marble Nighttime Light (NTL) composite and ancillary data layers (Zhang et al. 2015c, Wang et al. 2018), using spatial downscaling to estimate a 30 m product for changes on neighborhood scales (Román et al. 2018; Figure 21). These and other analyses demonstrate the utility of night lights in specifically examining impacts to electrical infrastructure, as opposed to other damage that may be more readily assessed via daytime sensing (e.g. flooding, structural damage).

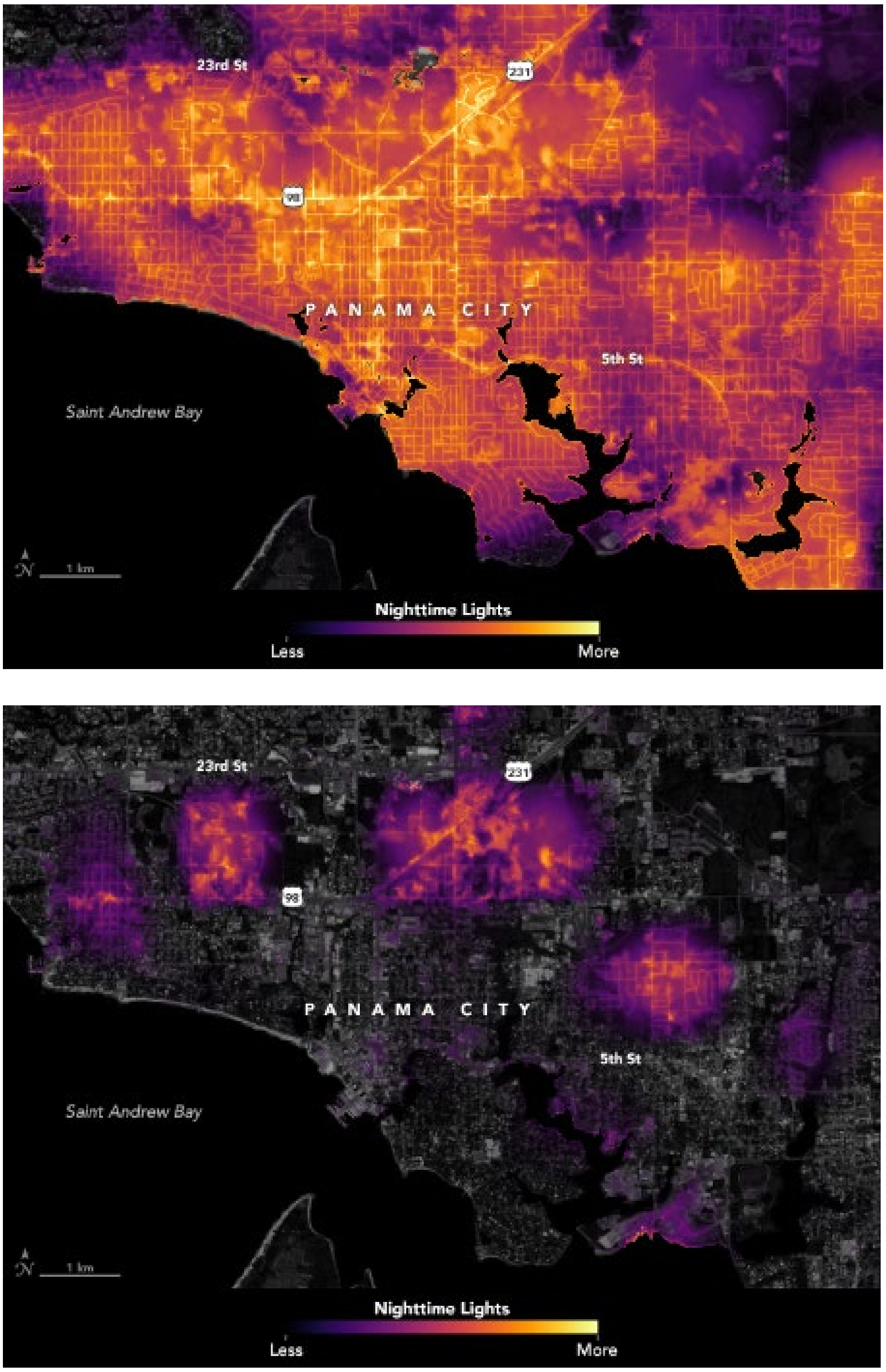

Figure 21: After making landfall as a category 4 storm on October 10, 2018, Hurricane Michael knocked out power for at least 2.5 million customers in the southeastern United States, according to the Edison Electric Institute. The images show where lights went out in Panama City, Florida, comparing the night lights before (top) and after (bottom) the hurricane (October 6th and 12th, 2018, respectively).

3.4 Monitoring armed conflicts

In addition to the environmental disasters discussed above, human-caused disasters also have strong impacts on night light emissions. Remote sensing of night lights therefore provides an opportunity to monitor conflicts, where data is often scarce and governmental reports may be biased (Witmer, 2015). High spatial resolution daytime images have been proved effective to achieve this purpose (American Association for the Advancement of Science 2013; Prins 2007), but building a link between conflicts and these remote sensing images sometimes requires human skills of image interpretation. Since there is a direct link between night-time lights and a number of socioeconomic parameters, dramatic decreases in night-time brightness may serve as an indicator for damage to infrastructure caused by armed conflicts. In addition to reductions in population size and Gross Domestic Product (GDP), decreases in light emissions also provide a warning that civilians are likely lacking a stable electricity supply, which is essential for both basic living and operation of hospitals.

A pioneering study in this topic examined the war effect in Chechnya and Georgia by using monthly DMSP/OLS composites (Witmer and O'Loughlin 2011), which were used to examine movement of refugees and burning oil fields caused by the wars A more comprehensive examination of global conflicts was undertaken by Li et al. (2013b) using time series of annual DMSP/OLS composites. These authors used 159 countries as research samples, and found that wars lead to a sharp reduction of night-time lights, that peace agreements are followed by restoration of night-time brightness levels, and that war-torn countries have larger fluctuations of night-time lights than peaceful countries.

Since that time, night-time light images have been employed to evaluate the violent conflicts in Syria (Li and Li 2014; Li et al. 2017; Figure 11a), Iraq (Li et al. 2018a; Li et al. 2015) and Yemen (Jiang et al. 2017) following the Arab Spring, showing that affected regions in these countries experienced dramatic reductions in light emissions after the conflict began (Figure 20). Examining all Arab countries following the onset of the Arab Spring, Levin et al. (2018) found that reductions in night-time brightness correlated with decreases in the number of tourists (using Flickr photos as indicator of visitation), with increases in asylum seeker numbers, and with increases in the numbers of deaths from conflicts. Levin et al. (2019) have also suggested that reductions of night-time lights may serve as an indicator of risk to UNESCO World Heritage Sites from armed conflicts. As is the case with environmental disasters, the development of NASA’s daily Black Marble product provides another step forward towards fine temporal monitoring of the effects of wars on internally displaced populations (Roman et al., 2018).

3.5 Holiday and ornamental lights, and political, historical, and cultural differences in lighting

While disasters are evident from a temporal reduction in light emissions, lighting associated with holidays can result in a temporary increase. The uniformities and variations between nighttime light signatures can provide new insights into how energy behaviors, motivated by social incentives and economic activity, vary across national and cultural boundaries (Figure 22). Temporal fluctuations in electricity demand may represent changes in individual and macro-scale energy behaviors, such as during major cultural events such as Christmas, New Year, and the Holy month of Ramadan. During the Christmas and New Year holidays in the USA, the patterns of total lighting electricity usage (units of Watt · hr) derived from nighttime radiance were shown to uniformly increase across US cities with diverse ethnicity and religious backgrounds (Román and Stokes, 2015). Román and Stokes suggest that this shows that in addition of being a religious holiday, Christmas and New Year are also celebrated as a civic holiday across the US through holiday lighting (Figure 23). Patterns of energy service demand observed through nightlight images during the Holy month of Ramadan can also indicate different religions as well as cultural observance practices. In the Middle East, cities with Muslim-majority population exhibit lighting peaks during and slightly after the 30 days of Ramadan compared to non-arab cities in Israel (Román and Stokes, 2015). Seasonal variations in nighttime lights have also been used to track patterns in ambient population (mainly tourists) in Greece (Stathakis and Baltas, 2018).

Lighting for cultural or celebratory purposes (such as light festivals; Giordano and Ong, 2017) may result in particularly bright emission signals compared to more functional lighting such as for streets and parking lots. For example, floodlighting of churches or other cultural objects often misses the facade, and can therefore be brightly visible on Suomi-NPP VIIRS DNB images (eg. Kyba et al. 2018c). Architectural lighting is often used to highlight significant buildings, and such lighting may only be on when special events are held or at certain times of the night (Meier 2018). This may present a challenge for night lights analyses, with the inconsistent temporal pattern contributing to the variability of night lights datasets (Coesfeld et al. 2018).

Administrative borders offer the possibility to observe clear contrasts between different countries or regions, an area where the high resolution color photographs from the ISS can be quite useful (Figure 22). The persistence of different lighting technologies in the former East and West Berlin and the extraordinary drop of light at the border between North and South Korea are well known examples. However, there are also large national differences between per capita light emissions in wealthy cities and countries (Kyba et. al 2015a, Sánchez de Miguel 2015; Levin and Zhang, 2017). The root causes behind these differences are in some cases not well understood (and may be related to different lighting standards between countries), and night lights data may therefore play a useful role in some investigations based on the social sciences.

Figure 22: Lighting differences between countries across borders, as seen from the ISS: China - North Korea - South Korea (ISS038-E-38280), US - Mexico (ISS030-E-213358), East and West Berlin (ISS035-E-17202).

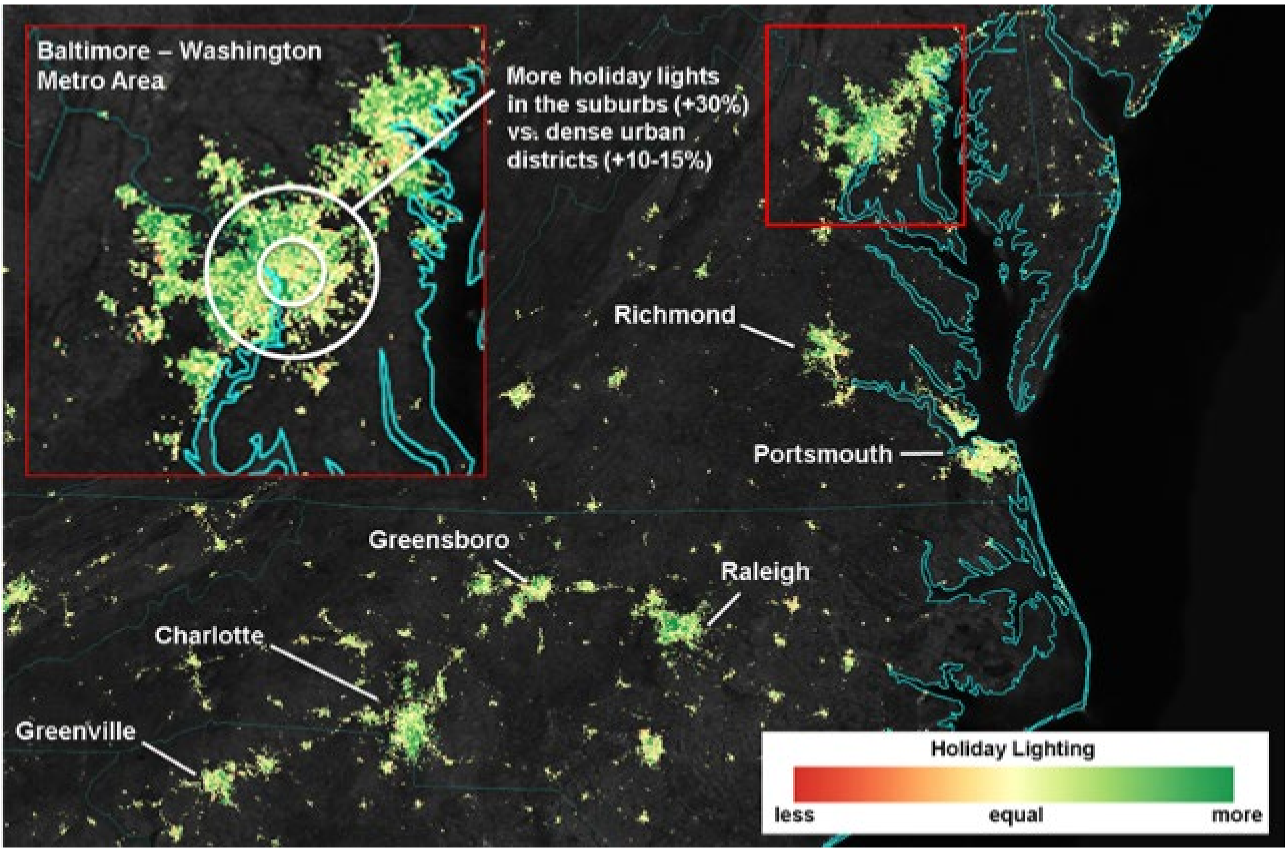

Figure 23: City lights shine brighter during the holidays in the United States when compared with the rest of the year, as shown using a new analysis of daily nighttime data from the VIIRS instrument onboard the NASA/NOAA Suomi NPP satellite (Roman and Stokes, 2015). Dark green pixels are areas where lights are 30 percent brighter, or more, during December. Because snow reflects so much light, only snow-free cities were analyzed. Holiday activity is shown to peak in the suburbs and peri-urban areas of major Southern US cities, where Christmas lights are prevalent. In contrast, most central urban districts, with compact dwelling types affording less space for light displays, experience a slight decrease or no change in energy service demand. The calculation is based on the relative change in lights between the Christmas holiday vs. the rest of the year. It is a simple ratio between the latter vs the former.

3.6 Astronomy

Astronomy is perhaps the oldest remote sensing discipline, with its goal to obtain information about objects at vast distances through observation of emitted, absorbed, scattered, or reflected light. Nearly all visible band astronomy is undertaken at night, because light scattered by sunlight in Earth's atmosphere outshines most celestial objects. The artificial light emitted by cities is similarly scattered by the atmosphere, and as a result one third of humans (including nearly 80% of North Americans) are no longer able to see the Milky Way from their homes (Falchi et al. 2016). This is an immense cultural loss (Gallaway, 2010). It also raises the cost of doing professional astronomy, as historically important and easily accessible sites such as Mount Wilson Observatory can no longer be used for research (Teare, 2000), and even remote sites are increasingly threatened by light pollution (Krisciunas et al. 2010, Aubé et al. 2018). Studies of night sky brightness and its changes are therefore important for amateur and professional astronomy.

Remote observation of upward light emissions is crucial for the study of artificial night sky brightness on large scales. These data can be used with radiative transfer models to predict night sky brightness on clear nights (Cinzano et al. 2001, Falchi et al. 2016). Both satellite imagery and the derived night sky brightness maps are used by the public to find locations for astronomical tourism (Collison et al. 2013, Hiscoks & Kyba 2017), and photometric indicators of visual night sky quality can be derived from ground based hemispherical photos (Duriscoe, 2016). The global spectral shift due to adoption of white LEDs is a major challenge for astronomy, both because the blue component of white light produces more skyglow (section 2.4), and because many current ground and space-based sensors are not sensitive to blue light (section 4.5, Figure 24). Ground based observations of night sky brightness are therefore crucial for calibrating skyglow models, and are necessary for long-term monitoring due to changes in lighting practice (Kyba, 2018a, Hyde et al. 2019). A related topic is studies using ground based instruments to measure the impacts of cloud cover on night sky brightness (eg. Kyba et al., 2011, 2012; Jechow et al., 2017b, 2019a), but in this case the aim is usually to better understand the ecological impacts of this form of global environmental change (see next section).

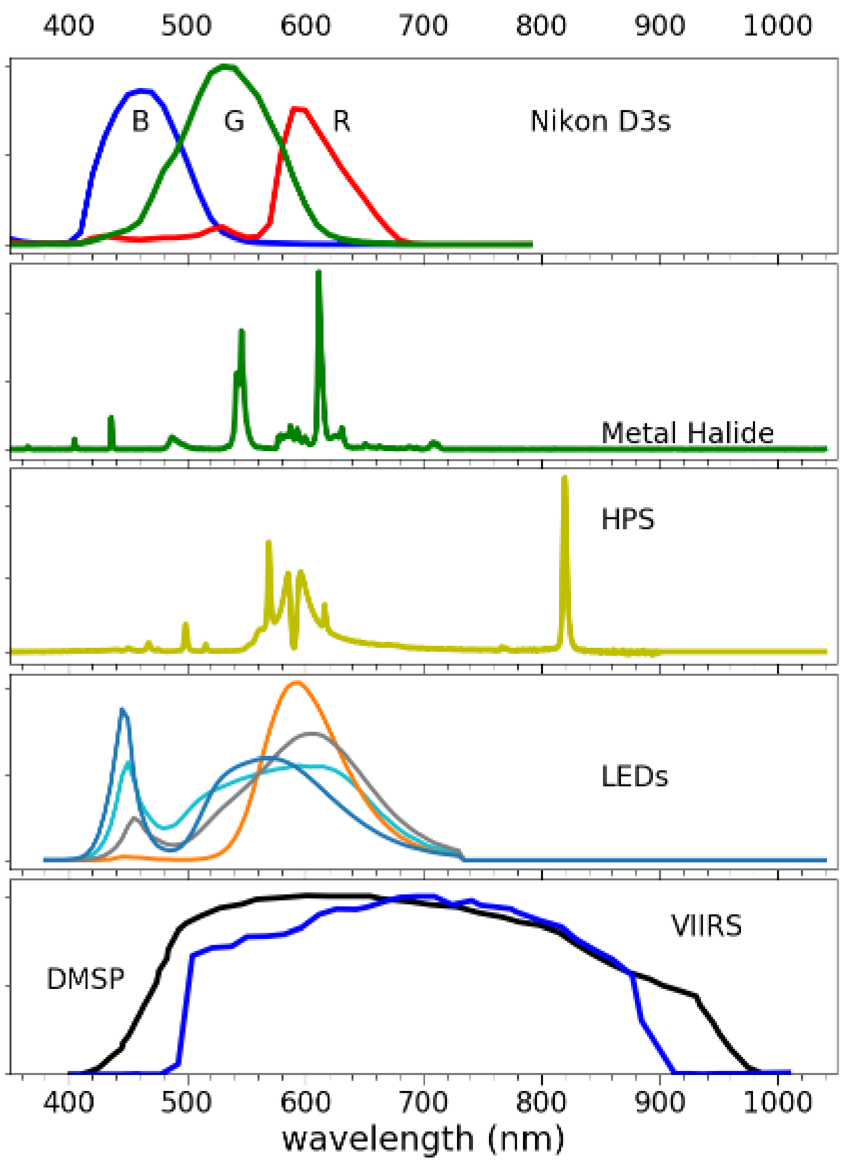

Figure 24: Spectral response of the most popular sensors and most popular spectra, from top to bottom. (a) the spectral response of the Nikon D3s Cameras used by the astronauts at the ISS; (b) a typical spectra of a Metal Halide lamp, popular on architectural lights; (c) a High pressure sodium light, popular until 2014 on streelighting; (d) LEDs of 5000K (blue), 4000K (cyan), 2700K (grey) and PC-Amber(amber), popular on street lighting; (e) representative spectral response of DMSP/OLS(black) and SNPP/VIIRS/DNB(blue). Sources: Sánchez de Miguel 2015, Tapia Ayuga et. al. 2015, Sánchez de Miguel et. al. 2017, Elvidge. et. al 1999 and Liao et. al. 2013.

3.7 Using night lights to estimate threats to ecosystems

Plants, animals, microorganisms, and entire ecological systems are affected by artificial light pollution, due to changes in behavior, physiology (including circadian rhythms), timing of activities, and disorientation, among many other reasons (Rich & Longcore, 2006; Navara & Nelson, 2007; Gaston et al., 2013, Russart & Nelson, 2018). As this is a very active area of research in biology and ecology (Davies & Smyth, 2018), many researchers make use of night lights data. For example, several studies have used the mosaics of DMSP/OLS stable lights (as one of several variables), to globally map the human footprint in terrestrial areas (Sanderson et al., 2002; Venter et al., 2016) as well as to map the human impact in marine areas (Halpern et al., 2008, 2015). In a similar fashion, night lights were used to globally map impervious surface area (Elvidge et al., 2007a) and to estimate human population at fine spatial resolutions (Bhaduri et al., 2002), as both impervious surface and population density are known to negatively impact biodiversity.

Using a calibrated set of DMSP/OLS images (1992-2010), Gaston et al. (2015) demonstrated that protected areas were indeed darker (DN < 5.5) than unprotected areas; however, they found that natural darkness has been eroding in many protected areas, and especially so in Europe, South and Central America, and in Asia, where there was a significant increase in mean nighttime lighting in 32-42% of all protected areas. In a following study, Koen et al. (2018) have found that areas with high species richness terrestrial and freshwater mammals, birds, reptiles, and amphibians, are suffering from encroachment of artificial lights. Marcantonio et al. (2015) used VIIRS/DNB data to show that a 10% reduction in light emissions near nature parks in Italy could lead to a 5–8% increase in the area suitable for high biodiversity. Social media (such as geotagged Flickr photos) has also been used in conjunction with night-time lights to estimate visitation of protected areas and the impact of human activity on them (Levin et al., 2015).

While most artificial lighting originates from land areas, marine ecosystems are not devoid of light pollution. As of 2010, Based on DMSP/OLS data (as of 2010), about 22% of the world's coastlines (except Antarctica) were subjected to light pollution based on DMSP/OLS data, with 54% of Europe's coastlines under light pollution, followed by Asia (34%) and Africa (22%) (Davies et al., 2014). Field experiments using an underwater spectrometer in the Gulf of Aqaba have observed artificial light in the blue band down to a depth of 25 m near the coast, and up to 5km from the coast at a depth of 5m depth at 5 km from the coast (Tamir et al., 2017).

3.8 Using night lights examine ecological light pollution

Studies which attempted to quantify the relationship between light pollution and presence or behaviour of species have mostly focused on specific organisms, such as sea turtles and birds (e.g. Van Doren et al., 2017). Using VIIRS/DNB data, La Sorte et al. (2017) showed that nocturnally migrating birds are attracted to urban lit areas, affecting their migration behaviour. In a follow-up study, Cabrera-Cruz et al. (2018) have shown that light pollution experienced by nocturnally migrating birds, is especially high during the migration season for species with smaller ranges. Recently, Horton et al. (2019) combined VIIRS/DNB with weather surveillance radar data to examine the exposure of migratory birds to light pollution, in order to provide data for targeted conservation actions. They found, for example, that over half of all migratory birds typically pass a single radar location within a single week, which suggests that targeted and relatively short term "lights out" campaigns for floodlit buildings could potentially greatly reduce the impact of light pollution on migratory birds.

Sea turtles represent one of the most studied groups, for which the negative impacts of artificial lights have been well known for decades (e.g. Witherington and Martin, 2000). Kamrowski et al. (2012, 2014) used DMSP/OLS imagery to identify which nesting sites of sea turtles along the Australian coastline are exposed to light pollution, and in which of these sites there was an increase in light pollution. Using finer spatial resolution imagery (ISS photographs and SAC-C), Mazor et al. (2013) have shown that nesting of sea turtles along the Mediterranean coast of Israel was negatively correlated with night-time brightness, and Weishampel et al. (2016) obtained similar results using DMSP data for nesting sea turtles in Florida, which was also confirmed by VIIRS data (Hu et al. 2018a). Given the differences between the light perceived by animals and humans (mostly horizontal light) and the light measured from space (mostly upwards reflected light; Katz and Levin, 2016), new ground based methods are developed to measure night-time brightness for ecological studies, e.g., using sky quality meters (Kelly et al., 2017) or hemispheric cameras (Pendoley et al., 2012). Jechow et al. (2019b) recently provided an overview of how a DSLR camera with a fisheye lens can be used for characterizing night time brightness over a full sphere, by taking two vertical plane photos. Such an approach is especially useful for studies on ecological light pollution, because the field of view of various species differs both in the horizontal as well as in the vertical plane.

Remote observations of night lights have also been used to examine the influence of light on bats, all of which are nocturnal, and many of which are extremely sensitive to artificial light. In a nationwide study of bats in France, Azam et al. (2016) combined

VIIRS/DNB data with landcover data to examine the relative effects of impervious surface, intensive agriculture, and light emission. They found that agriculture was the strongest negative influence on all four species tested, and that light emission also had a negative influence on 3 of the 4 species tested, and in all cases a stronger negative influence than impervious surface. Hale et al. (2015) used higher resolution (1 m) data from nighttime aerial photography and maps of tree cover together with observations of bats to examine how light modulates the impact of gaps in tree cover for bat flights. They found that the negative impact of light increases as crossing distance between trees increases. In a recent study, Straka et al. (2019) found that the lamp spectra also has important and species-dependent effects, using land cover data and a 1 m resolution map of light emission from Berlin (Kuechly et al. 2012) together with surveys of bat activity.

3.9 Epidemiology

In modern societies, exposure to artificial light is suspected as a contributing factor to some diseases (e.g. some cancers, obesity, and depression), through disruption of the circadian rhythm (Lunn et al. 2017) or sleep disturbance, as well as suppression of the hormone melatonin, which is related to ambient light intensities (Haim and Portnov, 2013; Cho et al., 2014). Space-based night light data allows studies of population exposures to artificial outdoor light, which can then be compared to data from either cohort studies or a set of patients and healthy controls. The “Light at Night hypothesis” for breast cancer was first proposed by Stevens (1987), who noted that if dim light is a risk factor, brightly lit communities could be expected to have higher levels of breast cancer. The first empirical analysis linking DMSP/OLS night lights data with breast cancer (BC) incidence was Kloog et al. (2008), which examined 147 urban localities in Israel. The study revealed a statistically significant association between ALAN and BC but not with lung cancer, which was used in the study as a negative control. Follow-up studies confirmed adverse effects of ALAN on BC and prostate cancer in worldwide cohorts (Kloog et al., 2009; 2010). Other studies investigated DSMP-derived ALAN data in conjunction with different health phenomena, including hormone-dependent cancers (Bauer et al., 2013; Rybnikova et al., 2015, 2016b; Portnov et al, 2016; James et al., 2017; Kim at al., 2017; Rybnikova et al., 2018), obesity (Rybnikova et al., 2016a; Rybnikova and Portnov, 2016; Koo et al., 2016), and sleep quality (Koo et al., 2016). These studies, carried out in different regions and population cohorts, provide mutually complementing evidence about significant associations between ALAN and a wide of range of adverse health phenomena.

A major question for this research is the extent to which remote observations of light match individual exposures. Kyba & Aronson (2015) argued that if ALAN is a cause of disease (rather than a correlate), then estimated risk factors should increase with increasing spatial resolution of remotely sensed data. Rybnikova and Portnov (2017) then compared results obtained from DMSP and VIIRS-DNB satellite images, and detected a stronger ALAN-BC association when using the higher spatial resolution VIIRS-DNB images. Recent studies have used even higher resolution multi-spectral images taken from the ISS. Both Garcia-Saenz et al. (2018) and Rybnikova and Portnov (2018) used ISS image data to conclude that exposures to short wavelength (blue) ALAN appear to have stronger effects on hormone-dependent cancer incidence than exposures to green and red light spectra. This conclusion is consistent with results of laboratory and small cohort studies, which emphasize potential health risks associated with short wavelength illumination (Lunn et al. 2017). Keshet-Sitton et al (2016) also demonstrated increased risk of breast cancer based on ground-level measurements rather than remote observations. Further work in this area will greatly benefit from improvements in resolution, coverage, and multispectral information from space-based sensors, as well as confirmation of the relevance of the data through ground-based measurements of a representative sample of individual exposures (Kyba & Spitschan 2019).

3.10 Lighting technology

For some applications, identification of lighting technology as well as their dynamics on short time scales is desirable. To discriminate lamp types using airborne or spaceborn systems, high spatial and spectral resolution is necessary (Figure 24). The ideal system would be to use a hyperspectral imaging spectrometer at low altitudes. Few studies with limited spatial coverage exist, such as the first ever performed over 1998 in Las Vegas, USA (Elvidge et al. 2005, Alamús et al. 2017, see section 2.3 for more). Elvidge et al. (2010) showed that it was in principle possible to discriminate light sources with multispectral sensors, using detailed spectral field measurements and a modeling approach for the pre LED technologies. This was later demonstrated in practice with an aerial survey over Birmingham, UK. In that study, Hale et al. (2013) used a standard DSLR camera and supportive field measurements, and achieved a high success rate of distinguishing between different vapor lamps, although the technique used was fully phenomenological. Sensor requirements for satellite based surveys were proposed (Elvidge et al. 2007 b,c) but few attempts have been performed. Using the hyperspectral data of a flight over Las Vegas

Metcalf (2012) and Tarda et. al. (2013) were able to determine different lighting technologies, Sánchez de Miguel (2015) used ISS images, and Zheng et al. (2018) were also able to distinguish high-pressure sodium (HPS) lamps from white LEDs using the new Jilin-1 satellite. However, there are fundamental limitations for multispectral sensors to distinguish between similar color light sources, like fluorescents/compact fluorescents and LEDs of same color temperature or HPS lamps and PC-Amber LEDs (Sánchez de Miguel et al. 2019b). It should also be noted that most of the research undertaken thus far has been done without radiometric calibrations of any kind or atmospheric corrections.

Ground-based measurements provide more freedom regarding temporal and spectral resolution (section 2.4). Several studies have used calibrated RGB cameras to track lighting remodelling from vapor lamps to LEDs (Kollath, 2016, Barentine, 2018), or short term dynamics like the switching off of specific lights to assess their contribution to skyglow (Cleaver, 1943; Jechow, 2018b). Ground-based measurements can provide a wider temporal range than space based sensors (section 4.3), and also fill in the blind spot of the lack of sensitivity to blue light from LEDs (section 4.6, Kyba et al. 2017). High frequency data, for example as measured using ground based SQM, can be used to remotely sense the contributions of different lighting types (streetlights, vehicles, residential light) due to their differing temporal patterns (Bará et al., 2018). Systems used in urban science show promising results at the cross section to remote sensing as shown by the “pulse of the city” studies with ground-based measurements, using a hyperspectral camera by unraveling aggregate human behavior patterns (Dobler, 2015), lighting types (Dobler, 2016) or temporal profiles using RGB images (Meier, 2018). In addition, the combination of several remote sensing techniques (AstMON, SQM, ISS images and Hyperspectral spectrograph [SAND] plus energy statistics) was used to trace the temporal evolution and population of the lighting technologies used in Madrid for an average night (Sánchez de Miguel, 2015).

3.11 Mapping fires, gas flares, and greenhouse gas emissions

Wildfires are a major force shaping natural ecosystems, and their ignition and propagation are influenced by both natural and anthropogenic factors. Whereas during the industrial period the global fire regime has shifted from one driven primarily by rainfall, to one driven by human influence on fire (ignition and suppression), in the future climate change may play a decisive role in global fire regime (Pechony and Shindell, 2010). Fire management therefore requires mapping fire in space and in time. It has long been known that visible light data from DMSP had a capability to detect biomass burning and natural gas flaring (Croft 1973, 1978; Figure 6b). In the mid-1990s a nightly biomass burning algorithm was developed for DMSP low light imaging data and regionally implemented (Elvidge et al., 1996). This involved a lit pixel detection algorithm and masking of persistent lights from cities, towns and gas flares. Later on, as the distribution of DMSP/OLS data was lowered to three hours, it was perceived that DMSP/OLS data can be used for operational fire monitoring (Elvidge et al., 2001b), and that active fire mapping using DMSP/OLS was able to detect more fires than MODIS (Chand et al., 2007).

A high correlation was identified between the total lit area of a country and total carbon dioxide (CO2) emission (Doll et al., 2000), and even better results were obtained using the VIIRS/DNB (Ou et al., 2015). The first global satellite estimates of flared gas volumes came from DMSP, with flaring sites identified manually based on circular haloes of glow present in the DMSP annual cloud-free nighttime lights (Elvidge et al., 2009a). With the advent of VIIRS, these capabilities have been substantially enhanced based on the nighttime detection of fires and flares in three spectral ranges: near infrared (NIR), shortwave infrared (SWIR) and midwave infrared (MWIR). The VIIRS Nightfire (VNF) algorithm detects the presence of sub-pixel infrared emitters, such as fires and flares in six spectral bands and uses Planck curve fitting to derive temperature, source area, and radiant heat using physical laws (Elvidge et al., 2013b), which is an improvement over satellite fire products which use one or two spectral bands (Elvidge et al., 2013c). Daily VNF datasets are available for download from https://www.ngdc.noaa.gov/eog/viirs/. The VNF data has been successfully used to map and classify industrial heat sources (Liu et al., 2018), as well as to conduct annual surveys of natural gas flaring locations and estimate flared gas volumes (Elvidge et al., 2015a). The advantage of VNF over both DMSP and traditional MWIR fire products is the ability to calculate variables such as temperature using physical laws. However, Elvidge et al. (2019) recently showed that the VIIRS/DNB retains a capability to detect combustion sources too small to trigger detection in VNF. These results indicate that more complete compilations of IR emitters could be achieved by adding a DNB fire product to complement VNF and other satellite derived fire products, as recently reviewed by Chuvieco et al. (2019).

3.12 Monitoring fisheries

The earliest reporting on nighttime satellite detection of fishing boats using massive lighting to attract catch, traces back to DMSP data (Croft, 1978; Figure 6c). From 2000 to 2012, NOAA provided regional near real time DMSP file transfer services to fishery agencies in Japan, Korea, Thailand, and Peru, where the boat detections were analyzed locally. However, an automatic algorithm for reporting boat locations was never developed for DMSP. The situation changed with VIIRS due to the large sizes of the images, making it impractical for most users to download the images for local analysis. In 2014, NOAA initiated the development of a VIIRS boat detection (VBD) algorithm. The initial algorithm was optimized for low moon conditions (Elvidge et al., 2015b) and produced high numbers of false detections from moonlit cloud and lunar glint features. This problem was resolved by adding a module which screens moonlit areas for lights found in DNB that are missing from the corresponding long wave infrared image based on a cross-correlation analysis. VBD is now produced globally with a nominal four-hour temporal latency, and is available online at https://eogdata.mines.edu/vbd/. In addition, NOAA provides near real time email and SMS alerts for VBD detections occurring in marine protected areas (MPAs) and fishery closures in Indonesia, Philippines and Thailand. The alerts now cover 989 individual areas, spanning 648,865 km^2, with 82,101 detections in 2017. VBD data have been successfully used to rate compliance levels in fishery closures in the Philippines and Vietnam (Elvide et al., 2018), and to map core fishing areas in the Philippines (Geronimo et al., 2018).

4. Research challenges, limitations of current sensors, and outlook for the future

4.1 Challenges of night light sensing and the differences between day vs. night sensing in the visible band

There are many challenges associated with observations of visible band light at night, and the remote sensing of socioeconomic parameters on the basis of such data. The most obvious of these are the dramatically reduced radiance and extreme dynamic range of night scenes in comparison to daytime remote sensing. Consider the scene in Figure 14. During daytime, the light source is the sun, shining from above the atmosphere. In a cloud free scene, rooftops, treetops, and open grassland or water areas are illuminated equally, and their radiance in the scene depends on their albedo. The typical dynamic range of the data is perhaps a factor of 50.

During the night, both celestial and artificial light sources are present. Areas appearing black in the night image are lit by natural sources like airglow and starlight, about 8 orders of magnitude fainter than direct sunlight. Streets are lit by reflected light from lamps, about 4 orders of magnitude fainter than direct sunlight (Hänel et al. 2018). Comparing the histograms of radiance over Berlin from a Landsat day-time image and a VIIRS/DNB night-time image, it can be observed that radiance at night was about 5 orders of magnitudes lower than at day time, and that the distribution at radiance at night-time is different, skewed towards dark areas, whereas during daytime it is distributed more normally (Figure 25). Whereas within Landsat 8 night-time images of Berlin, Las Vegas and other cities, the brightest sources mostly emitted light within the visible bands, bright sources of gas flares also emitted significantly in bands 6 and 7 of Landsat 8 (Levin and Phinn, 2016).

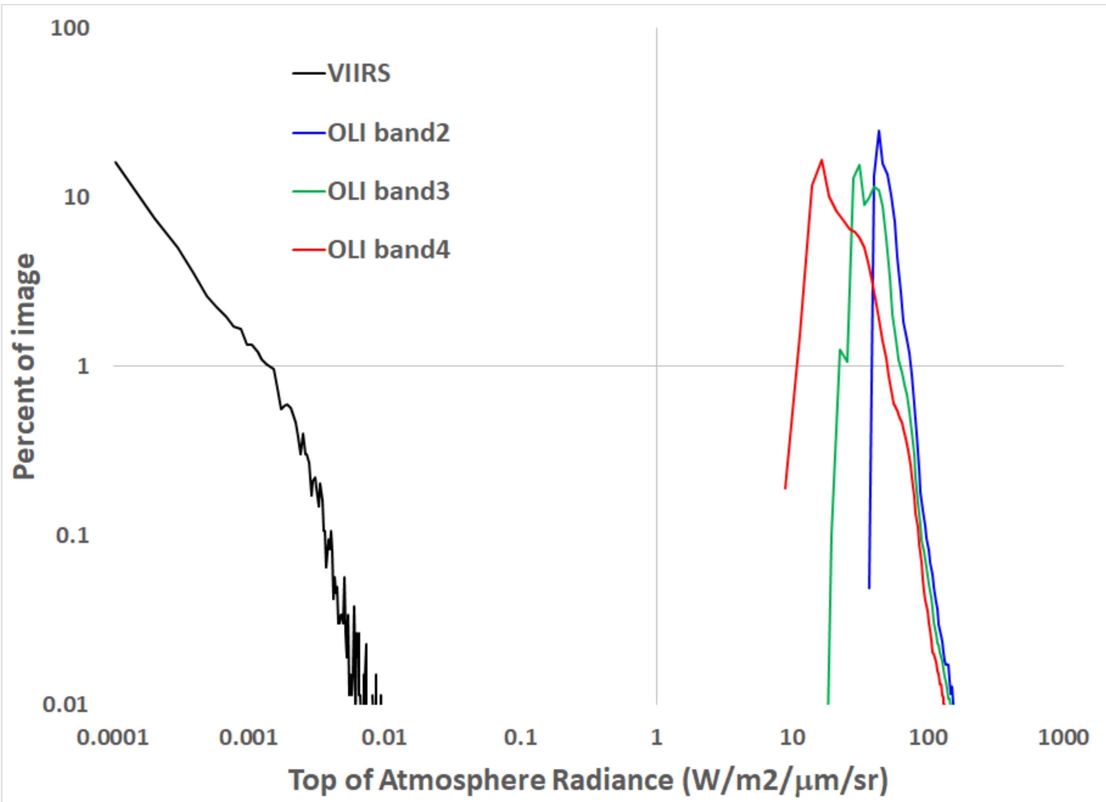

Figure 25: Histograms of top of atmosphere radiance for the images of Berlin of VIIRS and day-time Landsat OLI shown in Figure 14.

Some lamps (e.g., no cut-off or semi cut-off) radiate a portion of their light upwards without reflection (Cha et al., 2014), and can therefore have radiances approaching an order of magnitude of sunlight. Nighttime sensors that target to capture the radiance of all elements in an urban scene at high spatial resolution would therefore require an enormous instrumental dynamic range. In practice, this is never the case. At high spatial resolution, unlit areas are usually underexposed (as shown by Levin et al., 2014, using an EROS-B image), and lamps shining directly upward saturate the sensor. The problem of high dynamic range is reduced considerably at lower spatial resolution (as in Figure 14), because even in urban areas, most of the scene consists of areas that are not artificially lit (e.g. rooftops and treetops).

In daytime scenes, radiances change throughout the day due to changing solar illumination, atmospheric conditions and viewing geometry between the sensor, the target and the sun: the Bidirectional Reflectance Distribution Function (BRDF; Schaaf et al., 2002). In most cases, surface radiances themselves are not of interest, but rather derived quantities like reflectance within a spectral window, surface emissivity or surface temperature. At night, in many cases it is the radiance itself that we are interested in, but this value can be highly variable. Coesfeld et al. (2018) discusses the sources of these radiance changes, and their discussion is summarized and expanded upon here.

We begin with a hypothetical scenario to demonstrate the complexity of the spatial distribution of night lights. Imagine a very long wall that is 30 meters tall, with a single lamp mounted at 5 meters height, 5 meters away from the edge of the wall (Figure S1), which radiates in all directions. It can be immediately seen that when imaged from the left, the lamp is invisible, while when imaged from zenith or from the right, the lamp can be seen directly, as can the light reflected from the ground surface and the wall. If a space based instrument observes this scene on multiple days from multiple directions, the total radiance will change in an on-off fashion. Now consider the case where instead of radiating in all directions, the lamp shines all of its light directly on the wall (e.g. a well-directed floodlight). In this case, the radiance would go as $1-H(\theta-\pi/2)\cos\theta$, where θ is the angle between the observing direction and the normal of the wall, and H is the Heaviside step function. Viewed from the left, from directly above, or any view direction parallel with the wall's direction, the wall would appear to be black. When viewed from the right, the observed radiance would increase with both increasing nadir angle and increasing angular viewing distance from the wall's direction.

The scenarios described above were hypothetical, but are representative of two extremely common situations: first, screening (i.e. blocking) of artificial light by buildings, trees, or other objects, and second, radiation from vertical surfaces such as floodlit facades, light escaping windows, and illuminated signs. The imaging direction thus has a major impact on the radiance observed at night. Since this effect is determined by the local geometry, a general correction is not possible. At high spatial resolutions (Figure 26), the effect is quite obvious. At low spatial resolutions, the effect may be minimized to some extent due to averaging many local conditions, surface geometries such as hillsides or long parallel streets which can make the effect visible even at a spatial resolution of 750 meters.

Figure 26: Visibility of lit facades depends on perspective. The top image is a crop of an photograph taken from the South, so North facing facades are visible. The bottom image was taken from the North, so the South faces of buildings therefore appear dark. Photos taken by Alejandro Sanchez de Miguel and the Freie University"at Berlin during the EU COST Action ES1204 LoNNe. Figure and caption reproduced from Coesfeld et al. (2018),

Both DMSP/OLS and Suomi NPP/VIIRS DNB are wide-view sensors, with swath widths greater than 3000 km, which means they can accumulate angular observations varying in a large range. Angular observations sometimes are not preferred, because they often cause variation across geography that makes mosaicking or comparison over time a big challenge. However, angular information has been proved to carry valuable structural information and ironically is critical to normalize observations to the standard viewing-illuminating geometry, as seen in MODIS (Schaaf et al. 2002) and MISR (Multi-angle Imaging SpectroRadiometer) (Diner et al. 1989). Due to the variation in street layout and building height, nighttime light is also expected to vary accordingly (Kyba et al. 2015a). Angular observations from both DMSP/OLS and VIIRS/DNB may thus provide structural and vertical information about urban areas, especially in the east-west direction, given the characteristic scanning geometry of sun-synchronous sensors. Such information still remains under-utilized up to date, however preliminary results indicate that measured radiance is lower at nadir and increases towards the edge of the scan (Bai et al., 2015). In a recent paper, Li et al. (2019b), have confirmed that the viewing angle of VIIRS/DNB affects the amount of measured night-time brightness, and that building height should be incorporated to understand the relationship between the satellite viewing zenith angle and emitted night-time lights. A different group (Li et al. 2019c) have approached the problem from the other direction, using ground based all-sky imagery from Google Street View to examine how much light can escape to space, and how this is affected by changes in vegetation. Future research is required to extract this invaluable information from both DMSP/OLS and Suomi NPP/VIIRS DNB, and to remove angular effects from night-time products.

4.2 Uncertainties due to moonlight, aerosol/cloud contamination, and seasonal vegetation effects

Uncertainties originating from angular, diurnal, and seasonal variations in atmospheric and surface optical properties are also a primary source of measurement error in the nighttime lights (NTL). As demonstrated by Roman et al. (2018), characterizing these uncertainties is extremely crucial as a long-term record of NTL cannot be constrained directly from at-sensor top-of-atmosphere (TOA) radiances. The uncertainties can be separated into (1) environmental factors, such as moon light, cloud/aerosols, and surface albedo (interferes with the observed signal), and (2) errors stemming from seasonal variations in vegetation or in snow cover and associated surface properties, which can significantly affect estimates of seasonal and long-term trends (Figure 20).

Key to characterizing these factors is an accurate estimation of the surface Bidirectional Reflectance Distribution Function (BRDF, or reflectance anisotropy), a quantity that is governed by the angle and intensity of illumination – whether that illumination be solar or lunar (e.g., Miller and Turner, 2009) or from airglow emissions – and by the structural complexity of the surface. Roman et al. (2018) considered the semi-empirical RossThickLiSparse Reciprocal (RTLSR, or Ross-Li) BRDF model (Román et al., 2010; Roujean et al., 1992; Schaaf et al., 2011, 2002; Wang et al., 2018) to correct the effects of contamination through an external illumination in the NTL. This modeling approach is advantageous as it has been shown to capture a wide range of conditions affecting the VIIRS/DNB on a global basis. Similarly the RTLSR model also allows analytical inversion with a pixel-specific estimate of uncertainty in the model parameters and linear combinations thereof (Lucht and Roujean, 2000). Finally, the scheme is also flexible enough that other kernels can be easily adopted should any become available and should they be shown to be superior for a particular scenario.

Similar to day light sensing in visible band, NTL radiances also suffer from biases stemming from clouds and aerosols. A scene with opaque clouds can block the NTL radiance completely, whereas thinner and transparent or semi-transparent atmosphere blocks the radiance partially and scatters the light creating a fuzzy appearance (Elvidge et al., 2017). The vector radiative transfer modeling of the coupled atmosphere-surface system (Vermote and Kotchenova, 2008) can be used to compensate for aerosols, water vapor, and ozone impacts on the NTL radiances (Román et al., 2018). This correction mitigates errors stemming from poor-quality TOA retrievals, especially across regions with heavy aerosol loadings and at Moon/sensor geometries yielding stronger forward scatter contributions.

Seasonal variations such as those resulting from vegetation artifacts can also introduce challenges in the retrieval of satellite-derived NTL due to the canopy-level foliage along the ground-to-sensor geometry path. This effect occurs predominantly in urban areas where vegetation such as deciduous broadleaf canopies is present. The impact of this obstruction of surface light by the cyclical canopy results in reduction in the magnitude of NTL at city-wide scales (Levin, 2017; Levin and Zhang, 2017; Figure 20). This occlusion effect has been shown to be directly proportional in magnitude to the density and vertical distribution pattern of the canopy. Román et al.(2018) proposed to use gap fraction to correct the vegetation effect. These seasonal changes may be viewed as a noise (when aiming to estimate socio-economic properties from NTL) or as a signal (when aiming to estimate light pollution from NTL).

4.3 Challenges related to temporal sampling

In addition to the seasonal changes mentioned above, night lights are dynamic throughout the course of individual nights (Figure S2). Observations of night sky brightness show typical decreases of typically around 5% per hour (Kyba et al. 2015b, Falchi et al. 2016), with larger decreases earlier at night. The decrease in light emission can also be seen through horizontal imaging (Dobler et al. 2015, Meier 2018). Many municipalities intentionally dim or turn off street lights at late hours (Green et al. 2015), and these switch offs can produce very obvious signals in night sky brightness data (Puschnig et al. 2014, Sánchez de Miguel 2015, Jechow et al. 2018b). The typical spectra of artificial light emissions also appears to shift as the night progresses (Kyba et al. 2012, Aubé et al. 2016). This is presumably due to changes in the fraction of lights coming from different types of lamps. Observations of low resolution ground spectra or sky spectra could therefore potentially be used to differentiate the relative contributions of light sources at different times (Bará et al. 2018).

Orbital platforms with a (relatively) fixed overpass time, such as DMSP (early evening) or VIIRS DNB (~1:30am) have limited ability to view such temporal changes. Depending on the application, this may be a disadvantage (they do not get the full picture of light use) or an advantage (the observed radiance values are more consistent). Platforms with a non-fixed orbital time can fill in the gaps to some extent (Kyba et al. 2015a), but such imagery is then taken on different dates. Only a geostationary platform could allow continuous, or at least repeated, tracking of radiance changes throughout the full night (e.g. Zoogman et al. 2017). With routine and growing numbers of observational passes from Suomi-NPP, JPSS-1 (now NOAA-20) and subsequent JPSS series of satellites, nighttime light observations will become even more frequent, providing opportunities for multiple cloud-free observations per night and greater temporal frequency to quantify the stability of light sources, their magnitude, and time to restoration following a disaster event.

Outside of the tropics, there is an important interaction between imaging time and the seasons in which an orbital platform can acquire data about artificial lights. This is of particular importance for many cities in Europe. In Berlin, for example, astronomical night does not occur in the period between May 19 and July 27. If the satellite overpass time is displaced from midnight, this period is even longer. For a satellite with a 21:00 overpass time, Berlin would be illuminated by twilight from early April until the start of September. Restricting the available night window to the period September-March means that nights with snow cover will make up a much larger fraction of the dataset, especially at higher latitudes or elevations. Annual products for high latitude countries (e.g. Canada, Sweden, Norway, Finland, Iceland) are therefore likely to be biased upwards due to snow cover if the satellite overpass time is too far from midnight (Elvidge et al. 2001a).

4.4 Long-term instability of some light sources

Many light sources in countries with stable electricity emit relatively similar amounts of light from night to night. Coesfeld et al. (2018) reported that the distribution of radiances in the DNB monthly composite data for urban and suburban locations and airports was near normal, with a standard deviation of about 13-19%, depending on whether all months or only autumn months were considered. Other light sources such as ship ports, stadiums, and power plants had larger variations, while some other light sources are much more dynamic (Coesfeld et al., 2018). Wildfires appear only during the time they are active, and oil flares are not stable from year to year (Coesfeld et al., 2018). Large construction sites may be brightly lit for relatively long periods (Kuechly et al. 2012), and eventually replaced by less brightly lit buildings. Greenhouses are among the brightest objects on Earth, but may only lit during a portion of the year (Coesfeld et al., 2018). Special events such as large-scale outdoor concerts or light festivals (Figure S3) can also produce considerable light only for short periods. All these types of unstable lights pose a challenge for defining monthly and annual trends in light emissions.

4.5 Global spectral shift due to transitions to LEDs

The world is in the midst of a “lighting revolution” due to the development of light emitting diode (LED) technology (Pust et al. 2015). This is the fourth such revolution in the history of outdoor lighting: previous generations switched from oil to gas, gas to the first electric lights (arc lamps and incandescents), incandescent to high intensity discharge lamps (Riegel, 1973, Jakle, 2001, Isenstadt et al. 2014). Each new technology has not only allowed for an increase in light emission, but has also dramatically changed lighting spectra, and allowed new forms of illumination. The global transition to LED lights therefore has dramatic implications for remote sensing of night lights.

From a remote sensing perspective, there are two main consequences of the change towards LEDs. First, the “white” LEDs used for lighting outdoor areas have a broadband spectra, in dramatic contrast to the “line” type spectra of vapor lamps (Elvidge et al. 2010, Aubé et al. 2013; Figure 24). Much of the world was lit by orange colored high pressure sodium lamps at the start of the 21^{st} century, and existing broadband monitoring instruments designed for 20^{th} century lights can therefore easily mistake a change in spectrum for a decrease in emitted light (Kyba et al. 2015, Sánchez de Miguel et al. 2017). For similar reasons, the spectral change affects the perception of artificial lights by animals, and therefore the ecological impacts of such light (Longcore et al. 2018). Future research should be thus directed on examining the impacts of the transition of artificial lighting to LEDs on various topics, including ecological light pollution, human health, crime and car accidents, preferably using a before-after-control-impact (BACI) design, as in Plummer et al. (2016) and Manfrin et al. (2017).

The second major consequence of the introduction of LEDs is a change in illumination practices. For example, LEDs are more easily dimmed than vapor lamps, so lighting may become more temporally dynamic. Streetlights based on LEDs are less likely to directly emit light into the atmosphere, and may potentially result in less total emissions through more careful direction of the light (Kinzey et al. 2017). The most important change, however, may turn out to be a shift in the “typical” source of light observed from space, away from street lighting and towards lights emitted for advertising or artistic purposes (Kyba, 2018b). This spectral shift will likely affect the ability to existing sensors such as VIIRS/DNB to quantify artificial lights from space, given that it is not measuring incoming light in the blue band (Figure 24). Modelling work recently done by Bará et al. (2019) indicates that for certain transition scenarios (from HPS to LED), the VIIRS may detect reduction in artificial zenithal sky brightness, even if sky brightness in reality increases, due to the loss of the HPS line in the near-infra red, and the inability of the VIIRS to detect blue light. The emission of blue light from LED sources therefore requires future night-time sensos to include the blue channel (which is not covered by DMSP/OLS, VIIRS/DNB or Luojia-1), however blue light is scattered more (Kocifaj et al., 2019), and thus atmospheric haze removal techniques should be developed for night-time imagery, for future products.

4.6 Challenges in calibrating ground and space borne measurements

While night light remote sensing has benefited various applications, there are certain research gaps that need to be overcome in order to transform this data to be more quantitative. While in traditional optical remote sensing satellite images are atmospherically corrected to derive their reflectance values (Clark and Roush, 1984), it is not so clear which units should be used in night light imagery. The DMSP/OLS imagery products are distributed as stable lights or average lights x percent (DN values between 0 and 63). Often these products are used to calculate the total lit area or the total lights, however, these data are not in luminance units. Photometry is the measurement of the intensity of electromagnetic radiation in photometric units, like lumen/lux/etc, or magnitudes. Radiometry is the measurement of optical radiation, with some of the many typical units encountered are Watts/m^2 and photons/sec/steradian. The main difference between photometry and radiometry is that photometry is limited to the visible spectra as defined by the response of the human eye (Teikari 2007). Of relevance for such measurements, are the photopic and scotopic bands. Human photopic vision which allows color vision, takes place under daytime conditions as well as under artificial illumination, and is based on the properties of cone photoreceptors in the human retina. Human scotopic vision on the other hand, takes place under dark conditions, using the retinal rods alone, when humans perceive the world in "grey scale", and in comparison to photopic vision, scotopic vision is shifted towards shorter wavelengths, mostly between 454 and 549 nm (Elvidge et al., 2007b).

In recent years there have been some attempts to calibrate fine spatial resolution images to photometric units. Hale et al. (2013) used ground measurements of incident lux along linear transects to calibrate their aerial night light images into illuminance units. A different approach has been used by Cao and Bai (2014), who examined the temporal variability in light as measured by the VIIRS/DNB from various features which they expected to emit uniformly in different nights. Another approach for field mapping of night lights that can be used for calibrating aerial or space borne night light imagery is using ground networks of instruments such as the Sky Quality Meter (SQM, manufactured by Unihedron, measuring the brightness of the night sky in magnitudes per square arc second; http://www.unihedron.com/projects/darksky/), however ground networks aimed at monitoring light pollution are fairly recent (den Outer et al. 2011; Pun and So 2012; Zamorano et al., 2019). In an interesting study using Extech EasyView 30 light meters to map night brightness along a 10-m sampling grid on the Virginia Tech campus, brightness was measured twice: First with the light meter pointing upward to catch direct light from the light fixtures at 30 cm from the ground, then with the light meter pointing down to measure reflected light (Kim, 2012). Most ground networks of SQM are directed to measure zenith night sky brightness. In a study comparing the correspondence between an EROS-B night-time image, and ground measurements done with SQMs in three directions (downwards, horizontally and upwards), Katz and Levin (2016) have shown that the lowest correspondence was with ground measurements directed upwards (representing sky glow), whereas the strongest correspondence was found with ground measurements directed downwards (representing street light reflected by the surface). Thus, in addition to the inconsistency in the photometric units used for calibrating aerial night lights images, there is a gap with regards to how should one measure light on the ground so that it best corresponds with what an airborne or a space-borne captures.

4.7 Consistent nightlight time series across different platforms and sensors

Although the signal of change in the DMSP/OLS NTL time series is larger than the error signal and also large enough to render the error signal (noise) unimportant (Zhang and Seto, 2011), to facilitate accurate change analysis with NTL time series it is necessary to calibrate first to minimize differences caused mainly by satellite shift (Zhang et al., 2016). The challenge to achieve successful radiometric calibration of remote sensing imagery obtained at different times is to find invariant ground targets that can be used as references for reliable comparison over time. As the first attempt, Sicily, Italy was chosen as the reference site to calibrate the reference image F121999 and other images individually (Elvidge et al., 2009). These models were then applied to calibrate the entire time series from 1992 to 2008. This method successfully reduced differences caused by satellite shift to some order. However, models derived in Sicily might not be generalized to cover the entire globe, since noises introduced by various sources might not be geographically homogenous (Pandey et al., 2017). To address this problem, researchers studying regional urbanization dynamics have chosen local reference sites to derive their models so that they better fit their specific regions (Liu et al. 2011; Liu et al. 2012; Nagendra et al. 2012; Pandey et al. 2013). In an attempt to produce more generalized models for the entire globe, Wu et al. (2013) extended the Elvidge et al. (2009) method by selecting more reference sites, including Mauritius, Puerto Rico, and Okinawa, Japan in addition to Sicily, Italy. Despite that the Wu et al. (2013) method achieved improvement, the way they chose invariant regions was not essentially different than that applied by Elvidge et al. (2009) and also suffers from the limitation of subjectively choosing areas.

Li et al. (2013) designed an automatic method to find invariant pixels in Beijing, China to avoid subjective errors. This automatic method can minimize the bias introduced by subjective selection of invariant regions and has the potential to be extended to the entire globe. However, since the region of Beijing experienced dramatic changes in the past decades, this method might lead to overcorrection to the NTL time series. Furthermore, the iterative procedure to identify stable pixels is very computation intensive and thus cannot be directly implemented at the global scale, considering the gigantic amount of pixels. Zhang et al. (2016) designed a ridge sampling and regression method to calibrate the NTL time series over the entire globe. This method is based on a novel sampling strategy to identify pseudo-invariant features. Data points along a ridgeline-the densest part of a density plot generated between the reference image and the target image-were first identified and those data points were then used to derive calibration models to minimize inconsistencies in the NTL time series. In this way, only 63 pairs of data points were used to run a regression model for calibrating each target image, significantly reducing computation load. Since only the F152000 image was used as the reference image, target images close to the two ends of the time series might be over corrected due to the increased time intervals. Li and Zhou (2017) proposed a stepwise calibration approach to address that issue. They first reduced temporal inconsistency within each satellite segment and then systematically moved each satellite segment up or down to generate a temporally consistent NTL time series from 1992 to 2013, by making full use of the temporally neighbored image as a reference for calibration.

Each of the methods mentioned above has its strengths and shortages. A framework to assess and choose a right method for a specific application was proposed by Pandey et al. (2017). Future efforts are still needed to design better NTL calibrating methods. Furthermore, there is a huge gap between DMSP/OLS and VIIRS/DNB. A temporally consistent NTL time series extending from DMSP/OLS to VIIRS/DNB is highly desirable, yet still a huge challenge, due to differences in passing time, onboard calibration, spatial resolution, and other considerations (see Li et al., 2017, as well as Zheng et al., 2019, for examples of inter-calibration between DMSP/OLS and VIIRS/DNB). Ground-based stable and radiometrically calibrated light sources may offer a useful approach for inter-calibration between night-time lights sensors, as well as for validating the performance of these sensors, as attempted by Hu et al. (2018b) and Ryan et al. (2019).

4.8 Outlook for the future

4.8.1 The need for geostationary platforms

Despite the benefits of its unique information content, a significant limitation of current VIIRS DNB measurements is infrequent revisits, and hence poor temporal resolution across the night. The low earth-orbiting (LEO) satellite platform offers only 1-2 passes per night at low to mid-latitudes, meaning that the VIIRS DNB information must be used in 'snapshot mode.' With the addition of NOAA-20 in November 2017 to the same orbital plane as Suomi, there is now a 50-min update around 01:30 local time.

This second observation provides some information on the changing environment, but still cannot resolve parameter evolution or the diurnal cycle. For this, a geostationary-based (GEO) version of the DNB would be needed in order to overcome this principal limitation. Having a sensor that can provide low-light visible sensitivity from GEO would represent a significant advance over current nighttime imaging capabilities represented by the VIIRS DNB. A pioneering study on the temporal dynamics of urban lights was done by Dobler et al. (2015), using horizontal images from a fixed camera, every 10s over 22 nights, demonstrating the type of information which can be derived from continuous monitoring of artificial lights throughout the night. Frequent monitoring of the Earth at night from sunset to sunrise will allow researchers to uncover circadian patterns of human activity, not only to quantify temporal changes in light pollution, but also to better inform us on changes in ambient population during night-time, e.g., people working at night, or attending various night-time events.

Such a GEO platform would allow stare and thereby attain signal-to-noise on par or better (by a factor of 10) than the VIIRS/DNB. Dual proposing a nighttime GEO instrument as a star tracker, and conducting multiple intermittent read-outs over the ~20s sampling interval, would further allow the instrument to achieve the necessary navigation and stability requirements for this measurement to attain 700 m resolution. It would be very useful, but not required, to coordinate nighttime GEO operations with a contemporary geostationary sensor (e.g., the Advanced Baseline Imager on GOES-R) to leverage additional spectral information from those sensors. As noted in Miller et al. (2013), combining the visible band with near infrared (conventional) and thermal bands would further expand the utility of the low-light observations. For instance, a geostationary lowlight visible sensor, combined with shortwave and thermal infrared bands from co-located ABI observations, would be able to retrieve both cloud optical depth and effective particle size via moonlight, leading to improved estimates of cloud water path.

So far, the only occasion that a sensor acquired a full night-time image of the entire hemisphere (as a geostationary satellite would be able to do) showing artificial lights was in the ESA - Rosetta mission. In three occasions the prove ESA - Rosetta made flybys over the Earth to get the gravitational assistants it needed to change direction to its main scientific goal, the comet 67P/Churiumov-Guerasimenko. The team took images of the Earth during these flybys, and currently these images still the only images of the Earth at night taken from a position where it is possible to see the full earth at night (other images available are renders or mosaics of individual images or scans). These images where taken with the camera OSIRIS (Keller et. al. 2007) on the filters “Blue”, “Green”, “Orange”. Unfortunately, these images are only available on the raw format and Level 3 calibration. The difficulty of their reduction and georeferencing have therefore limited their use in peer review publications, although they are freely available at the ESA archive (https://archives.esac.esa.int/psa/) (Figure 27).

Figure 27: OSIRIS view of Earth by night. This is a composite of four images combined to show the illuminated crescent of Earth and the cities of the northern hemisphere. The images were acquired with the OSIRIS Wide Angle Camera (WAC) during Rosetta's second Earth swing-by on 13 November. This image showing islands of light created by human habitation (from the Nile River on the upper left side, to eastern China on the upper right side) was taken with the OSIRIS WAC at 19:45 CET, about 2 hours before the closest approach of the spacecraft to Earth. At the time, Rosetta was about 80 000 km above the Indian Ocean where the local time approached midnight. The image was taken with a five-second exposure of the WAC with the red filter. This image showing Earth's illuminated crescent was taken with the WAC at 20:05 CET as Rosetta was about 75 000 km from Earth. The crescent seen is around Antarctica. The image is a colour composite combining images obtained at various wavelengths. Source: http://www.esa.int/spaceinimages/Images/2007/11/OSIRIS_view_of_Earth_by_night

4.8.2 Spectral information

Artificial lighting sources vary in their emission spectra from the sun's emission and from each other (Aubé et al., 2013; Figure 24). To better estimate the negative effects of light pollution, various spectral indices have been proposed, including the Melatonin Suppression Index (MSI), the Induced Photosynthesis Index (IPI) and the Star Light Index (SLI) (Aubé et al., 2013), which also allow to compare the impacts of different lamp types on different species based on their spectral response curves (Longcore et al., 2018). With hyperspectral data, the major types of artificial lighting sources can be separated (Dobler et al., 2016). However, the majority of available space borne sensors are panchromatic, with only ISS photos and the new Jilin-1 satellite offering RGB color images (Table 1). As noted above, the panchromatic channel on the DMSP/OLS and VIIRS/DNB does not cover the blue light, thereby important spectral information is missing, which will become even more crucial as more cities change their street lighting technology to LED (Kyba et al., 2015a). Future night-time sensors designed for monitoring artificial lights should therefore include the blue band, and offer several spectral bands in the VIS-NIR range, so as to enable the identification of lighting types, and so as to fit human scotopic and photopic vision (Elvidge et al., 2007b). Investigating the optimal spectral band combination, Elvidge et al. (2010) concluded that the best set of spectral bands (in terms of cost and efficiency) would include at least four bands: the blue, green, red and NIR (as on Landsat). Such a combination of bands which will enable the identification of major types of lighting, and will also allow the estimation of the luminous efficacy of radiation, and the correlated color temperature, but not will enable to estimate other properties, such as the color rendering index (Elvidge et al., 2010). With the transition to LEDs, we are facing the global challenge of how to reduce light pollution, in spite of this new technology which allows to light up more areas at lower costs. One direction can be the application of light pollution metrics (such as developed by Aubé et al., 2013 and by Longcore et al., 2018) which will be placed on packages of bulb, to better inform consumers on possible light pollution impacts, similar to information provided on food packages concerning their ingredients, allergens, and dietary information (Tangari and Smith, 2012).

4.8.3 Spatial resolution

Numerous studies have made great use of available night-time sensors (mostly DMSP/OLS and VIIRS/DNB) to study the spatial and temporal patterns of artificial light at night, and the anthropogenic and physical variables explaining it, at global, regional and national levels. However, most studies of night lights were not able to examine spatial patterns at the neighborhood or street level due to the lack of sensors with fine spatial resolution (Table 1). The spatial resolution of the majority of night-time space borne sensors is below 100 m, and freely available images of cities at spatial resolution which is better than 100 m are only available from astronaut photographs taken from the ISS. However, these images are not taken regularly, and are of varying radiometric and spatial quality. Night-time images with high spatial resolution (< 5 m) have been shown to enable the mapping and classification of individual lighting sources (e.g., Metcalf, 2012; Hale et al., 2013), and can enable us to better understand the nightscape as experience by animals within urban areas (Bennie et al., 2014b). However, high spatial resolution such as offered now by commercial satellites (such as EROS-B and Jilin-1) may not be needed for all applications. Indeed, several papers have shown that high spatial resolution of night time images did not improve our ability to explain spatial patterns of light pollution, and that better correlations were obtained at spatial resolutions of 50 – 100 m (Katz and Levin, 2016) or even at coarser spatial resolutions (e.g., Anderson et al., 2010). This result may relate to the combined artefact of night-time images becoming darker and with greater contrast between dark and bright areas with increasing spatial resolution (Kyba et al., 2015a; Katz and Levin, 2016). At high spatial resolutions there may also be greater differences between ground measurements of night-time brightness in the horizontal direction, and space borne measurements of night-time brightness, which only capture upward emissions of artificial lights (Katz and Levin, 2016). Indeed, in their evaluation of the required spatial resolution of a concept mission termed as NightSat, Elvidge et al. (2007b) estimated that a sensor with a spatial resolution of 50 – 100 m would suffice to present the major night-time features which are common to urban and rural areas. Such medium spatial resolution will also enable global monitoring of the Earth at night at a frequent revisit time, without requiring a constellation with too many satellites. With the rise in launch and use of cubesats (such as Planet Labs; Strauss, 2017), and the recent launch of the Luojia-1 cubesat (Jiang et al., 2018), this may offer a relatively cheap approach for providing global coverage of the Earth at night, at finer spatial resolutions than currently available. An additional research challenge, which relates to the need to better quantify the exposure to light pollution, requires us to develop methods to quantify and understand the differences between human exposure to night-time brightness both indoors (based on ground based sensors or on smart wearable technology, mobile device platforms or embedded platforms; Ko et al., 2015) vs. the exposure to night-time brightness outdoors (as measured by satellites).

5. Conclusions

Images of artificial lights at night directly observe human activity from space, and therefore enable a number of remote sensing applications either unique to night light sensing (e.g. monitoring illegal fishing, remotely sensing lighting technologies) or strongly complementing other types of remote sensing (e.g. evaluating the impacts of armed conflicts and disasters and the recovery from them, quantifying temporary and seasonal changes in population, studying urban change). The field of remote sensing of night lights has greatly expanded since the early 2000s, thanks to an increase in the number and quality of space and ground based sensors able to measure low levels of light in the visible band. This development has also had a major impact on the study of light pollution, which has grown in parallel with remote sensing of night lights. Nevertheless, despite the demonstrated value of night lights data, the sensors, algorithms, and products for night lights still lag far behind the state of the art in remote sensing based on reflected daylight, or in other spectral ranges. In particular, night lights data are generally taken at lower resolutions, lack temporal coverage, and most importantly lack multi- or hyperspectral data. This is of particular concern at the moment, because of the global shift in the night lights spectra due to the adoption of LED lights.

New and improved sensors and algorithms will not only allow a host of new remote sensing applications based on night lights data, they will also have a dramatic influence on our understanding of human influence on one of the most threatened environments on Earth's land surface: the night. In stark contrast to many other environmental stressors such as climate change due to greenhouse gasses or chemical pollution, reductions in light emissions reduce the degree of light pollution and its environmental impact immediately. Whereas reducing greenhouse gas levels requires coordinated global action, light pollution depends overwhelmingly on local actors. Many of the transitions needed to achieve a sustainable society, such as emissions free transportation, are difficult problems that still require considerable research and likely changes in behavior. Methods to eliminate waste light, on the other hand, are already well known (e.g. Falchi et al. 2011); lights must simply be directed more carefully (which LEDs can help with), in many cases overall light levels must be reduced, and in other cases, lights can simply be turned off. Fortunately, it has been demonstrated that reductions in overall light emission can be accomplished while actually improving vision over current practice (e.g. Narendran et al. 2016).

The main challenge facing the transition to sustainable lighting is one of awareness. Future night lights data will play a key role in this regard. The data will be used to visualize changes in light emission and light pollution, identify and quantify emissions from specific polluters, and evaluate the effectiveness of light pollution mitigation strategies.

Acknowledgements

CCMK acknowledges funding from the European Union's Horizon 2020 research and innovation programme under grant agreement no. 689443 via project GEOEssential, and funding from the Helmholtz Association Initiative and Networking Fund under grant ERC-RA-0031. Some aspects of this manuscript were based upon work from COST Action ES1204 LoNNe (Loss of the Night Network), supported by COST (European Cooperation in Science and Technology). ASdM acknowledges funding from the EMISS@N project (NERC grant NE/P01156X/1) and the Cities at Night project. QLZ acknowledges funding from the One Hundred Talents Program of the Chinese Academy of Science ([2015], No. 70). AJ is supported by the Leibniz Association, Germany within the ILES (SAW-2015-IGB-1) and CONNECT (SAW-K45/2017) projects and by the IGB Leibniz Institute through the Frontiers in Freshwater Science project (IGB Frontiers 2017). Black Marble product suite data created at NASA's Goddard Space Flight Center with support from the NASA's Earth Observing System Data and Information System, Terrestrial Ecology, and Group on Earth Observations programs under grants NNH16ZDA001N-GEO-0055 and NNH17ZDA001N-TASNPP-0007. Finally, we would like to pay our respects to Abraham Haim, who passed away this January. Abraham was a leader in the field of ecological and health impacts of artificial light, and was involved in a number of studies relating remotely sensed night lights data to human health impacts.

References

Abrahams, A., Oram, C., & Lozano-Gracia, N. (2018). Deblurring dmsp nighttime lights: a new method using gaussian filters and frequencies of illumination. *Remote Sensing of Environment, 210*, 242-258.

Akbari, H., Menon, S., & Rosenfeld, A. (2009). Global cooling: increasing world-wide urban albedos to offset co 2. *Climatic Change, 94*(3-4), 275-286.

Alamús, R., Bará, S., Corbera, J., Escofet, J., Palà, V., Pipia, L., & Tardà, A. (2017). Ground-based hyperspectral analysis of the urban nightscape. *ISPRS Journal of Photogrammetry and Remote Sensing*, *124*, 16-26.

Álvarez-Berríos, N.L., Parés-Ramos, I.K., & Aide, T.M. (2013). Contrasting patterns of urban expansion in Colombia, Ecuador, Peru, and Bolivia Between 1992 and 2009. *Ambio, 42*, 29-40.

Amaral, S., Câmara, G., Monteiro, A. M. V., Quintanilha, J. A., & Elvidge, C. D. (2005). Estimating population and energy consumption in Brazilian Amazonia using DMSP night-time satellite data. *Computers, Environment and Urban Systems*, 29(2), 179-195.

American Association for the Advancement of Science (2013). Conflict in Aleppo, Syria: A Retrospective Analysis. In https://www.aaas.org/aleppo_retrospective

Anderson, S. J., Tuttle, B. T., Powell, R. L., & Sutton, P. C. (2010). Characterizing relationships between population density and nighttime imagery for Denver, Colorado: issues of scale and representation. *International Journal of Remote Sensing*, *31*(21), 5733-5746.

Andreić, Ž., & Andreić, D. (2010). Some Aspects of Light Pollution in the Near Infrared. In 3rd International Symposium for Dark-sky Parks and 3rd International Dark-sky Camp.

Aubé, M., & Kocifaj, M. (2012). Using two light-pollution models to investigate artificial sky radiances at Canary Islands observatories. *Monthly Notices of the Royal Astronomical Society*, *422*(1), 819-830.

Aubé, M., Roby, J., & Kocifaj, M. (2013). Evaluating potential spectral impacts of various artificial lights on melatonin suppression, photosynthesis, and star visibility. *PloS one*, *8*(7), e67798.

Aubé, M. (2015). Physical behaviour of anthropogenic light propagation into the nocturnal environment. *Phil. Trans. R. Soc. B*, *370*(1667), 20140117.

Aubé, M., Kocifaj, M., Zamorano, J., Lamphar, H. S., & de Miguel, A. S. (2016). The spectral amplification effect of clouds to the night sky radiance in Madrid. *Journal of Quantitative Spectroscopy and Radiative Transfer*, *181*, 11-23.

Aubé, M., Simoneau, A., Wainscoat, R., & Nelson, L. (2018). Modelling the effects of phosphor converted LED lighting to the night sky of the Haleakala Observatory, Hawaii. *Monthly Notices of the Royal Astronomical Society*, *478*(2), 1776-1783.

Aubrecht, C., Elvidge, C. D., Ziskin, D., Baugh, K. E., Tuttle, B., Erwin, E., & Kerle, N. (2009). Observing power blackouts from space-A disaster related study. *EGU General Assembly: Geophysical Research Abstracts; European Geosciences Union: Vienna, Austria*, 1-2.

Azam, C., Le Viol, I., Julien, J. F., Bas, Y., & Kerbiriou, C. (2016). Disentangling the relative effect of light pollution, impervious surfaces and intensive agriculture on bat activity with a national-scale monitoring program. Landscape Ecology, 31(10), 2471-2483.

Bai, Y., Cao, C., & Shao, X. (2015). Assessment of scan-angle dependent radiometric bias of Suomi-NPP VIIRS day/night band from night light point source observations. In *Earth Observing Systems XX* (Vol. 9607, p. 960727). International Society for Optics and Photonics.

Ban, Y., Jacob, A., & Gamba, P. (2015). Spaceborne sar data for global urban mapping at 30 m resolution using a robust urban extractor. *Isprs Journal of Photogrammetry & Remote Sensing*, 103, 28-37.

Bará, S., Espey, B., Falchi, F., Kyba, C. C. M., & Nievas Rosillo, M. (2015). Report of the 2014 LoNNe intercomparison campaign. *URL: http://eprints. ucm. es/32989/(Accessed 13 May 2016)*.

Bará, S. (2017). Characterizing the zenithal night sky brightness in large territories: how many samples per square kilometre are needed?. *Monthly Notices of the Royal Astronomical Society*, 473(3), 4164-4173.

Bará, S., Rodríguez-Arós, Á., Pérez, M., Tosar, B., Lima, R. C., de Miguel, A. S., & Zamorano, J. (2018). Estimating the relative contribution of streetlights, vehicles and residential lighting to the urban night sky brightness. *Lighting Research Tecnhology*. https://doi.org/10.1177/1477153518808337.

Bará, S., Rigueiro, I., & Lima, R. C. (2019). Monitoring transition: expected night sky brightness trends in different photometric bands. *Journal of Quantitative Spectroscopy and Radiative Transfer*, 106644. https://doi.org/10.1016/j.jqsrt.2019.106644

Barentine, J. C., Walker, C. E., Kocifaj, M., Kundracik, F., Juan, A., Kanemoto, J., & Monrad, C. K. (2018). Skyglow changes over Tucson, Arizona, resulting from a municipal LED street lighting conversion. *Journal of Quantitative Spectroscopy and Radiative Transfer*, *212*, 10-23.

Bauer SE, Wagner SE, Burch J, Bayakly R, Vena JE. (2013) A case-referent study: light at night and breast cancer risk in Georgia. *International Journal of Health Geographies,* 12, 23.

Baugh, K., Elvidge, C. D., Ghosh, T., & Ziskin, D. (2010). Development of a 2009 stable lights product using DMSP-OLS data. *Proceedings of the Asia-Pacific Advanced Network*, 30, 114-130.

Belward, A. S., & Skøien, J. O. (2015). Who launched what, when and why; trends in global land-cover observation capacity from civilian earth observation satellites. *ISPRS Journal of Photogrammetry and Remote Sensing*, 103, 115-128.

Bennett, M. M., & Smith, L. C. (2017). Advances in using multitemporal night-time lights satellite imagery to detect, estimate, and monitor socioeconomic dynamics. *Remote Sensing of Environment*, 192, 176-197.

Bennie, J., Davies, T. W., Duffy, J. P., Inger, R., & Gaston, K. J. (2014a). Contrasting trends in light pollution across Europe based on satellite observed night time lights. *Scientific Reports*, *4*, 3789.

Bennie, J., Davies, T. W., Inger, R., & Gaston, K. J. (2014b). Mapping artificial lightscapes for ecological studies. *Methods in Ecology and Evolution*, 5, 534-540.

Bhaduri, B., Bright, E., Coleman, P., & Dobson, J. (2002). LandScan. *Geoinformatics*, *5*(2), 34-37.

Biggs, J. D., Fouché, T., Bilki, F., & Zadnik, M. G. (2012). Measuring and mapping the night sky brightness of Perth, Western Australia. Monthly Notices of the Royal Astronomical Society, 421(2), 1450-1464.

STV(2011),Bron/Broen,https://www.svt.se/bron/

Burne, B. H. (1972). Pollution by light. *The Lancet*, 299(7751), 642.

Cabrera-Cruz, S. A., Smolinsky, J. A., & Buler, J. J. (2018). Light pollution is greatest within migration passage areas for nocturnally-migrating birds around the world. *Scientific Reports*, *8*(1), 3261.

Calegari,G. R., Nasi, N. and Celino, I.(2018): "Human Computation vs. Machine Learning: an Experimental Comparison for Image Classification", *Human Computation Journal*, 5 (1), 13-30, DOI: 10.15346/hc.v5i1.2, 2018.

Cao, X., Hu, Y., Zhu, X., Shi, F., Zhuo, L., & Chen, J. (2019). A simple self-adjusting model for correcting the blooming effects in DMSP-OLS nighttime light images. *Remote Sensing of Environment*, 224, 401-411.

Cha, J. S., Lee, J. W., Lee, W. S., Jung, J. W., Lee, K. M., Han, J. S., & Gu, J. H. (2014). Policy and status of light pollution management in Korea. *Lighting Research & Technology*, *46*(1), 78-88.

Cao, C., & Bai, Y. (2014). Quantitative analysis of VIIRS DNB nightlight point source for light power estimation and stability monitoring. *Remote Sensing*, 6(12), 11915-11935.

Cao, X., Chen, J., Imura, H., & Higashi, O. (2009). A SVM-based method to extract urban areas from DMSP-OLS and SPOT VGT data. *Remote Sensing of Environment, 113*, 2205-2209.

Cao, C., Shao, X., & Uprety, S. (2013). Detecting light outages after severe storms using the S-NPP/VIIRS day/night band radiances. *IEEE Geoscience and Remote Sensing Letters*, *10*(6), 1582-1586.

Castrence, M., Nong, D.H., Tran, C.C., Young, L., & Fox, J. (2014). Mapping Urban Transitions Using Multi-Temporal Landsat and DMSP-OLS Night-Time Lights Imagery of the Red River Delta in Vietnam. *Land, 3*, 148-166.

Chand, T. K., Badarinath, K. V. S., Murthy, M. S. R., Rajshekhar, G., Elvidge, C. D., & Tuttle, B. T. (2007). Active forest fire monitoring in Uttaranchal State, India using multi-temporal DMSP-OLS and MODIS data. *International Journal of Remote Sensing*, 28(10), 2123-2132.

Chen, X., & Nordhaus, W.D. (2011). Using luminosity data as a proxy for economic statistics. *Proceedings of the National Academy of Sciences, 108*, 8589-8594.

Chen, Z., Yu, B., Song, W., Liu, H., Wu, Q., Shi, K., & Wu, J. (2017). A new approach for detecting urban centers and their spatial structure with nighttime light remote sensing. *IEEE Transactions on Geoscience and Remote Sensing*, 55(11), 6305-6319.

Cho, Y., Ryu, S. H., Lee, B. R., Kim, K. H., Lee, E., & Choi, J. (2015). Effects of artificial light at night on human health: A literature review of observational and experimental studies applied to exposure assessment. Chronobiology International, 32(9), 1294-1310.

Chuvieco, E., Mouillot, F., van der Werf, G. R., San Miguel, J., Tanasse, M., Koutsias, N., ... & Heil, A. (2019). Historical background and current developments for mapping burned area from satellite Earth observation. Remote Sensing of Environment, 225, 45-64.

Cinzano, P., Falchi, F., & Elvidge, C. D. (2001). The first world atlas of the artificial night sky brightness. *Monthly Notices of the Royal Astronomical Society*, *328*(3), 689-707.

Clark, R. N., & Roush, T. L. (1984). Reflectance spectroscopy: Quantitative analysis techniques for remote sensing applications. *Journal of Geophysical Research: Solid Earth*, *89*(B7), 6329-6340.

Clark, H., Pinkovskiy, M., & Sala-i-Martin, X. (2017). China's GDP Growth May be Understated. In: National Bureau of Economic Research

Coesfeld, J., Anderson, S., Baugh, K., Elvidge, C., Schernthanner, H., & Kyba, C. (2018). Variation of individual location radiance in VIIRS DNB monthly composite images. *Remote Sensing*, 10(12), 1964.

Cleaver, O. P. (1943). Control of Coastal Lighting in Anti-Submarine Warfare (No. 746). Engineer Board Fort Belvoir VA.

Collier, P. (1994). Innovative military mapping using aerial photography in the First World War: Sinai, Palestine and Mesopotamia 1914–1919. *The Cartographic Journal*, *31*(2), 100-104.

Collison, F. M., & Poe, K. (2013). "Astronomical tourism": The astronomy and dark sky program at Bryce Canyon National park. *Tourism Management Perspectives*, 7, 1-15.

Colomb, R., Alonso, C., & Nollmann, I. (2003). SAC-C mission and the international am constellation for earth observation. *Acta Astronautica*, 52(9-12), 995-1006.

Croft, T.A., (1973), Burning waste gas in oil fields, *Nature*, 245, 375-376.

Croft, T.A., (1978), Night-time images of the Earth from space, Scientific American, 239, 68-79.

Croft, T. A. (1979). The brightness of lights on Earth at night, digitally recorded by DMSP satellite (No. 80-167). US Geological Survey.

Crutzen, P. J. (2002). Geology of mankind. *Nature*, 415(6867), 23.

Dashora, A., Lohani, B., & Malik, J. N. (2007). A repository of earth resource information–CORONA satellite programme. Current Science, 92(7), 926-932.

Davies, T. W., & Smyth, T. (2018). Why artificial light at night should be a focus for global change research in the 21st century. *Global Change Biology*, *24*(3), 872-882.

Davies, T. W., Duffy, J. P., Bennie, J., & Gaston, K. J. (2014). The nature, extent, and ecological implications of marine light pollution. *Frontiers in Ecology and the Environment*, *12*(6), 347-355.

den Outer, P., Lolkema, D., Haaima, M., Hoff, R. V. D., Spoelstra, H., & Schmidt, W. (2011). Intercomparisons of nine sky brightness detectors. *Sensors*, *11*(10), 9603-9612.

Dickinson, L. G., Boselly III, S. E., & Burgmann, W. S. (1974). Defense Meteorological Satellite Program (DMSP)-User's Guide (No. AWS-TR-74-250). Air Weather Service Scott AFB IL.

Diner, D. J., Bruegge, C. J., Martonchik, J. V., Ackerman, T. P., Davies, R., Gerstl, S. A., ... & Danielson, E. D. (1989). MISR: A multiangle imaging spectroradiometer for geophysical and climatological research from EOS. *IEEE Transactions on Geoscience and Remote Sensing*, *27*(2), 200-214.

Dobler, G., Ghandehari, M., Koonin, S. E., Nazari, R., Patrinos, A., Sharma, M. S., ... & Wurtele, J. S. (2015). Dynamics of the urban lightscape. *Information Systems*, *54*, 115-126.

Dobler, G., Ghandehari, M., Koonin, S. E., & Sharma, M. S. (2016). A Hyperspectral Survey of New York City Lighting Technology. *Sensors*, *16*(12), 2047.

Doll, C. N. (2008). CIESIN thematic guide to night-time light remote sensing and its applications. Center for International Earth Science Information Network of Columbia University, Palisades, NY.

Doll, C. H., Muller, J. P., & Elvidge, C. D. (2000). Night-time imagery as a tool for global mapping of socioeconomic parameters and greenhouse gas emissions. *AMBIO: a Journal of the Human Environment*, *29*(3), 157-162.

Doll, C.N.H., Muller, J.-P., & Morley, J.G. (2006). Mapping regional economic activity from night-time light satellite imagery. *Ecological Economics, 57*, 75-92

Duriscoe, D. M., Luginbuhl, C. B., & Moore, C. A. (2007). Measuring Night-Sky Brightness with a Wide-Field CCD Camera. *Publications of the Astronomical Society of the Pacific*, *119*(852), 192.

Duriscoe, D. M. (2016). Photometric indicators of visual night sky quality derived from all-sky brightness maps. Journal of Quantitative Spectroscopy and Radiative Transfer, 181, 33-45.

Edison, T. A. (1880). The Success of the Electric Light. N. American Rev., 131(287), 295–300.

Ehrlich, D., Estes, J. E., & Singh, A. (1994). Applications of NOAA-AVHRR 1 km data for environmental monitoring. International Journal of Remote Sensing, 15(1), 145-161.

Elvidge, C. D., Kroehl, H. W., Kihn, E. A., Baugh, K. E., Davis, E. R., & Hao, W. M. (1996). Algorithm for the retrieval of fire pixels from DMSP operational linescan system data. *Biomass burning and global change: Remote sensing, modeling and inventory development, and biomass burning in Africa*, *1*, 73-85.

Elvidge, C. D., Baugh, K. E., Kihn, E. A., Kroehl, H. W., Davis, E. R., & Davis, C. W. (1997a). Relation between satellite observed visible-near infrared emissions, population, economic activity and electric power consumption. *International Journal of Remote Sensing*, 18(6), 1373-1379.

Elvidge, C. D., Baugh, K. E., Kihn, E. A., Kroehl, H. W., & Davis, E. R. (1997b). Mapping city lights with nighttime data from the DMSP Operational Linescan System. *Photogrammetric Engineering and Remote Sensing*, 63(6), 727-734.

Elvidge, C. D., Baugh, K. E., Hobson, V. R., Kihn, E. A., & Kroehl, H. W. (1998). Detection of fires and power outages using DMSP-OLS data. *Remote Sensing Change Detection: Environmental Monitoring Methods and Applications*, 123-135. Ann Arbor Press: Chelsea, MI, USA.

Elvidge, C. D., Baugh, K. E., Dietz, J. B., Bland, T., Sutton, P. C., & Kroehl, H. W. (1999). Radiance calibration of DMSP-OLS low-light imaging data of human settlements. *Remote Sensing of Environment*, *68*(1), 77-88.

Elvidge, C. D., Imhoff, M. L., Baugh, K. E., Hobson, V. R., Nelson, I., Safran, J., ... & Tuttle, B. T. (2001a). Night-time lights of the world: 1994–1995. *ISPRS Journal of Photogrammetry and Remote Sensing*, 56(2), 81-99.

Elvidge, C. D., Nelson, I., Hobson, V. R., Safran, J., & Baugh, K. E. (2001b). Detection of fires at night using DMSP-OLS data. Global and Regional Vegetation Fire Monitoring from Space: Planning a Coordinated International Effort (Eds. Frank J. Ahern, Johann G. Goldammer and Christopher 0. Justice), 125-144. SPB Academic Publishing bv/The Hague/The Netherlands.

Elvidge, C. D., & Green, R. O. (2005). High-and low-altitude AVIRIS observations of nocturnal lighting. Proceedings of the 13th JPL Airborne Earth Science Workshop, Pasadena, California, May 24-27, 2005

Elvidge, C. D., Tuttle, B. T., Sutton, P. C., Baugh, K. E., Howard, A. T., Milesi, C., ... & Nemani, R. (2007a). Global distribution and density of constructed impervious surfaces. *Sensors*, 7(9), 1962-1979.

Elvidge, C. D., Cinzano, P., Pettit, D. R., Arvesen, J., Sutton, P., Small, C., ... & Weeks, J. (2007b). The Nightsat mission concept. *International Journal of Remote Sensing*, 28(12), 2645-2670.

Elvidge, C. D., Safran, J., Tuttle, B., Sutton, P., Cinzano, P., Pettit, D., ... & Small, C. (2007c). Potential for global mapping of development via a nightsat mission. *GeoJournal*, 69(1-2), 45-53.

Elvidge, C. D., Ziskin, D., Baugh, K. E., Tuttle, B. T., Ghosh, T., Pack, D. W., ... & Zhizhin, M. (2009a). A fifteen year record of global natural gas flaring derived from satellite data. *Energies*, 2(3), 595-622.

Elvidge, C.D., Sutton, P.C., Ghosh, T., Tuttle, B.T., Baugh, K.E., Bhaduri, B., & Bright, E. (2009b). A global poverty map derived from satellite data. *Computers & Geosciences, 35*, 1652-1660.

Elvidge, C. D., Erwin, E. H., Baugh, K. E., Ziskin, D., Tuttle, B. T., Ghosh, T., & Sutton, P. C. (2009c). Overview of DMSP nightime lights and future possibilities. In 2009 Joint Urban Remote Sensing Event (pp. 1-5). IEEE.

Elvidge, C. D., Keith, D. M., Tuttle, B. T., & Baugh, K. E. (2010). Spectral identification of lighting type and character. *Sensors*, 10(4), 3961-3988.

Elvidge, C., Baugh, K., Anderson, S., Sutton, P., & Ghosh, T. (2012). The Night Light Development Index (NLDI): a spatially explicit measure of human development from satellite data. *Social Geography, 7*, 23-35

Elvidge, C. D., Baugh, K. E., Zhizhin, M., & Hsu, F. C. (2013a). Why VIIRS data are superior to DMSP for mapping nighttime lights. In *Proceedings of the Asia-Pacific Advanced Network* (Vol. 35, No. 62).

Elvidge, C. D., Zhizhin, M., Hsu, F. C., & Baugh, K. E. (2013b). VIIRS nightfire: Satellite pyrometry at night. *Remote Sensing*, *5*(9), 4423-4449.

Elvidge, C. D., Zhizhin, M., Hsu, F. C., & Baugh, K. (2013c). What is so great about nighttime VIIRS data for the detection and characterization of combustion sources. Proceedings of the Asia-Pacific Advanced Network, 35(0), 33.

Elvidge, C. D., Zhizhin, M., Baugh, K., Hsu, F. C., & Ghosh, T. (2015a). Methods for global survey of natural gas flaring from visible infrared imaging radiometer suite data. *Energies*, *9*(1), 14.

Elvidge, C. D., Zhizhin, M., Baugh, K., & Hsu, F. C. (2015b). Automatic boat identification system for VIIRS low light imaging data. *Remote Sensing*, *7*(3), 3020-3036.

Elvidge, C. D., Baugh, K., Zhizhin, M., Hsu, F. C., & Ghosh, T. (2017). VIIRS night-time lights. *International Journal of Remote Sensing*, 38(21), 5860-5879.

Elvidge, C. D., Ghosh, T., Baugh, K., Zhizhin, M., Hsu, F. C., Katada, N. S., Penalosa, W., & Hung, B. Q. (2018). Rating the effectiveness of fishery closures with Visible

Infrared Imaging Radiometer Suite boat detection data. *Frontiers in Marine Science*, section Marine Conservation and Sustainability, *5*, 132.

Elvidge, C. D., Zhizhin, M., Baugh, K., Hsu, F. C., & Ghosh, T. (2019). Extending nighttime combustion source detection limits with short wavelength VIIRS Data. *Remote Sensing*, 11(4), 395.

Falchi, F., Cinzano, P., Elvidge, C. D., Keith, D. M., & Haim, A. (2011). Limiting the impact of light pollution on human health, environment and stellar visibility. *Journal of Environmental Management*, 92(10), 2714-2722.

Falchi, F., Cinzano, P., Duriscoe, D., Kyba, C. C., Elvidge, C. D., Baugh, K., ... & Furgoni, R. (2016). The new world atlas of artificial night sky brightness. *Science Advances*, *2*(6), e1600377.

Farges, T., & Blanc, E. (2016). Characteristics of lightning, sprites, and human-induced emissions observed by nadir-viewing cameras on board the International Space Station. Journal of Geophysical Research: *Atmospheres*, 121(7), 3405-3420.

Fiorentin, P., Bettanini, C., Lorenzini, E., Aboudan, A., Colombatti, G., Ortolani, S., & Bertolo, A. (2018, June). MINLU: An Instrumental Suite for Monitoring Light Pollution from Drones or Airballoons. In 2018 5th IEEE International Workshop on Metrology for AeroSpace (MetroAeroSpace) (pp. 274-278). IEEE.

Fouquet, R., & Pearson, P. J. (2006). Seven centuries of energy services: The price and use of light in the United Kingdom (1300-2000). *The Energy Journal*, 139-177.

Forbes, D.J. (2013). Multi-scale analysis of the relationship between economic statistics and DMSP-OLS night light images. *Giscience & Remote Sensing, 50*, 483-499

Gallaway, T. (2010). On light pollution, passive pleasures, and the instrumental value of beauty. *Journal of Economic Issues*, *44*(1), 71-88.

Garcia-Saenz A., Sánchez de Miguel A., Espinosa A., Valentín A., Aragonés N., Llorca J., Amiano P., Martín Sánchez V., Guevara M., Capelo R., Tardón A., Peiró-Pérez R., Jiménez-Moleón JJ., Roca-Barceló A., Pérez-Gómez B., Dierssen-Sotos T., Fernández-Villa T., Moreno-Iribas C., Moreno V., García-Pérez J., Castaño-Vinyals G., Pollán M., Aubé M., Kogevinas M. (2018) Evaluating the association between artificial light-at-night exposure and breast and prostate cancer risk in Spain (MCC-Spain study). *Environmental Health Perspectives* 126(4):047011

Gaston, K. J., Bennie, J., Davies, T. W., & Hopkins, J. (2013). The ecological impacts of nighttime light pollution: a mechanistic appraisal. *Biological Reviews*, *88*(4), 912-927.

Gaston, K. J., Duffy, J. P., & Bennie, J. (2015). Quantifying the erosion of natural darkness in the global protected area system. *Conservation Biology*, *29*(4), 1132-1141.

Geronimo, R., Franklin, E., Brainard, R., Elvidge, C., Santos, M., Venegas, R., & Mora, C. (2018). Mapping Fishing Activities and Suitable Fishing Grounds Using Nighttime Satellite Images and Maximum Entropy Modelling. *Remote Sensing*, *10*(10), 1604.

Ges, X., Bará, S., García-Gil, M., Zamorano, J., Ribas, S. J., & Masana, E. (2018). Light pollution offshore: zenithal sky glow measurements in the Mediterranean coastal waters. *Journal of Quantitative Spectroscopy and Radiative Transfer*, 210, 91-100.

Ghosh, T., Powell, R.L., Elvidge, C.D., Baugh, K.E., Sutton, P.C., & Anderson, S. (2010). Shedding light on the global distribution of economic activity. *The Open Geography Journal, 3*, 148-161

Giordano, E., & Ong, C. E. (2017). Light festivals, policy mobilities and urban tourism. *Tourism Geographies*, *19*(5), 699-716.

Gillespie, T. W., Frankenberg, E., Fung Chum, K., & Thomas, D. (2014). Night-time lights time series of tsunami damage, recovery, and economic metrics in Sumatra, Indonesia. Remote Sensing Letters, 5(3), 286-294.

Goldblatt, R., Stuhlmacher, M. F., Tellman, B., Clinton, N., Hanson, G., Georgescu, M., ... & Balling, R. C. (2018). Using Landsat and nighttime lights for supervised pixel-based image classification of urban land cover. *Remote Sensing of Environment*, *205*, 253-275.

Green, J., Perkins, C., Steinbach, R., & Edwards, P. (2015). Reduced street lighting at night and health: a rapid appraisal of public views in England and Wales. *Health & place*, *34*, 171-180.

Guo, W., Lu, D., Wu, Y., & Zhang, J. (2015). Mapping impervious surface distribution with integration of snnp viirs-dnb and modis ndvi data. *Remote Sensing, 7*(9), 12459-12477.

Gutman, P. (2007). Ecosystem services: foundations for a new rural–urban compact. *Ecological Economics, 62*(3), 383-387.

Haim, A., & Portnov, B. A. (2013). *Light pollution as a new risk factor for human breast and prostate cancers* (p. 168). Dordrecht: Springer.

Hale, J. D., Davies, G., Fairbrass, A. J., Matthews, T. J., Rogers, C. D., & Sadler, J. P. (2013). Mapping lightscapes: spatial patterning of artificial lighting in an urban landscape. *PloS one*, 8(5), e61460.

Hale, J. D., Fairbrass, A. J., Matthews, T. J., Davies, G., & Sadler, J. P. (2015). The ecological impact of city lighting scenarios: exploring gap crossing thresholds for urban bats. Global Change Biology, 21(7), 2467-2478.

Halpern, B. S., Walbridge, S., Selkoe, K. A., Kappel, C. V., Micheli, F., D'agrosa, C., ... & Fujita, R. (2008). A global map of human impact on marine ecosystems. *Science*, *319*(5865), 948-952.

Halpern, B. S., Frazier, M., Potapenko, J., Casey, K. S., Koenig, K., Longo, C., ... & Walbridge, S. (2015). Spatial and temporal changes in cumulative human impacts on the world’s ocean. *Nature communications*, *6*, 7615.

Hansen, M. C., Potapov, P. V., Moore, R., Hancher, M., Turubanova, S. A. A., Tyukavina, A., ... & Kommareddy, A. (2013). High-resolution global maps of 21st-century forest cover change. *Science*, 342(6160), 850-853.

Hänel, A., Posch, T., Ribas, S. J., Aubé, M., Duriscoe, D., Jechow, A., ... & Spoelstra, H. (2018). Measuring night sky brightness: methods and challenges. *Journal of Quantitative Spectroscopy and Radiative Transfer*. 205, 278-290.

Hao, R., Yu, D., Sun, Y., Cao, Q., Liu, Y., & Liu, Y. (2015). Integrating multiple source data to enhance variation and weaken the blooming effect of DMSP-OLS light. *Remote Sensing*, 7(2), 1422-1440.

He, C., Shi, P., Li, J., Chen, J., Pan, Y., Li, J., ... & Ichinose, T. (2006). Restoring urbanization process in China in the 1990s by using non-radiance-calibrated DMSP/OLS nighttime light imagery and statistical data. *Chinese Science Bulletin*, *51*(13), 1614-1620.

Henderson, V., Storeygard, A., & Weil, D.N. (2011). A bright idea for measuring economic growth. *American Economic Review, 101*, 194-199

Henderson, J.V., Storeygard, A., & Weil, D.N. (2012). Measuring economic growth from outer space. *American Economic Review, 102*, 994-1028

Henderson, J.V., Squires, T.L., Storeygard, A., & Weil, D.N. (2016). The Global Spatial Distribution of Economic Activity: Nature, History, and the Role of Trade. *National Bureau of Economic Research Working Paper Series, No. 22145*

Hiscocks, P. D., & Kyba, C. (2017). Maps of Light Pollution. *Journal of the Royal Astronomical Society of Canada*, *111*, 154.

Hoag, A. A., Schoening, W. E., & Coucke, M. (1973). City sky glow monitoring at Kitt Peak. *Publications of the Astronomical Society of the Pacific*, 85(507), 503.

Hoornweg, D., Freire, M., Lee, M. J., Bhada-Tata, P., & Yuen, B. (2011). *Cities and climate change: responding to an urgent agenda*. The World Bank.

Horton, K. G., Nilsson, C., Van Doren, B. M., La Sorte, F. A., Dokter, A. M., & Farnsworth, A. (2019). Bright lights in the big cities: migratory birds' exposure to artificial light. Frontiers in Ecology and the Environment.

Hölker, F., Wolter, C., Perkin, E. K., & Tockner, K. (2010a). Light pollution as a biodiversity threat. *Trends in Ecology & Evolution*, 25(12), 681-682.

Hölker, F., Moss, T., Griefahn, B., Kloas, W., Voigt, C. C., Henckel, D., ... & Franke, S. (2010b). The dark side of light: a transdisciplinary research agenda for light pollution policy. *Ecology and Society*, 15(4).

Hsu, F. C., Baugh, K. E., Ghosh, T., Zhizhin, M., & Elvidge, C. D. (2015). DMSP-OLS radiance calibrated nighttime lights time series with intercalibration. *Remote Sensing*, *7*(2), 1855-1876.

Hu, K., Qi, K., Guan, Q., Wu, C., Yu, J., Qing, Y., ... & Li, X. (2017). A scientometric visualization analysis for night-time light remote sensing research from 1991 to 2016. Remote Sensing, 9(8), 802.

Hu, Z., Hu, H., & Huang, Y. (2018a). Association between nighttime artificial light pollution and sea turtle nest density along Florida coast: A geospatial study using VIIRS remote sensing data. *Environmental Pollution*, *239*, 30-42.

Hu, S., Ma, S., Yan, W., Lu, W., & Zhao, X. (2018b). Feasibility of a specialized ground light source for night-time low-light calibration. International Journal of Remote Sensing, 39(8), 2543-2559.

Huang, Q., Yang, X., Gao, B., Yang, Y., & Zhao, Y. (2014). Application of DMSP/OLS nighttime light images: A meta-analysis and a systematic literature review. *Remote Sensing*, 6(8), 6844-6866.

Hurley S., Goldberg D., Nelson D., Hertz A., Horn-Ross P.L., Bernstein L., and Reynolds P. (2014) Light at Night and Breast Cancer Risk Among California Teachers, *Epidemiology*; 25(5): 697–706.

Hyde E., Frank S., Barentine J. C, Kuechly H., Kyba, C. C. (2019). Testing for changes in light emissions from certified International Dark Sky Places. International Journal of Sustainable Lighting, 21(1), 11-19.

Imhoff, M.L., Lawrence, W.T., Stutzer, D.C., & Elvidge, C.D. (1997). A technique for using composite DMSP/OLS "city lights" satellite data to map urban area. *Remote Sensing of Environment*, 61, 361-370.

Isenstadt, S., Petty, M. M., & Neumann, D. (2014). *Cities of light: Two centuries of urban illumination*. Routledge.

Jakle, J. A. (2001). *City lights: Illuminating the American night (landscapes of the night)*. John Hopkins University Press, Baltimore, MD, USA.

James P., Bertrand KA, Hart JE, Schernhammer ES, Tamimi RM, and Laden F. (2017) Outdoor Light at Night and Breast Cancer Incidence in the Nurses' Health Study II., *Environmental Health Perspectives,* 125(8), 087010.

Jean, N., Burke, M., Xie, M., Davis, W. M., Lobell, D. B., & Ermon, S. (2016). Combining satellite imagery and machine learning to predict poverty. *Science*, *353*(6301), 790-794.

Jechow, A., Kolláth, Z., Lerner, A., Hänel, A., Shashar, N., Hölker, F., & Kyba, C. (2017a). Measuring light pollution with fisheye lens imagery from a moving boat, a proof of concept. *International Journal of Sustainable Lighting* 19, 15-25.

Jechow, A., Kolláth, Z., Ribas, S. J., Spoelstra, H., Hölker, F., & Kyba, C. C. (2017b). Imaging and mapping the impact of clouds on skyglow with all-sky photometry. *Scientific Reports*, *7*(1), 6741.

Jechow, A., Hölker, F., & Kyba, C. (2018a). How dark can it get at night? Examining how clouds darken the sky via all-sky differential photometry. *arXiv preprint arXiv:1807.10593*.

Jechow, A., Ribas, S. J., Domingo, R. C., Hölker, F., Kolláth, Z., & Kyba, C. C. (2018b). Tracking the dynamics of skyglow with differential photometry using a digital camera with fisheye lens. *Journal of Quantitative Spectroscopy and Radiative Transfer*, *209*, 212-223.

Jechow, A., Hölker, F., & Kyba, C. C. (2019a). Using all-sky differential photometry to investigate how nocturnal clouds darken the night sky in rural areas. Scientific reports, 9(1), 1391.

Jechow, A., Kyba, C., & Hölker, F. (2019b). Beyond All-Sky: Assessing Ecological Light Pollution Using Multi-Spectral Full-Sphere Fisheye Lens Imaging. Journal of Imaging, 5(4), 46.

Jiang, W., He, G., Long, T., & Liu, H. (2017). Ongoing conflict makes Yemen dark: From the perspective of nighttime light. *Remote Sensing, 9*, 798

Jiang, W., He, G., Long, T., Guo, H., Yin, R., Leng, W., ... & Wang, G. (2018). Potentiality of Using Luojia 1-01 Nighttime Light Imagery to Investigate Artificial Light Pollution. *Sensors*, *18*(9), 2900.

Justice, C. O., Townshend, J. R. G., Vermote, E. F., Masuoka, E., Wolfe, R. E., Saleous, N., ... & Morisette, J. T. (2002). An overview of MODIS Land data processing and product status. *Remote sensing of Environment*, 83(1-2), 3-15.

Kamrowski, R. L., Limpus, C., Moloney, J., & Hamann, M. (2012). Coastal light pollution and marine turtles: assessing the magnitude of the problem. *Endangered Species Research*, *19*(1), 85-98.

Kamrowski, R. L., Limpus, C., Jones, R., Anderson, S., & Hamann, M. (2014). Temporal changes in artificial light exposure of marine turtle nesting areas. *Global Change Biology*, *20*(8), 2437-2449.

Katz, Y., & Levin, N. (2016). Quantifying urban light pollution—A comparison between field measurements and EROS-B imagery. *Remote Sensing of Environment*, 177, 65-77.

Keller, H. U., Barbieri, C., Lamy, P., Rickman, H., Rodrigo, R., Wenzel, K. P., ... & Bailey, M. E. (2007). OSIRIS–The scientific camera system onboard Rosetta. *Space Science Reviews*, 128(1-4), 433-506.

Kelly, I., Leon, J. X., Gilby, B. L., Olds, A. D., & Schlacher, T. A. (2017). Marine turtles are not fussy nesters: a novel test of small-scale nest site selection using structure from motion beach terrain information. PeerJ, 5, e2770.

Keshet-Sitton, A., Or-Chen, K., Huber, E., & Haim, A. (2017). Illuminating a risk for breast cancer: A preliminary ecological study on the association between streetlight and breast cancer. Integrative Cancer Therapies, 16(4), 451-463.

Kim, M. (2012). Modeling nightscapes of designed spaces–case studies of the University of Arizona and Virginia Tech campuses. In *13th international conference on Information Technology in landscape architecture proceedings* (pp. 455-463).

Kim K.Y., Lee E., Kim Y.J. and Kim J. (2017) The association between artificial light at night and prostate cancer in Gwangju City and South Jeolla Province of South Korea, *Chronobiology International*, 34(2), 203-211.

Kinzey, B. R., Perrin, T. E., Miller, N. J., Kocifaj, M., Aube, M., & Lamphar, H. A. (2017). *An investigation of LED street lighting's impact on sky glow* (No. PNNL-26411). Pacific Northwest National Lab.(PNNL), Richland, WA (United States).

Kloog I., Haim A. Richard G. Stevens R.G., Barchana M. and B.A. Portnov (2008) Light at Night Co-distributes with Incident Breast Cancer but not Lung Cancer in the Female Population of Israel, *Chronobiology International,* 25(1), 65–81.

Kloog I., Haim, A. Stevens R.G. and B.A. Portnov (2009a) The Global Co-Distribution of Light at Night (LAN) and Cancers of Prostate, Colon and Lung in Men, *Chronobiology International*, 26(1), 108 - 125.

Kloog I., Stevens R.G., Haim, A. and B.A. Portnov (2010) Nighttime light level co-distributes with breast cancer incidence worldwide, *Cancer Causes & Control,* 21, 2059–2068.

Ko, P. R. T., Kientz, J. A., Choe, E. K., Kay, M., Landis, C. A., & Watson, N. F. (2015). Consumer sleep technologies: a review of the landscape. Journal of Clinical Sleep Medicine, 11(12), 1455-1461.

Kocifaj, M. (2017). Retrieval of angular emission function from whole-city light sources using night-sky brightness measurements. *Optica*, *4*(2), 255-262.

Kocifaj, M., Solano-Lamphar, H. A., & Videen, G. (2019). Night-sky radiometry can revolutionize the characterization of light-pollution sources globally. Proceedings of the National Academy of Sciences, 116(16), 7712-7717.

Koen, E. L., Minnaar, C., Roever, C. L., & Boyles, J. G. (2018). Emerging threat of the 21st century lightscape to global biodiversity. Global Change Biology, 24(6), 2315-2324.

Kohiyama, M., Hayashi, H., Maki, N., Higashida, M., Kroehl, H. W., Elvidge, C. D., & Hobson, V. R. (2004). Early damaged area estimation system using DMSP-OLS night-time imagery. *International Journal of Remote Sensing*, *25*(11), 2015-2036.

Kolláth, Z., Dömény, A., Kolláth, K., & Nagy, B. (2016). Qualifying lighting remodelling in a Hungarian city based on light pollution effects. *Journal of Quantitative Spectroscopy and Radiative Transfer*, *181*, 46-51.

Kong, W., Cheng, J., Liu, X., Zhang, F., Fei, T. (2019). Incorporating nocturnal UAV side-view images with VIIRS data for accurate population estimation: a test at the urban administrative district scale. International Journal of Remote Sensing. https://doi.org/10.1080/01431161.2019.1615653

Koo YS, Song JY, Joo EY, Lee HJ, et al. (2016). Outdoor artificial light at night, obesity, and sleep health: Cross-sectional analysis in the KoGES study. *Chronobiology International*, 33 (3), 301–14.

Kotarba, A. Z., & Aleksandrowicz, S. (2016). Impervious surface detection with nighttime photography from the International Space Station. *Remote Sensing of Environment*, 176, 295-307.

Krisciunas, K., Bogglio, H., Sanhueza, P., & Smith, M. G. (2010). Light pollution at high zenith angles, as measured at Cerro Tololo Inter-American Observatory. *Publications of the Astronomical Society of the Pacific*, *122*(889), 373.

Kruse, F. A., & Elvidge, C. D. (2011, March). Identifying and mapping night lights using imaging spectrometry. In *Aerospace Conference*, 2011 IEEE (pp. 1-6). IEEE.

Kuechly, H. U., Kyba, C. C., Ruhtz, T., Lindemann, C., Wolter, C., Fischer, J., & Hölker, F. (2012). Aerial survey and spatial analysis of sources of light pollution in Berlin, Germany. *Remote Sensing of Environment*, 126, 39-50.

Kuffer, M., Pfeffer, K., Sliuzas, R., Taubenböck, H., Baud, I., & van Maarseveen, M. (2018). Capturing the Urban Divide in Nighttime Light Images From the International Space Station. *IEEE Journal of Selected Topics in Applied Earth Observations and Remote Sensing*.

Kyba, C. C., Ruhtz, T., Fischer, J., & Hölker, F. (2011). Cloud coverage acts as an amplifier for ecological light pollution in urban ecosystems. *PloS one*, *6*(3), e17307.

Kyba, C. C. M., Ruhtz, T., Fischer, J., & Hölker, F. (2012). Red is the new black: how the colour of urban skyglow varies with cloud cover. *Monthly Notices of the Royal Astronomical Society*, *425*(1), 701-708.

Kyba, C. C., & Hölker, F. (2013). Do artificially illuminated skies affect biodiversity in nocturnal landscapes? *Landscape Ecology* 28, 1637-1640.

Kyba, C. C., Wagner, J. M., Kuechly, H. U., Walker, C. E., Elvidge, C. D., Falchi, F., ... & Hölker, F. (2013a). Citizen science provides valuable data for monitoring global night sky luminance. *Scientific Reports*, 3, 1835.

Kyba, C. C., Ruhtz, T., Lindemann, C., Fischer, J., & Hölker, F. (2013b). Two camera system for measurement of urban uplight angular distribution. In *AIP Conference Proceedings* (Vol. 1531, No. 1, pp. 568-571). AIP.

Kyba, C., Garz, S., Kuechly, H., de Miguel, A. S., Zamorano, J., Fischer, J., & Hölker, F. (2015a). High-resolution imagery of earth at night: new sources, opportunities and challenges. *Remote Sensing*, 7(1), 1-23.

Kyba, C. C., Tong, K. P., Bennie, J., Birriel, I., Birriel, J. J., Cool, A., ... & Ehlert, R. (2015b). Worldwide variations in artificial skyglow. *Scientific Reports*, *5*, 8409.

Kyba, C. C., & Aronson, K. J. (2015). Assessing exposure to outdoor lighting and health risks. *Epidemiology*, *26*(4), e50.

Kyba, C. C., Kuester, T., de Miguel, A. S., Baugh, K., Jechow, A., Hölker, F., ... & Guanter, L. (2017). Artificially lit surface of Earth at night increasing in radiance and extent. *Science Advances*, 3(11), e1701528.

Kyba, C. C. (2018a). Is light pollution getting better or worse? *Nature Astronomy*, *2*(4), 267.

Kyba, C. C. M. (2018b). A proposed method for estimating regional and global changes in energy consumption for outdoor lighting, presented at 5th International Conference on Artificial Light at Night, Snowbird, USA, 12-14 November, 2018.

Kyba, C. C., Mohar, A., Pintar, G., & Stare, J. (2018c). A shining example of sustainable church lighting using the EcoSky LED: 96% reduction in energy consumption, and dramatic reduction of light pollution. *International Journal of Sustainable Lighting*, *20*(1), 1-10.

Kyba, C. C. M., & Spitschan, M. (2019). Comment on 'Domestic light at night and breast cancer risk: a prospective analysis of 105000 UK women in the Generations Study'. British Journal of Cancer, 120(2), 276.

La Sorte, F. A., Fink, D., Buler, J. J., Farnsworth, A., & Cabrera-Cruz, S. A. (2017). Seasonal associations with urban light pollution for nocturnally migrating bird populations. *Global Change Biology*, *23*(11), 4609-4619.

Lauer, D. T., Morain, S. A., & Salomonson, V. V. (1997). The Landsat program: Its origins, evolution, and impacts. *Photogrammetric Engineering and Remote Sensing*, 63(7), 831-838.

Laforet, V. and Pettit, D.R.(2015), Air,Press Syndication Group,ISBN-9780996058728

Levin, N. (2017). The impact of seasonal changes on observed nighttime brightness from 2014 to 2015 monthly VIIRS DNB composites. *Remote Sensing of Environment*, 193, 150-164.

Levin, N., & Duke, Y. (2012). High spatial resolution night-time light images for demographic and socio-economic studies. *Remote Sensing of Environment*, 119, 1-10.

Levin, N., & Phinn, S. (2016). Illuminating the capabilities of Landsat 8 for mapping night lights. *Remote Sensing of Environment*, 182, 27-38.

Levin, N., Johansen, K., Hacker, J. M., & Phinn, S. (2014). A new source for high spatial resolution night time images—The EROS-B commercial satellite. *Remote Sensing of Environment*, 149, 1-12.

Levin, N., Kark, S., & Crandall, D. (2015). Where have all the people gone? Enhancing global conservation using night lights and social media. *Ecological Applications*, *25*(8), 2153-2167.

Levin, N., Ali, S., & Crandall, D. (2018). Utilizing remote sensing and big data to quantify conflict intensity: The Arab Spring as a case study. *Applied Geography*, *94*, 1-17.

Levin, N., Ali, S., Crandall, D., & Kark, S. (2019). World Heritage in danger: Big data and remote sensing can help protect sites in conflict zones. *Global Environmental Change*, 55, 97-104.

Li, X., & Li, D. (2014). Can night-time light images play a role in evaluating the Syrian Crisis? *International Journal of Remote Sensing, 35*, 6648-6661Li, X., & Zhou, Y. (2017). Urban mapping using DMSP/OLS stable night-time light: a review. *International Journal of Remote Sensing*, 38(21), 6030-6046.

Li, X., & Zhou, Y. (2017). Urban mapping using DMSP/OLS stable night-time light: a review. *International Journal of Remote Sensing*, 38(21), 6030-6046.

Li, X., Xu, H., Chen, X., & Li, C. (2013a). Potential of NPP-VIIRS nighttime light imagery for modeling the regional economy of China. *Remote Sensing, 5*, 3057-3081

Li, X., Chen, F., & Chen, X. (2013b). Satellite-observed nighttime light variation as evidence for global armed conflicts. *IEEE Journal of Selected Topics in Applied Earth Observations and Remote Sensing, 6*, 2302-2315

Li, X., Zhang, R., Huang, C., & Li, D. (2015). Detecting 2014 Northern Iraq Insurgency using night-time light imagery. *International Journal of Remote Sensing, 36*, 3446-3458

Li, D., Zhao, X., & Li, X. (2016). Remote sensing of human beings–a perspective from nighttime light. *Geo-spatial Information Science*, 19(1), 69-79.

Li, X., Li, D., Xu, H., & Wu, C. (2017). Intercalibration between DMSP/OLS and VIIRS night-time light images to evaluate city light dynamics of Syria's major human settlement during Syrian Civil War. *International Journal of Remote Sensing*, 38(21), 5934-5951.

Li, X., Liu, S., Jendryke, M., Li, D., & Wu, C. (2018a). Night-Time Light Dynamics during the Iraqi Civil War. *Remote Sensing, 10*, 858

Li, X., Zhao, L., Li, D., & Xu, H. (2018b). Mapping urban extent using Luojia 1-01 nighttime light imagery. *Sensors*, 18(11), 3665.

Li, X., Li, X., Li, D., He, X., & Jendryke, M. (2019a). A preliminary investigation of Luojia-1 night-time light imagery. *Remote Sensing Letters*, 10(6), 526-535.

Li, X., Ma, R., Zhang, Q., Li, D., Liu, S., He, T., & Zhao, L. (2019b). Anisotropic characteristic of artificial light at night–Systematic investigation with VIIRS DNB multi-temporal observations. *Remote Sensing of Environment*, 233, 111357. https://doi.org/10.1016/j.rse.2019.111357

Li, X., Duarte, F., & Ratti, C. (2019c). Analyzing the obstruction effects of obstacles on light pollution caused by street lighting system in Cambridge, Massachusetts. Environment and Planning B: Urban Analytics and City Science, 2399808319861645.

Liu, Z., He, C., Zhang, Q., Huang, Q., & Yang, Y. (2012). Extracting the dynamics of urban expansion in China using DMSP-OLS nighttime light data from 1992 to 2008. *Landscape and Urban Planning, 106*, 62-72.

Liu, X., H. Guohua, A. Bin, L. Xia, and Q. Shi. (2015). A Normalized Urban Areas Composite Index (Nuaci) Based on Combination of Dmsp-Ols and Modis for Mapping Impervious Surface Area. *Remote Sensing* 7 (12): 17168–17189. doi:10.3390/rs71215863.

Liu, Y., Hu, C., Zhan, W., Sun, C., Murch, B., & Ma, L. (2018). Identifying industrial heat sources using time-series of the VIIRS Nightfire product with an object-oriented approach. *Remote Sensing of Environment*, 204, 347-365.

Longcore, T., & Rich, C. (2004). Ecological light pollution. *Frontiers in Ecology and the Environment,* 2(4), 191-198.

Longcore, T., Rich, C., Mineau, P., MacDonald, B., Bert, D. G., Sullivan, L. M., ... & Manville II, A. M. (2012). An estimate of avian mortality at communication towers in the United States and Canada. PLoS one, 7(4), e34025.

Longcore, T., Rodríguez, A., Witherington, B., Penniman, J. F., Herf, L., & Herf, M. (2018). Rapid assessment of lamp spectrum to quantify ecological effects of light at night. *Journal of Experimental Zoology Part A: Ecological and Integrative Physiology*. DOI: 10.1002/jez.2184

Lu, D., & Weng, Q. (2002). Use of impervious surface in urban land-use classification. *Remote Sensing of Environment, 102*(1), 146-160.

Luginbuhl, C. B., Duriscoe, D. M., Moore, C. W., Richman, A., Lockwood, G. W., & Davis, D. R. (2009). From the ground up II: Sky glow and near-ground artificial light propagation in Flagstaff, Arizona. *Publications of the Astronomical Society of the Pacific*, *121*(876), 204.

Lunn, R. M., Blask, D. E., Coogan, A. N., Figueiro, M. G., Gorman, M. R., Hall, J. E., ... & Stevens, R. G. (2017). Health consequences of electric lighting practices in the modern world: A report on the National Toxicology Program's workshop on shift work at night, artificial light at night, and circadian disruption. *Science of the Total Environment*, *607*, 1073-1084.

Ma, T., Zhou, C., Pei, T., Haynie, S., & Fan, J. (2012). Quantitative estimation of urbanization dynamics using time series of DMSP/OLS nighttime light data: A comparative case study from China's cities. *Remote Sensing of Environment, 124*, 99-107.

Ma, T., Zhou, Y., Zhou, C., Haynie, S., Pei, T., & Xu, T. (2015). Night-time light derived estimation of spatio-temporal characteristics of urbanization dynamics using DMSP/OLS satellite data. *Remote Sensing of Environment*, 158, 453-464.

Manfrin, A., Singer, G., Larsen, S., Weiß, N., van Grunsven, R. H., Weiß, N. S., ... & Hölker, F. (2017). Artificial light at night affects organism flux across ecosystem boundaries and drives community structure in the recipient ecosystem. Frontiers in Environmental Science, 5, 61.

Marcantonio, M., Pareeth, S., Rocchini, D., Metz, M., Garzon-Lopez, C. X., & Neteler, M. (2015). The integration of Artificial Night-Time Lights in landscape ecology: A remote sensing approach. Ecological Complexity, 22, 109-120.

Marchant, P. R. (2004). A demonstration that the claim that brighter lighting reduces crime is unfounded. British Journal of Criminology, 44(3), 441-447.

Marchant, P. (2017). Why lighting claims might well be wrong. International Journal of Sustainable Lighting, 19(1), 69-74.

Mazor, T., Levin, N., Possingham, H. P., Levy, Y., Rocchini, D., Richardson, A. J., & Kark, S. (2013). Can satellite-based night lights be used for conservation? The case of nesting sea turtles in the Mediterranean. *Biological Conservation*, *159*, 63-72.

McDonald, R. A. (1995). Corona: success for space reconnaissance, a look into the Cold War, and a revolution in intelligence. *Photogrammetric Engineering & Remote Sensing*, 61(6), 689-720.

Meier, J. M. (2018). Temporal Profiles of Urban Lighting: Proposal for a research design and first results from three sites in Berlin. *International Journal of Sustainable Lighting*, *20*(1), 11-28.

Metcalf, J. P. (2012). Detecting and Characterizing nighttime lighting using multispectral and hyperspectral imaging (Doctoral dissertation, Monterey, California. Naval Postgraduate School).

Mills, G. (2010). Cities as agents of global change. *International Journal of Climatology, 27*(14), 1849-1857.

Miller, S. D., Mills, S. P., Elvidge, C. D., Lindsey, D. T., Lee, T. F., & Hawkins, J. D. (2012). Suomi satellite brings to light a unique frontier of nighttime environmental sensing capabilities. *Proceedings of the National Academy of Sciences*, 109(39), 15706-15711.

Miller, S. D., W. C. Straka, III, S. P. Mills, C. D. Elvidge, T. F. Lee, J. E. Solbrig, A. Walther, A. K. Heidinger, and S. C. Weiss (2013): Illuminating the Capabilities of the Suomi National Polar-Orbiting Partnership (NPP) Visible Infrared Imaging Radiometer Suite (VIIRS) Day/Night Band. *Remote Sensing*, 5**(**12**)**, 6717-6766.

Miller, S.D., W. C. Straka III, J. Yue, C. J. Seaman, S. Xu, C. D. Elvidge, L. Hoffman, and I. Azeem, (2018). The Dark Side of Hurricane Matthew: Unique Perspectives from the VIIRS Day/Night Band, *Bulletin of the American Meteorological Society*, available as an Early Online Release (https://journals.ametsoc.org/doi/pdf/10.1175/BAMS-D-17-0097.1)

Miller, S. D., and R. E. Turner, 2009: A dynamic lunar spectral irradiance dataset for NPOESS/VIIRS Day/Night Band nighttime environmental applications, *IEEE Transactions on Geoscience and Remote Sensing*, 47(7), 2316-2329.

Min, B., & Gaba, K. M. (2014). Tracking electrification in Vietnam using nighttime lights. *Remote Sensing*, *6*(10), 9511-9529.

Min, B., Gaba, K. M., Sarr, O. F., & Agalassou, A. (2013). Detection of rural electrification in Africa using DMSP-OLS night lights imagery. *International Journal of Remote Sensing*, *34*(22), 8118-8141.

Minh Hieu, Nguyen. (2016). Transfer Learning for Classification of Nighttime Images. Zenodo. http://doi.org/10.5281/zenodo.1452011

Moreno Burgos V.,Palacios Morena M.,Carrasco Díaz D., (2010), In: Documento Final del Grupo de trabajo 21 de Conama 10 Teledetección y sensores medioambientales.

Murphy, R. E., Barnes, W. L., Lyapustin, A. I., Privette, J., Welsch, C., DeLuccia, F., ... & Kealy, P. S. (2001). Using VIIRS to provide data continuity with MODIS. In Geoscience and Remote Sensing Symposium, 2001. IGARSS'01. IEEE 2001 International (Vol. 3, pp. 1212-1214). IEEE.

Nagendra, H., Lucas, R., Honrado, J.P., Jongman, R.H.G., Tarantino, C., Adamo, M., & Mairota, P. (2012). Remote sensing for conservation monitoring: Assessing protected areas, habitat extent, habitat condition, species diversity, and threats. *Ecological Indicators*.

Narendran, N., Freyssinier, J. P., & Zhu, Y. (2016). Energy and user acceptability benefits of improved illuminance uniformity in parking lot illumination. *Lighting Research & Technology*, *48*(7), 789-809.

Nakićenović, N. (2012). Summary for Policy Makers. *In Global Energy Assessment: Toward a Sustainable Future*; Cambridge University Press: Hong Kong, China, pp. 16–18.

Nateghi, R., Guikema, S. D., & Quiring, S. M. (2014). Forecasting hurricane-induced power outage durations. *Natural Hazards*, *74*(3), 1795-1811.

Navara, K. J., & Nelson, R. J. (2007). The dark side of light at night: physiological, epidemiological, and ecological consequences. *Journal of Pineal Research*, *43*(3), 215-224.

Nordhaus, W. D. (1996). Do real-output and real-wage measures capture reality? The history of lighting suggests not. In *The economics of new goods* (pp. 27-70). University of Chicago Press.

Ocaña, F., Sánchez de Miguel,A. ,Conde, A. (2016). Low cost multi-purpose balloon-borne platform for wide-field imaging and video observation*, Proc.SPIE*, 9906, 9,doi :10.1117/12.2233001

Ou, J., Liu, X., Li, X., Li, M., & Li, W. (2015). Evaluation of NPP-VIIRS nighttime light data for mapping global fossil fuel combustion CO2 emissions: a comparison with DMSP-OLS nighttime light data. *PloS one*, *10*(9), e0138310.

Ouyang, Z., Lin, M., Chen, J., Fan, P., Qian, S. S., & Park, H. (2019). Improving estimates of built-up area from night time light across globally distributed cities through hierarchical modeling. *Science of The Total Environment*, 647, 1266-1280.

Pack, D.W., & Hardy, B. S. (2016). CubeSat Nighttime Lights. 30th Annual AAIA/USU Conference on Small Satellites.

Pack, D., Hardy, B., & Longcore, T. (2017). Studying the Earth at night from CubeSats. 31st Annual AAIA/USU Conference on Small Satellites.

Pack, D.W., Coffman, C.M., Santiago, J.R., & Russell, R.W. (2018). Earth remote sensing results from the CUbesat MULtispectral Observing System, CUMULOS. In *AGU Fall Meeting Abstracts*.

Pack, D. W., Coffman, C. M., & Santiago, J. R. (2019). A Year in Space for the CUbesat MULtispectral Observing System: CUMULOS. In *33rd Annual AIAA/USU Conference on Small Satellites*. SSC19-XI-01.

Painter, K. (1996). The influence of street lighting improvements on crime, fear and pedestrian street use, after dark. Landscape and Urban Planning, 35(2-3), 193-201.

Pandey, B., Joshi, P. K., & Seto, K. C. (2013). Monitoring urbanization dynamics in india using dmsp/ols night time lights and spot-vgt data. *International Journal of Applied Earth Observations & Geoinformation*, 23(1), 49-61.

Pandey, B., Zhang, Q., & Seto, K. C. (2017). Comparative evaluation of relative calibration methods for dmsp/ols nighttime lights. *Remote Sensing of Environment*, 195, 67-78.

Pauwels, Julie ; Le Viol,Isabelle ; Azam, Clémentine ; Valet, Nicolas ; Julien, Jean-François; Bas, Yves; Lemarchand, Clément; Sánchez de Miguel, Alejandro; Kerbiriou, Christian (2019). Accounting for artificial light impact on bat activity for a biodiversity-friendly urban planning, *Landscape and Urban Planning*, 183, 12-25.

Pawson, S. M., & Bader, M. F. (2014). LED lighting increases the ecological impact of light pollution irrespective of color temperature. *Ecological Applications*, 24(7), 1561-1568.

Pechony, O., & Shindell, D. T. (2010). Driving forces of global wildfires over the past millennium and the forthcoming century. Proceedings of the National Academy of Sciences, 107(45), 19167-19170.

Peña-García, A., Hurtado, A., & Aguilar-Luzón, M. C. (2015). Impact of public lighting on pedestrians' perception of safety and well-being. *Safety Science*, *78*, 142-148.

Pendoley, K. L., Verveer, A., Kahlon, A., Savage, J., & Ryan, R. T. (2012, January). A novel technique for monitoring light pollution. In *International Conference on Health, Safety and Environment in Oil and Gas Exploration and Production*. Society of Petroleum Engineers.

Pettit, D. (2009). Exploring the frontier: science of opportunity on the International Space Station. *Proceedings of the American Philosophical Society*, *153*(4), 381-402.

Plummer, K. E., Hale, J. D., O'Callaghan, M. J., Sadler, J. P., & Siriwardena, G. M. (2016). Investigating the impact of street lighting changes on garden moth communities. Journal of Urban Ecology, 2(1), juw004.

Portnov B.A., Stevens R.G., Samociuk H., Wakefield D. and Gregorio D.I. (2016) Light at Night and Breast Cancer Incidence in Connecticut: An Ecological Study of Age Group Effects, *Science of the Total Environment,* 572, 1020-1024.

Pritchard, S. B. (2017). The trouble with darkness: NASA's Suomi satellite images of Earth at night. Environmental History, 22(2), 312-330.

Prins, E. (2007). Use of low cost Landsat ETM+ to spot burnt villages in Darfur, Sudan. *International Journal of Remote Sensing, 29*, 1207-1214

Pun, C. S. J., & So, C. W. (2012). Night-sky brightness monitoring in Hong Kong. *Environmental Monitoring and Assessment*, *184*(4), 2537-2557.

Pun, C. S. J., So, C. W., Leung, W. Y., & Wong, C. F. (2014). Contributions of artificial lighting sources on light pollution in Hong Kong measured through a night sky brightness monitoring network. *Journal of Quantitative Spectroscopy and Radiative Transfer*, *139*, 90-108.

Puschnig, J., Posch, T., & Uttenthaler, S. (2014). Night sky photometry and spectroscopy performed at the Vienna University Observatory. *Journal of Quantitative Spectroscopy and Radiative Transfer*, *139*, 64-75.

Pust, P., Schmidt, P. J., & Schnick, W. (2015). A revolution in lighting. *Nature Materials*, *14*(5), 454.

Rao, P. K., Holmes, S. J., Anderson, R. K., Winston, J. S., & Lehr, P. E. (1990). Weather Satellites: Systems, Data, and Environmental Applications. American Meteorological Society, Boston.

Regan, Jason, (2018), Spanish Company Deploys Drones to Battle Light Pollution,https://dronelife.com/2018/02/13/spanish-company-deploys-drones-battle-light-pollution/

Rich, C., & Longcore, T. (Eds.). (2006). *Ecological consequences of artificial night lighting*. Island Press.

Riegel, K. W. (1973). Light Pollution: Outdoor lighting is a growing threat to astronomy. *Science*, 179(4080), 1285–1291.

Román, M. O., & Stokes, E. C. (2015). Holidays in lights: Tracking cultural patterns in demand for energy services. *Earth's Future*, 3(6), 182-205.

Román, M. O., Wang, Z., Sun, Q., Kalb, V., Miller, S. D., Molthan, A., ... & Seto, K. C. (2018). NASA's Black Marble nighttime lights product suite. *Remote Sensing of Environment*, 210, 113-143.

Román, M. O., Stokes, E. C., Shrestha, R., Wang, Z., Schultz, L., Carlo, E. A. S., ... & Ji, C. (2019). Satellite-based assessment of electricity restoration efforts in Puerto Rico after Hurricane Maria. PloS one, 14(6), e0218883. doi:10.1371/journal.pone.0218883

Rosebrugh, D.W., (1935). Sky-Glow from large cities, *Journal of the Royal Astronomical Society of Canada*, 29, 79

Roy, D. P., Wulder, M. A., Loveland, T. R., Woodcock, C. E., Allen, R. G., Anderson, M. C., ... & Scambos, T. A. (2014). Landsat-8: Science and product vision for terrestrial global change research. *Remote Sensing of Environment*, 145, 154-172.

Royé, Dominic (2018), https://twitter.com/dr_xeo/status/993770291431079936

Russart, K. L., & Nelson, R. J. (2018). Artificial light at night alters behavior in laboratory and wild animals. Journal of Experimental Zoology Part A: Ecological and Integrative Physiology, 329(8-9), 401-408.

RTVE, (2013), España a ras de cielo - España de Noche, http://www.rtve.es/alacarta/videos/espana-a-ras-de-cielo/espana-ras-cielo-espana-noche/4692661/

Ruhtz, T., Kyba, C. C. M., Posch, T. Puschnig, J., Kuechly, H. (2015) Lichtmesskampagne Zentralraum Oberösterreich Erfassung des abgestrahlten Lichts mit einem nächtlichen Überflug

Russell, B. (1935). In Praise of Idleness and Other Essays. Routledge.

Ryan, R. E., Pagnutti, M., Burch, K., Leigh, L., ruggles, t., cao, c., ... & helder, d. (2019). the Terra Vega active light source: a first step in a new approach to perform nighttime absolute radiometric calibrations and early results calibrating the VIIRS DNB. Remote Sensing, 11(6), 710.

Rybnikova N. and Portnov B.A. (2016) Artificial Light at Night and Obesity: Does the Spread of Wireless Information and Communication Technology Play a Role? *International Journal of Sustainable Lighting* 35, 16-20.

Rybnikova N. and Portnov B.A. (2017) Outdoor Light and Breast Cancer Incidence: A Comparative Analysis of DMSP and VIIRS-DNB Satellite Data, *International Journal of Remote Sensing,* 38(21), 1-10.

Rybnikova N. and Portnov B.A. (2018) Population-level Study Links Short Wavelength Nighttime Illumination with Breast Cancer Incidence in a Major Metropolitan Area, *Chronobiology International,* 2018.

Rybnikova N., Haim A. and Portnov B.A. (2015) Artificial Light at Night (ALAN) and Breast Cancer Incidence Worldwide: A Revisit of Earlier Findings with Analysis of Current Trends, *Chronobiology International,* 32(6), 757–773.

Rybnikova N., Haim A. and Portnov B.A. Does Artificial Light-At-Night (ALAN) Exposure Contribute to the Worldwide Obesity Pandemic? (2016a) *Int. Journal of Obesity*, 40(5), 815-823.

Rybnikova N., Haim A. and Portnov B.A. (2016b) Is Prostate Cancer Incidence Worldwide Linked to Artificial Light at Night Exposures? Review of Earlier Findings and Analysis of Current Trends, *Archives of Environmental and Occupational Health*, 72(2), 111-122.

Rybnikova N., Stevens R., Gregorio D., Samociuk H., Portnov B.A. Kernel Density Analysis Reveals a Halo Pattern of Breast Cancer Incidence in Connecticut (2018) *Spatial and Spatio-temporal Epidemiology,* 26, 143–151.

Sabbatini, M. (2014) NightPod-Nodding Mechanism for the ISS; Technical Report Experiment Record #9337; European Space Agency: Noordwijk, The Netherlands.

Sánchez de Miguel, A. and Zamorano, J. (2012), https://guaix.fis.ucm.es/node/1557

Sánchez de Miguel, A., Zamorano, J., Gómez, Castaño, J., Pascual S, (2013) European street lighting power consumption estimation using DMSP/OLS images, ALAN Conference.

Sánchez de Miguel, A., Zamorano, J., Pascual, S., López Cayuela, M., Ocaña, F., Challupner, P., ... & de Miguel, E. (2013). ISS nocturnal images as a scientific tool against light pollution: Flux calibration and colors. Highlights of Spanish Astrophysics VII; Springer: Berlin, Germany, 1, 916-919.

Sánchez de Miguel, A. , Castaño, J. G., Zamorano, J., Pascual, S., Ángeles, M., Cayuela, L., ... & Kyba, C. C. (2014). Atlas of astronaut photos of Earth at night. *Astronomy & Geophysics*, 55(4), 4-36.

Sánchez de Miguel, A. (2015). Variación espacial, temporal y espectral de la contaminación lumínica y sus fuentes: Metodología y resultados (Doctoral dissertation, Universidad Complutense de Madrid).

Sánchez de Miguel, A., Aubé, M., Zamorano, J., Kocifaj, M., Roby, J., & Tapia, C. (2017). Sky Quality Meter measurements in a colour-changing world. *Monthly Notices of the Royal Astronomical Society*, *467*(3), 2966-2979.

Sánchez de Miguel, A., Lucía García, Jaime Zamorano, Jesús Gallego, José Gómez, Daniel Lombraña, … Esteban González. (2018). DarkSkies Project (Cities At Night - 2014) [Data set]. Zenodo. http://doi.org/10.5281/zenodo.1255130

Sánchez de Miguel, A., Kyba, C.C.M., Zamorano, J., Aubé, M., Gallego, J. (2019a) The nature of the diffuse light near cities detected in nighttime satellite imagery. arXiv preprint arXiv:1908.05482.

Sánchez de Miguel, A., Kyba, C. C., Aubé, M., Zamorano, J., Cardiel, N., Tapia, C., ... & Gaston, K. J. (2019b). Colour remote sensing of the impact of artificial light at night (I): The potential of the International Space Station and other DSLR-based platforms. Remote Sensing of Environment, 224, 92-103.

Sanderson, E. W., Jaiteh, M., Levy, M. A., Redford, K. H., Wannebo, A. V., & Woolmer, G. (2002). The human footprint and the last of the wild: the human footprint is a global map of human influence on the land surface, which suggests that human beings are stewards of nature, whether we like it or not. *AIBS Bulletin*, *52*(10), 891-904.

Sandau, R. (2010). Status and trends of small satellite missions for Earth observation. *Acta Astronautica*, 66(1-2), 1-12.

Sadler, P. (2018). Detecting cities in aerial night-time images by learning structural invariants using single reference augmentation, https://arxiv.org/abs/1810.08597

Schaaf, C. B., Gao, F., Strahler, A. H., Lucht, W., Li, X., Tsang, T., ... & Lewis, P. (2002). First operational BRDF, albedo nadir reflectance products from MODIS. *Remote sensing of Environment*, *83*(1-2), 135-148.

Schmidt W., (2015), AtlasNederland Verlicht, NachtMeetnet.

Sen, A., Kim, Y., Caruso, D., Lagerloef, G., Colomb, R., Yueh, S., & Le Vine, D. (2006). Aquarius/SAC-D mission overview. In *Sensors, Systems, and Next-Generation Satellites* X (Vol. 6361, p. 63610I). International Society for Optics and Photonics.

Shi, K., Huang, C., Yu, B., Yin, B., Huang, Y., & Wu, J. (2014). Evaluation of NPP-VIIRS night-time light composite data for extracting built-up urban areas. *Remote Sensing Letters*, 5(4), 358-366.

Simi, C. G., Kindsfather, R., Pickard, H., Howard, W., Norton, M. C., & Dixon, R. (1995, November). HERCULES/MSI: a multispectral imager with geolocation for STS-70. In Remote Sensing for Agriculture, Forestry, and Natural Resources (Vol. 2585, pp. 267-283). International Society for Optics and Photonics.

Small, C. (2005). A global analysis of urban reflectance. *International Journal of Remote Sensing, 26*, 661-682.

Small, C., & Elvidge, C. D. (2013). Night on Earth: Mapping decadal changes of anthropogenic night light in Asia. *International Journal of Applied Earth Observation and Geoinformation*, 22, 40-52.

Small, C., Pozzi, F., & Elvidge, C. (2005). Spatial analysis of global urban extent from DMSP-OLS night lights. *Remote Sensing of Environment, 96*, 277-291.

Solano Lamphar, H. A., & Kocifaj, M. (2016). Urban night-sky luminance due to different cloud types: A numerical experiment. *Lighting Research & Technology*, *48*(8), 1017-1033.

Stark, H., Brown, S. S., Wong, K. W., Stutz, J., Elvidge, C. D., Pollack, I. B., ... & Parrish, D. D. (2011). City lights and urban air. *Nature Geoscience*, 4(11), 730.

Stathakis, D., & Baltas, P. (2018). Seasonal population estimates based on night-time lights. *Computers, Environment and Urban Systems*, 68, 133–141.

Stefanov, W. L., Evans, C. A., Runco, S. K., Wilkinson, M. J., Higgins, M. D., & Willis, K. (2017). Astronaut photography: Handheld camera imagery from low earth orbit. *Handbook of Satellite Applications*, 847-899.

Steinbach, R., Perkins, C., Tompson, L., Johnson, S., Armstrong, B., Green, J., ... & Edwards, P. (2015). The effect of reduced street lighting on road casualties and crime in England and Wales: controlled interrupted time series analysis. J Epidemiol Community Health, 69(11), 1118-1124.

Stevens, R. G. (1987). Electric power use and breast cancer: a hypothesis. American Journal of Epidemiology, 125(4).

Straka, T. M., Wolf, M., Gras, P., Buchholz, S., & Voigt, C. C. (2019). Tree cover mediates the effect of artificial light on urban bats. Frontiers in Ecology and Evolution, 7, 91.

Strauss, M. (2017). Planet Earth to get a daily selfie. *Science*, 355, 782-783.

Sullivan III, W. T. (1989). A 10 km resolution image of the entire night-time Earth based on cloud-free satellite photographs in the 400–1100 nm band. *International Journal of Remote Sensing*, *10*(1), 1-5.

Tamir, R., Lerner, A., Haspel, C., Dubinsky, Z., & Iluz, D. (2017). The spectral and spatial distribution of light pollution in the waters of the northern Gulf of Aqaba (Eilat). *Scientific Reports*, *7*, 42329.

Tangari, A. H., & Smith, R. J. (2012). How the temporal framing of energy savings influences consumer product evaluations and choice. Psychology & Marketing, 29(4), 198-208.

Tardà, A., Palà, V., Arbiol, R., Pérez, F., Viñas, O., Pipia, L., & Martínez, L. (2011). Detección de la iluminación exterior urbana nocturna con el sensor aerotransportado CASI 550. International Geomatic Week, Barcelona, Spain.

Tapia Ayuga, C., Sánchez de Miguel, A., & Zamorano Calvo, J. (2015). *LICA--UCM lamps spectral database*. LICA Reports. Madrid.

Townsend, A. C., & Bruce, D. A. (2010). The use of night-time lights satellite imagery as a measure of Australia's regional electricity consumption and population distribution. *International Journal of Remote Sensing*, 31(16), 4459-4480.

United Nations (2014). *World Urbanization Prospects: The 2014 Revision*, Highlights. Department of Economic and Social Affairs. Population Division, United Nations.

Van Doren, B. M., Horton, K. G., Dokter, A. M., Klinck, H., Elbin, S. B., & Farnsworth, A. (2017). High-intensity urban light installation dramatically alters nocturnal bird migration. *Proceedings of the National Academy of Sciences*, *114*(42), 11175-11180.

Venter, O., Sanderson, E. W., Magrach, A., Allan, J. R., Beher, J., Jones, K. R., ... & Levy, M. A. (2016). Sixteen years of change in the global terrestrial human footprint and implications for biodiversity conservation. *Nature Communications*, *7*, 12558.

Vermote, E. F., El Saleous, N., Justice, C. O., Kaufman, Y. J., Privette, J. L., Remer, L., ... & Tanre, D. (1997). Atmospheric correction of visible to middle-infrared EOS-MODIS data over land surfaces: Background, operational algorithm and validation. *Journal of Geophysical Research: Atmospheres*, *102*(D14), 17131-17141.

Walczak, K., Gyuk, G., Kruger, A., Byers, E., & Huerta, S. (2017). NITESat: A High Resolution, Full-Color, Light Pollution Imaging Satellite Mission. *International Journal of Sustainable Lighting*, 19(1), 48-55.

Walker, M. F. (1970). The California site survey. *Publications of the Astronomical Society of the Pacific*, *82*(487), 672.

Walker, M. F. (1973). Light pollution in California and Arizona. *Publications of the Astronomical Society of the Pacific*, 85(507), 508-519.

Walker, C. E., Pompea, S. M., & Isbell, D. (2008, June). GLOBE at night 2.0: On the road toward IYA 2009. In EPO and a Changing World: Creating Linkages and Expanding Partnerships (Vol. 389, p. 423).

Wang, W., Cheng, H., & Zhang, L. (2012). Poverty assessment using DMSP/OLS night-time light satellite imagery at a provincial scale in China. *Advances in Space Research, 49*, 1253-1264

Wang, Z., Román, M. O., Sun, Q., Molthan, A. L., Schultz, L. A., & Kalb, V. L. (2018). Monitoring Disaster-Related Power Outages Using NASA Black Marble Nighttime Light Product. *ISPRS-International Archives of the Photogrammetry, Remote Sensing and Spatial Information Sciences*, 1853-1856.

Wei, Y., Liu, H., Song, W., Yu, B., & Xiu, C. (2014). Normalization of time series DMSP-OLS nighttime light images for urban growth analysis with pseudo invariant features. *Landscape and Urban Planning*, *128*, 1-13.

Weishampel, Z. A., Cheng, W. H., & Weishampel, J. F. (2016). Sea turtle nesting patterns in Florida vis-à-vis satellite-derived measures of artificial lighting. *Remote Sensing in Ecology and Conservation*, *2*(1), 59-72.

Welch, R. (1980). Monitoring urban population and energy utilization patterns from satellite data. *Remote Sensing of Environment*, 9(1), 1-9.

Weng, Q. (2009). Thermal infrared remote sensing for urban climate and environmental studies: Methods, applications, and trends. *ISPRS Journal of Photogrammetry and Remote Sensing*, *64*(4), 335-344.

Witherington, B. E., & Martin, R. E. (2000). Understanding, assessing, and resolving light-pollution problems on sea turtle nesting beaches.

Witmer, F. D. (2015). Remote sensing of violent conflict: Eyes from above. *International Journal of Remote Sensing*, *36*(9), 2326-2352.

Witmer, F.D.W., & O'Loughlin, J. (2011). Detecting the effects of wars in the Caucasus regions of Russia and Georgia using radiometrically normalized DMSP-OLS nighttime lights imagery. *Giscience & Remote Sensing, 48*, 478-500.

Wu, J., He, S., Peng, J., Li, W., & Zhong, X. (2013). Intercalibration of DMSP-OLS night-time light data by the invariant region method. *International Journal of Remote Sensing, 34*, 7356-7368.

Xu, H., Yang, H., Li, X., Jin, H., & Li, D. (2015). Multi-Scale measurement of regional inequality in Mainland China during 2005–2010 using DMSP/OLS night light imagery and population density grid data. *Sustainability, 7*, 13469

Xu, Y., Knudby, A., & Côté-Lussier, C. (2018). Mapping ambient light at night using field observations and high-resolution remote sensing imagery for studies of urban environments. *Building and Environment*, *145*, 104-114.

Yair, Y., Rubanenko, L., Mezuman, K., Elhalel, G., Pariente, M., Glickman-Pariente, M., ... & Inoue, T. (2013). New color images of transient luminous events from dedicated observations on the International Space Station. *Journal of Atmospheric and Solar-Terrestrial Physics*, 102, 140-147.

Yi, K., Tani, H., Li, Q., Zhang, J., Guo, M., & Bao, Y., et al. (2014). Mapping and evaluating the urbanization process in northeast china using dmsp/ols nighttime light data. *Sensors, 14*(2), 3207-3226.

Yu, B., Shi, K., Hu, Y., Huang, C., Chen, Z., & Wu, J. (2015). Poverty Evaluation Using NPP-VIIRS Nighttime Light Composite Data at the County Level in China. *Ieee Journal of Selected Topics in Applied Earth Observations and Remote Sensing, 8*, 1217-1229.

Zamorano Calvo, J., Sánchez de Miguel, A., Pascual Ramírez, S., Gómez Castaño, J., Ramírez Moreta, P., & Challupner, P. (2011). ISS nocturnal images as a scientific tool against Light Pollution.

Zamorano, J., Sánchez de Miguel, A. , Alfaro, E., Martínez-Delgado, D., Ocaña, F., Nievas, M., & Castaño, J. G. (2013, May). NIXNOX project: Enjoy the dark skies of Spain. In Highlights of Spanish Astrophysics VII (pp. 962-970).

Zamorano, J., de Miguel, A. S., Ocaña, F., Pila-Diez, B., Castaño, J. G., Pascual, S., ... & Nievas, M. (2016). Testing sky brightness models against radial dependency: A dense two dimensional survey around the city of Madrid, Spain. *Journal of Quantitative Spectroscopy and Radiative Transfer*, 181, 52-66.

Zamorano, J., Tapia, C., Pascual, S., García, C., González, R., González, E., ... & Solano, E. (2019, March). Night Sky Brightness monitoring in Spain. In Highlights on Spanish Astrophysics X, Proceedings of the XIII Scientific Meeting of the Spanish Astronomical Society held on July 16-20, 2018, in Salamanca, Spain, ISBN 978-84-09-09331-1. B. Montesinos, A. Asensio Ramos, F. Buitrago, R. Schödel, E. Villaver, S. Pérez-Hoyos, I. Ordóñez-Etxeberria (eds.) p. 599-604 (pp. 599-604).

Zhang, Q., Pandey, B., & Seto, K. C. (2016). A robust method to generate a consistent time series from dmsp/ols nighttime light data. *IEEE Transactions on Geoscience & Remote Sensing, 54*(10), 5821-5831.

Zhang, Q., Schaaf, C., & Seto, K. C. (2013). The vegetation adjusted NTL urban index: A new approach to reduce saturation and increase variation in nighttime luminosity. *Remote Sensing of Environment*, *129*, 32-41.

Zhang, Q., & Seto, K.C. (2011). Mapping urbanization dynamics at regional and global scales using multi-temporal DMSP/OLS nighttime light data. *Remote Sensing of Environment, 115*, 2320-2329.

Zhang, J. C., Ge, L., Lu, X. M., Cao, Z. H., Chen, X., Mao, Y. N., & Jiang, X. J. (2015a). Astronomical Observing Conditions at Xinglong Observatory from 2007 to 2014. *Publications of the Astronomical Society of the Pacific*, *127*(958), 1292.

Zhang, Q., Levin, N., Chalkias, C., Letu, H. (2015b). Nighttime light remote sensing -- Monitoring human societies from outer space. Chapter 11 in *Remote Sensing Handbook*, Volume 3, pp. 289-310 (Edited by Thenkabail, P.S.). Taylor and Francis.

Zhang, Q., Li, B., Thau, D., & Moore, R. (2015c). Building a better urban picture: Combining day and night remote sensing imagery. *Remote Sensing*, *7*(9), 11887-11913.

Zhao, X., YU, B., Liu, Y., Yao, S., Lian, T., Chen, L., Yang, C., Chen, Z., Wu, J. (2018) NPP-VIIRS DNB Daily Data in Natural Disaster Assessment: Evidence from Selected Case Studies. *Remote Sensing*, *10*(10), 1526; doi:10.3390/rs10101526

Zhao, M., Zhou, Y., Li, X., Cao, W., He, C., Yu, B., ... & Zhou, C. (2019). Applications of satellite remote sensing of nighttime light observations: advances, challenges, and perspectives. *Remote Sensing*, 11(17), 1971.

Zheng, Q., Weng, Q., Huang, L., Wang, K., Deng, J., Jiang, R., ... & Gan, M. (2018). A new source of multi-spectral high spatial resolution night-time light imagery—JL1-3B. *Remote Sensing of Environment*, 215, 300-312.

Zheng, Q., Weng, Q., & Wang, K. (2019). Developing a new cross-sensor calibration model for DMSP-OLS and Suomi-NPP VIIRS night-light imageries. *ISPRS Journal of Photogrammetry and Remote Sensing*, 153, 36-47.

Zhou, Y., Smith, S. J., Elvidge, C. D., Zhao, K., Thomson, A., & Imhoff, M. (2014). A cluster-based method to map urban area from dmsp/ols nightlights. *Remote Sensing of Environment, 147*(18), 173-185.

Zhou, Y., Smith, S. J., Zhao, K., Imhoff, M., Thomson, A., & Bondlamberty, B., et al. (2015). A global map of urban extent from nightlights. *Environmental Research Letters, 10*(5).

Zhou, Y., Li, X., Asrar, G. R., Smith, S. J., & Imhoff, M. (2018). A global record of annual urban dynamics (1992–2013) from nighttime lights. *Remote Sensing of Environment*, *219*, 206-220.

Zhu, Z., Zhou, Y., Seto, K. C., Stokes, E. C., Deng, C., Pickett, S. T., & Taubenböck, H. (2019). Understanding an urbanizing planet: Strategic directions for remote sensing. Remote Sensing of Environment, 228, 164-182.

Zoogman, P., Liu, X., Suleiman, R. M., Pennington, W. F., Flittner, D. E., Al-Saadi, J. A., ... & Janz, S. J. (2017). Tropospheric emissions: Monitoring of pollution (TEMPO). *Journal of Quantitative Spectroscopy and Radiative Transfer*, 186, 17-39.

List of Figure Captions

Figure 1: Lighting changes in Calgary, Alberta (Canada) between 24/12/2010 (top) and 28/11/2015 (bottom). The neighborhood at left has converted from high pressure sodium to white LED lights, while the highway at right is newly illuminated with sodium lamps. The area has a roughly 7.5x3 km extent. Images based on astronaut photographs ISS026-E-12438 and ISS045-E-155029.

Figure 2: Space borne sensors with night-time lights capabilities, as a function of the year from which digital night-time images are available, and the spatial resolution of the sensor.

Figure 3: Cumulative number of papers on artificial lights in the Artificial Light at Night (ALAN) Research Literature Database (n = 2545) (http://alandb.darksky.org/, accessed September 16th, 2019). Also shown are papers where the title of the paper included the word pollution (n = 271), and papers published in remote sensing journals or where either one of the words “remote”, “sensing”, “satellite”, “DMSP”, “VIIRS”, “Luojia”, “SQM” appeared in the title of the paper or that Chris Elvidge was one of the co-authors (n = 380). The green line shows the yearly numbers of papers cited in our manuscript (n = 372).

Figure 4: Lunar eclipse over North America on 2014/10/08, viewed by VIIRS DNB. At far right, the eclipse had not yet begun, and the instrument observed clouds illuminated by full moonlight. The next strip was taken with the moon partially eclipsed, and the dark strip when the moon was near to fully eclipsed. The final strip (at left) was taken one day earlier. Image prepared by Christopher Kyba based on image and data processing by NOAA's National Geophysical Data Center. Image available under a CC BY license at https://tinyurl.com/us-eclipse-20141008.

Figure 5: DMSP local times at the ascending equatorial crossing.

Figure 6: DMSP colorized night lights. The white represents lights generated from electricity, the red shading shows fires, the pink shading indicates light from squid fishing boats, and the blue spots are gas flares from oil rigs. Each is one year's worth of data. The differentiation of fires, boats, electric lights and gas flares was all done by temporal analysis (do the lights stay constant and do they move). The instrument itself is not able to distinguish between them. Zoomed in areas are shown for northern Europe (b), Japan and Korea (c), western Africa (d), and northern South America (e). Source of dataset: https://sos.noaa.gov/datasets/nighttime-lights-colorized/

Figure 7: Section of the first global map of DMSP nighttime lights, produced by mosaicking film segments by Woody Sullivan, University of Washington.

Figure 8: NGDC's first map of DMSP nighttime lights, produced from 29 orbits and no cloud screening.

Figure 9: NGDC's second generation DMSP nighttime lights product produced with cloud-screening from 236 orbits acquired in a six month period in 1995.

Figure 10: DMSP radiance nighttime lights for St. Louis, Missouri.

Figure 11: False color composites of DMSP stable lights version 4, showing: (a) decrease in lights following the war in Syria; (b) expansion of roads in the United Arab Emirates (UAE); (c) the lit border between India and Pakistan; (d) urbanization in China; (e) economic decline in Ukraine and Moldova following the collapse of the Soviet Union; (f) temporal changes in activity of oil wells in Nigeria.

Figure 12: Night lights of the Levant, Astronaut photograph ISS053-E-50422, taken on 28/9/2017, 00:10:11 GMT. At the bottom of the image the densely populated Delta of the Nile can be seen, while the center of the image covers Israel, the West Bank, Jordan and Lebanon. The consequences of the conflict in Syria are hinted in this photo, where Syria is mostly dark, in contrast with lit towns and cities in Turkey to the north.

Figure 13: The number of night-time ISS photos identified by the Cities at Night crowdsourcing project (http://citiesatnight.org/index.php/maps/). Note that in several ISS missions many night-time photos were taken, while in other mission hardly any night-time photos were taken. The data shown does not include the recent three years.

Figure 14: Berlin at day and night: (a) Landsat 8 OLI, April 2017, true color composite; (b) Astronaut photography from the International Space Station, ISS047-E-29989, March 2016; (c) Luojia01 night-time image, August 25th, 2018; (d) VIIRS/DNB October 2016.

Figure 15: (a) The number of night-time ISS photos identified by the Cities at Night crowdsourcing project (http://citiesatnight.org/index.php/maps/), within 100x100 km grid cells;. (b) The number of all night-time Luojia-1 images acquired so far (n = 8675, May 2019), as received from Wuhan University, with 250x250 km grid cells.

Figure 16: A vertical aerial photograph taken during a raid on Berlin on the night of 2-3 September 1941. The broad wavy lines are the tracks of German searchlights and anti-aircraft fire. Also illuminated by the flash-bomb in the lower half of the photograph are the Friedrichshain gardens and sports stadium, St Georgs Kirchhof and Balten Platz.

Figure 17: All-sky luminance map based on a photograph taken 15 kilometers outside of Berlin's city limits (30 km from the city center). Photograph and image processing by Andreas Jechow. The dashed line shows 40^{o} from zenith (equivalently 50^{o} elevation). A natural starlit sky has a luminance near 0.2-0.3 mcd/m^2 (Hanel et al 2018).

Figure 18: Night-time hemispheric photo at Emily Bay, Norfolk Island, Australia (April 6th, 2018, 21:52 local time). The upper image shows the raw image, while the bottom image presents sky brightness as calculated by the Sky Quality Camera software. The bright light at the east (azimuth 112, left side of the image) is the moon rising over the horizon. Notice the difference between bright clouds above artificial light sources, and the dark clouds above dark areas. Photo taken by Noam Levin.

Figure 19: Mean VIIRS radiance values in July 2014 at the country level (averaging all cities within a country), as a function of national GDP per capita. Based on data from Levin and Zhang (2017). Note that GDP on its own is not enough to explain night-time brightness differences of urban areas between countries. Additional variables include albedo, whether countries have natural gas and oil resources, and lighting standards, among other factors.

Figure 20: Temporal changes in monthly VIIRS night-time brightness, demonstrating various patterns (each of the sites was normalized between its own minimum and maximum values).

Aleppo, Syria: dramatic decrease in night-time lights due to the war in Syria.
El Zaatari refugee camp, Jordan: influx of refugees from Syria makes this refugee camp one of the largest cities in Jordan.
Dubai, UAE: A global city and a business hub in the Middle East, with a growing economy.
San Juan, Puerto Rico: Hurricane Maria (September 20th, 2017) led to power outages throughout Puerto Rico.
Caracas, Venezuela: In 2014 Venezuela entered an economic recession, with a decrease in its GDP, evident in a decrease of night lights in its capital city.
Juliaca, Peru: A seasonal pattern is evident in night-time lights, commonly attributed to seasonal changes in albedo related to vegetation and snow cover.

Figure 21: After making landfall as a category 4 storm on October 10, 2018, Hurricane Michael knocked out power for at least 2.5 million customers in the southeastern United States, according to the Edison Electric Institute. The images show where lights went out in Panama City, Florida, comparing the night lights before (top) and after (bottom) the hurricane (October 6th and 12th, 2018, respectively).

Figure 22: Lighting differences between countries across borders, as seen from the ISS: China - North Korea - South Korea (ISS038-E-38280), US - Mexico (ISS030-E-213358), East and West Berlin (ISS035-E-17202).

Figure 23: City lights shine brighter during the holidays in the United States when compared with the rest of the year, as shown using a new analysis of daily nighttime data from the VIIRS instrument onboard the NASA/NOAA Suomi NPP satellite (Roman and Stokes, 2015). Dark green pixels are areas where lights are 30 percent brighter, or more, during December. Because snow reflects so much light, only snow-free cities were analyzed. Holiday activity is shown to peak in the suburbs and peri-urban areas of major Southern US cities, where Christmas lights are prevalent. In contrast, most central urban districts, with compact dwelling types affording less space for light displays, experience a slight decrease or no change in energy service demand. The calculation is based on the relative change in lights between the Christmas holiday vs. the rest of the year. It is a simple ratio between the latter vs the former.

Figure 24: Spectral response of the most popular sensors and most popular spectra, from top to bottom. (a) the spectral response of the Nikon D3s Cameras used by the astronauts at the ISS; (b) a typical spectra of a Metal Halide lamp, popular on architectural lights; (c) a High pressure sodium light, popular until 2014 on streelighting; (d) LEDs of 5000K (blue), 4000K (cyan), 2700K (grey) and PC-Amber(amber), popular on street lighting; (e) representative spectral response of DMSP/OLS(black) and SNPP/VIIRS/DNB(blue). Sources: Sánchez de Miguel 2015, Tapia Ayuga et. al. 2015, Sánchez de Miguel et. al. 2017, Elvidge. et. al 1999 and Liao et. al. 2013.

Figure 25: Histograms of top of atmosphere radiance for the images of Berlin of VIIRS and day-time Landsat OLI shown in Figure 14.

Figure 26: Visibility of lit facades depends on perspective. The top image is a crop of an photograph taken from the South, so North facing facades are visible. The bottom image was taken from the North, so the South faces of buildings therefore appear dark. Photos taken by Alejandro Sanchez de Miguel and the Freie University"at Berlin during the EU COST Action ES1204 LoNNe. Figure and caption reproduced from Coesfeld et al. (2018), available under a Creative Commons Attribution license (CC-BY 4.0).

Figure 27: OSIRIS view of Earth by night. This is a composite of four images combined to show the illuminated crescent of Earth and the cities of the northern hemisphere. The images were acquired with the OSIRIS Wide Angle Camera (WAC) during Rosetta's second Earth swing-by on 13 November. This image showing islands of light created by human habitation (from the Nile River on the upper left side, to eastern China on the upper right side) was taken with the OSIRIS WAC at 19:45 CET, about 2 hours before the closest approach of the spacecraft to Earth. At the time, Rosetta was about 80 000 km above the Indian Ocean where the local time approached midnight. The image was taken with a five-second exposure of the WAC with the red filter. This image showing Earth's illuminated crescent was taken with the WAC at 20:05 CET as Rosetta was about 75 000 km from Earth. The crescent seen is around Antarctica. The image is a colour composite combining images obtained at various wavelengths. Source: http://www.esa.int/spaceinimages/Images/2007/11/OSIRIS_view_of_Earth_by_night

Tables

Table 1

Table 1. Comparison of available space-borne sensors for night-lights mapping, sorted by spatial resolution.

Sensor	Spatial resolution (m)	Operational years	Temporal resolution	Products	Radiometric range	Spectral bands	Main references
DMSP/OLS	3000	Digital archive available for 1992-2013	Global coverage can be obtained every 24 hours	Stable lights, Radiance calibrated, Average DN	10^{-6} to 10^{-9} watts/cm^2/ sr/µm 6 bit Min detectable signal 4 10-5 W/m/sr	Panchromatic 400-1100 nm	Doll 2008; Elvidge et al. 1997b, 2009c
VIIRS/DNB	740	Launched in Oct 2011	Daily images can be downloaded.	Monthly Cloud-free composites available from April 2012 onwards in radiance units of nano-Watts/(cm^2*sr). Daily corrected product, VNP46A1, available since mid-2019 (NASA Black Marble).	14 bit Min detectable signal 3 10-5 W/m/sr	Panchromatic 505-890 nm	Miller et al. 2012; Elvidge et al., 2013, 2017; Roman et al., 2018 https://viirsland.gsfc.nasa.gov/ https://ladsweb.modaps.eosdis.nasa.gov/search/order/1/VNP46A1--5000

Aerocube 4	500	Experimental cubesat, 2014	Sporadic	N\A	Detection threshold of about 20 nW/cm2/sr to achieve SNR of 4 or more	RGB	Pack and Hardy, 2016; Pack et al., 2017
SAC-C HSTC	300	Launched in Nov 2000	Sporadic	N\A	8 bit	Panchromatic 450-850 nm	Colomb et al. 2003
SAC-D HSC	200-300	Launched in June 2011	Sporadic	N\A	10 bit	Panchromatic 450-900 nm	Sen et al. 2006
Astronauts photographs onboard the International Space Station (ISS)	5-200	From 2003 onwards (since mission ISS006)	Photos taken irregularly	Photos can be searched and downloaded from: http://eol.jsc.nasa.gov/	8-14 bit	RGB	Doll 2008; Levin and Duke 2012; Kyba et al., 2014; Sánchez de Miguel et al., 2014
CUMULOS	150	Experimental cubesat, 2018	Sporadic	N\A	N\A	Panchromatic	Pack et al., 2018, 2019
LuoJia1-01	130	Launched June 2018	15 day revisit time	Freely available	DN values with lab calibration	Panchromatic, 460-980 nm	Li et al., 2018b, 2019a
Aerocube 5	124	Experimental cubesat, 2015	Sporadic	N\A	Detection threshold of about 20 nW/cm2/sr to achieve SNR of 4 or more	RGB	Pack and Hardy, 2016; Pack et al., 2017

Landsat 8	15-30	Launched in 2013	Night time images acquired irregularly	Freely available	14 bit Only very bright objects are detected	Seven bands	Roy et al., 2014; Levin and Phinn, 2016
Jilin-1 (JL1-3B)	0.9	Launched January 2017	Commercial satellite, acquires images on demand	N\A	8 bit	430–512 nm (blue), 489–585 nm (green) and 580–720 nm (red)	Zheng et al., 2018 https://www.cgsatellite.com/imagery/luminous-imagery/
JL1-07/08	< 1	Launched January 2018	Commercial satellite, acquires images on demand	N\A	N\A	Panchromatic and multi-spectral (blue, green, red, red edge, and near-infrared bands)	Zhao et al., 2019
EROS-B	0.7	Night lights images offered since mid-2013	Commercial satellite, acquires images on demand	N\A	16 bit	Panchromatic	Levin 2014; Katz and Levin, 2016